SYNTHESIS, CHARACTERIZATION AND APPLICATIONS OF NEW PHOTOCURABLE AND BIODEGRADABLE ELASTOMERS

Jinrong Liu

A dissertation submitted to the faculty of the University of North Carolina at Chapel Hill in partial fulfillment of the requirements for the degree of Doctor of Philosophy in the Materials Science

Chapel Hill
2008

Approved By:

Dr. Valerie V.S. Ashby

Dr. Ed T. Samulski

Dr. Yue Wu

Dr. Sergei S.Sheiko

Dr. Nancy Allbritton

ABSTRACT

JINRONG LIU: SYNTHESIS, CHARACTERIZATION AND APPLICATIONS OF NEW PHOTOCURABLE AND BIODEGRADABLE ELASTOMERS

(Under the direction of Dr. Valerie V.S. Ashby and Dr. Ed T. Samulski)

Biodegradable elastomers have attracted a great deal of interest due to their potential applications in the biomedical field. Based on the advantages of the photocuring method, a new series of photocurable and biodegradable elastomers were designed. By using step growth polymerization, polyester liquids with different composition and molecular weights were synthesized. After endcapping with methacrylate groups, these liquids can be easily fabricated into completely amorphous elastomers by UV exposure for 1 min at room conditions. The prepared elastomers presented a wide range of mechanical properties (G = 0.1-10 MPa) and a fast degradation rate (16% after 5 week incubation in PBS). The *in vitro* and *in vivo* biocompatibility studies of the elastomers indicated that these elastomers were good candidates as tissue engineering scaffolds. Meanwhile, the functionality of these photocurable elastomers was expanded by incorporation of amine containing monomers, and new elastomers were prepared to explore their potential as drug carrier systems. Monodispersed elastomeric particles were fabricated out of these amine containing materials by PRINT^{TM} technology. These particles showed pH sensitive drug release of Doxorubicin (a hydrophobic drug model) and Minocycline chloride (a hydrophilic drug model), and the release profiles can be further tuned by the incorporation of a disulfide crosslinker.

This work is dedicated to my family for their support and love as well as my colleagues and friends.

TABLE OF CONTENTS

.

LIST OF TABLES

Table

LIST OF FIGURES

Figure

LIST OF ABBREVIATIONS AND SYMBOLS

AA	Adipic acid
AFM	Atomic force microscopy
ATRP	Atom transfer radical polymerization
DCC	Dicyclohexylcarbodiimide
DEAP	2,2-Diethoxyacetophenone
DEG	Diethylene glycol
DLL	D,L-lactide
DLS	Dynamic light scattering
DMAP	4-Dimethylaminopyridine
DOX	Doxorubicin
DPBS	Dulbecco's Phosphate Buffered Saline
DSC	Differential scanning calorimetry
ε-CL	ε-Caprolactone
EG	Ethylene glycol
EMEM	Eagle minimal essential medium
FBS	Fetal bovine serum
FTIR	Fourier transform infrared spectroscopy
GPC	Gel permeation chromatography
H&E	Hematoxylin and eosin
HMA	Trans-β-hydromuconic acid
HPLC	High performance liquid chromatography
MCH	Minocycline hydrochloride
MTS	Masson’s trichrome stain
NMR	Nuclear magnetic resonance

PBS	Phosphate buffered saline
PCL	Poly(caprolactone)
PCLA	Poly(caprolactone *co* L-lactide)
PDI	Polydispersity index
PEG	Poly(ethylene glycol)
PEUU	Poly(ester urethane)urea
PGA	Polyglycolide
PGS	Poly(glycerol sebacate)
PIP	1,4-Bis (2-hydroxyethyl)piperazine
PLA	Polylactide
PLGA	Poly(lactide-glycol acid)
POC	Poly (diol citrate)
PRINT	Particle Replication in Non-wetting Templates
PTFE	Polytetrafluoroethylene
RMS	Root mean square roughness
SDBV	Small diameter blood vessels
SEM	Scanning electron microscopy
Sn(Oct)	Stannous 2-ethylhexanoate
TEG	Tetraethylene glycol
TGA	Thermogravimetric ananlysis
THF	Tetrohydrofuran
TMC	Trimethylene carbonate
TPE	Thermoplastic elastomers
UV	Ultraviolet

T_g	Glass transition temperature
G	Young's Modulus
T_m	Melting temperature
δ	Chemical shift
σ	Tension stress
ε	Tension strain
Ra	Arithmetic roughness

CHAPTER 1

INTRODUCTION TO BIODEGRADABLE ELASTOMERS AND THEIR APPLICATIONS IN BIOMEDICAL FIELDS

An elastomer is a polymer that exhibits enormous extensibility up to several hundred percent, compared with a few percent for ordinary solids, and has the ability to recover its original shape and dimensions on release of stress. These materials can be covalently crosslinked or connected in a network by physical associations such as small crystalline domains.[1] Because of their special mechanical properties, elastomers have been broadly applied in industry. For example, they have been used as auto tires, conveyor belts, footwear, cables, etc. Elastomers have been important materials for the development of biomedical engineering and have been used as gloves, catheters, and hand and foot joint replacements.[2] In tissue engineering, elastomeric scaffolds have been used to support and orient cell growth for the generation of replacement tissue. The mechanical properties of the elastomer are designed to resemble soft tissues, thereby withstanding repeated dynamic loads without causing mechanical stimuli to the surrounding tissues.

There are two categories of elastomers: thermoplastic elastomers and thermoset elastomers. Thermoplastic elastomers, which are elastomeric at the use temperatures, are physically crosslinked block copolymers, where one block of the copolymer chains aggregate to form glassy domains and effectively crosslink the soft segments. Because physical crosslinking is reversible upon heating and cooling, thermoplastic elastomers are less dimensionally and thermally stable than their thermoset counterparts. Thermoset elastomers are formed by the chemical crosslinking of polymer chains, which is an irreversible process. These materials are increasingly used in engineering applications because of their excellent stability at elevated temperatures and under physical stress. They are dimensionally stable under a wide variety of conditions due to their rigid

network structure and will not flow when heated.[3] Therefore, thermoset elastomers have a performance advantage over thermoplastic elastomers, although the latter presents lower processing costs.

Many kinds of elastomers have been studied to date, and this chapter will focus on synthetically fabricated elastomers, especially those designed to be biodegradable for medical applications. The essential reason for interest in biodegradable materials is the desire to have a device that can be used as an implant and does not require a second surgical procedure for removal.

This chapter will be divided into two sections. In the first section, representative synthetic methods used for making biodegradable thermoplastic elastomers and thermoset elastomers will be reviewed with an emphasis on thermoset elastomers, as they can maintain structural integrity upon implantation inside body.[1] In the second section, the applications of these materials in the biomedical field, especially as scaffolds and drug release carriers will be discussed.

1.1 Synthesis of biodegradable elastomers

1.1.1 Synthesis of biodegradable thermoplastic elastomers (TPE)

Biodegradable thermoplastic elastomers can be prepared as diblock, triblock or multiblock copolymers. Generally diblock and triblock copolymers can self-organize into well-defined morphologies while multiblock copolymers microphase-separate into less-defined phases.[4]

Many biodegradable diblock and triblock copolymers have been reported in the literature.[4-12] Generally one block is formed first with reactive endgroups, followed by the formation of alternate blocks. Depending on the composition of the polymer chains, the block copolymers can be A-B diblocks[8,9], A-B-A triblocks[4,10,11] or A-B-C triblocks[12]. Multiblock copolymers can be synthesized by chain extending low molecular weight prepolymers.[13-22]

Herein, representative examples of these elastomers, their synthesis and the corresponding mechanical and thermal properties will be discussed.

1.1.1.1 A-B diblock copolymers

Moon Suk Kim *et al.* used living cationic polymerization to prepare poly(isobutylene-*b*-ε-caprolactone) diblocks for making biodegradable thermoplastic elastomer (Scheme 1-1).[9] This new synthetic method involved the combination of living cationic polymerization of isobutylene and living cationic ring-opening polymerization of ε-CL. These synthetic conditions afforded well-defined poly(isobutylene-*b*-ε-caprolactone) diblock without unfavorable backbiting or transesterification reactions. This simple methodology yielded a thermoplastic elastomer with a semicrystalline, biodegradable end segment. T_g and T_m were found to be -60 °C and 60 °C, respectively.

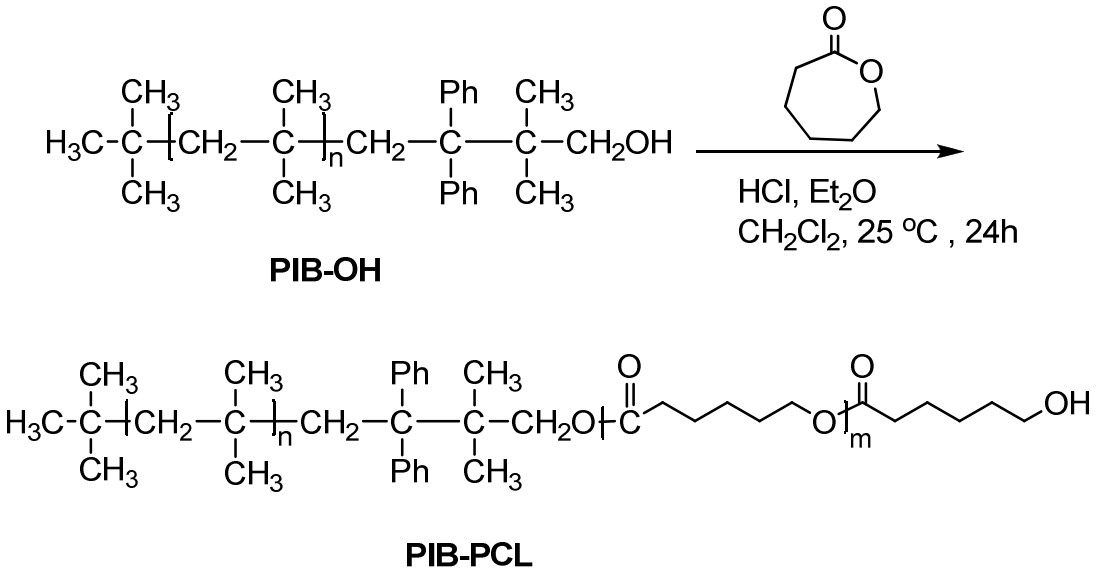

Figure 1-1. Living cationic polymerization preparation of poly(isobutylene-*b*-ε-caprolactone) diblocks by Moon Suk Kim *et al.*

1.1.1.2 A-B-A triblock copolymers

A more effective network formation can be achieved by A-B-A triblock copolymers. Hiki *et al.* reported a telechelic poly([RS]-3-hydroxybutyrate) prepared using the ring-opening polymerization of [RS]-*b*-butyrolactone and 1,4-butanediol as the initiator (Figure 1-2).[7] The subsequent copolymerization with L-lactide afforded highly elastomeric A-B-A type triblock copolyesters. The Young's modulus of the copolymer films increased from 30 to 160 MPa and the elongation at break decreased from 200 to 86% with increasing PLLA composition (44-69%) and increasing crystallinity (9-23%). The T_g values ranged from 15-47 ºC.

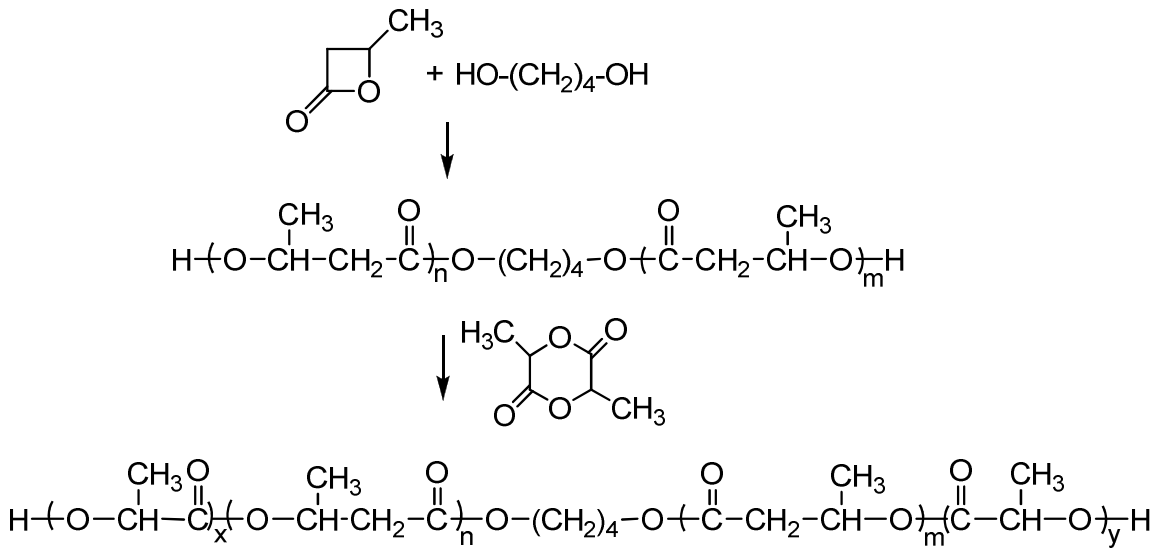

Figure 1-2. Ring-opening polymerization [RS]-*b*-butyrolactone in the presence of 1,4-butanediol and copolymerization with L-lactide by Hiki *et al.*

1.1.1.3 A-B-C triblock copolymers

Elisa Zini *et al.* prepared novel (L-lactide-glycolide-trimethylene carbonate) terpolymers via sequential ring-opening polymerization of the cyclic monomers using low-toxicity zirconium (IV) acetylacetonate as the initiator (Figure 1-3).[12] The glass transition temperature of the terpolymers ranged from 12 to 42 ºC, and the Young's modulus ranged from 3-1541 MPa. The obtained polymers showed shape memory properties, which can reform to their original shapes, and they recovered the permanent shape near body temperature. This property be beneficial in minimally invasive surgery. The combination of low toxicity and shape memory properties made the triblock copolymers promising for biomedical applications.

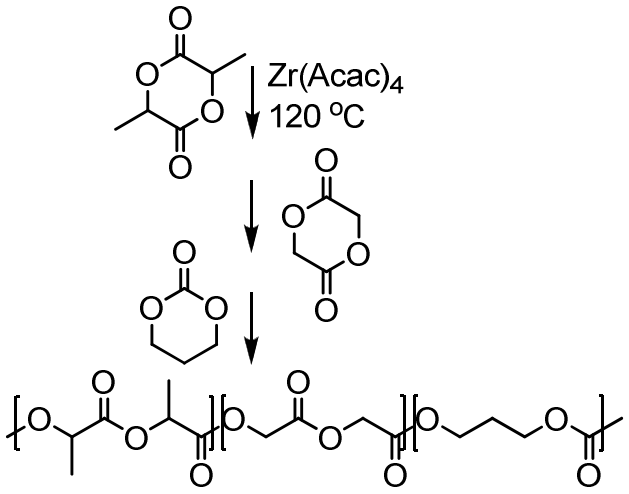

Figure 1-3. Novel (L-lactide-glycolide-trimethylene carbonate) terpolymers by Elisa Zini *et al.*

1.1.1.4 Multiblock thermoplastic elastomers

Polyurethanes are the most prevalent class of multiblock thermoplastic elastomers.[13-22] Low molecular weight polyesters are used as the soft segments to yield biodegradable polyurethanes. Cohn *et al.* synthesized PCL/PLA thermoplastic elastomers, where poly(L-lactic acid) generated the hard blocks and poly(caprolactone) created the soft segments along the copolymeric backbone with hexamethylene diisocyanate as a chain extender. This led to a family of biodegradable poly(ester-urethane) multiblock copolymers.[19] The multiblock copolymers displayed enhanced mechanical properties, with ultimate tensile strength values near 32 MPa, Young's modulus as low as 30 MPa and elongation at break values well above 600% (Figure 1-4). These copolymers exhibited T_g values approximately -30 °C and T_m values near 42 °C.

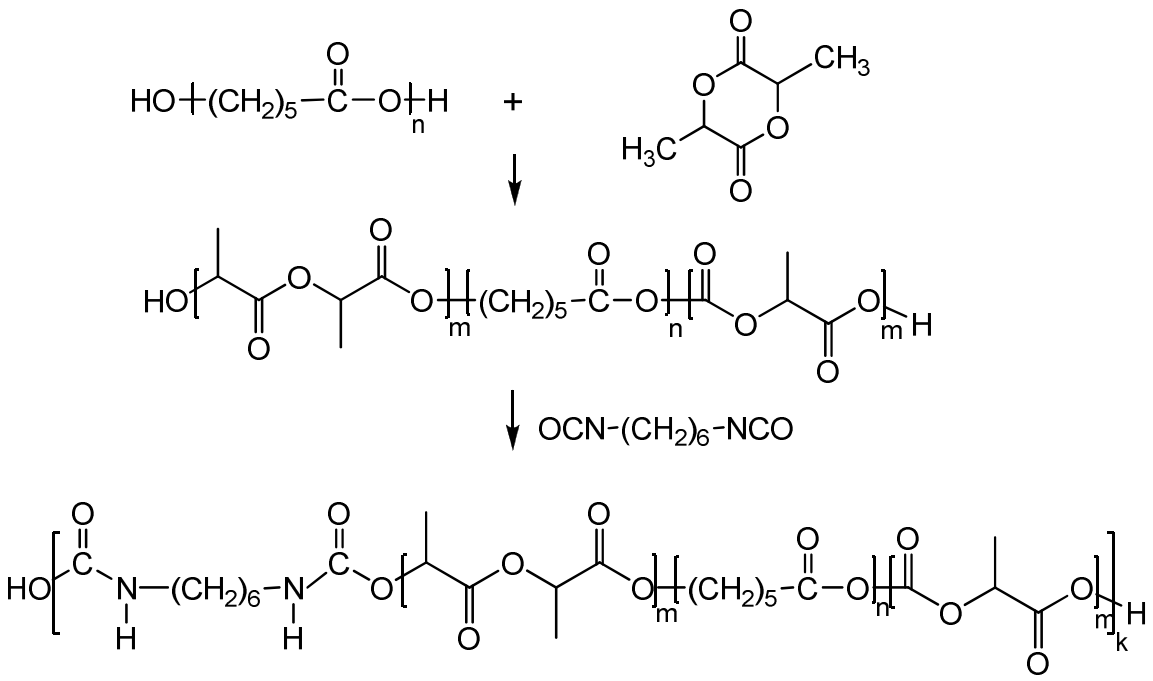

Figure 1-4. Synthesis and structure of PCLA multiblock copolymers by Cohn *et al.*

In addition to poly(ester-urethane)s, poly(urethane urea)s have also been explored to afford better mechanical properties. [21,22] Guan *et al.* synthesized a family of biodegradable poly(ester-urethane)ureas based on poly(caprolactone) and butyl diisocyanate. The polymers were highly flexible, with tensile strengths ranging from 9.2 to 29 MPa and breaking strains from 660 to 895% (Figure 1-5).[22] They further improved the hydrophilicity and biodegradation rate of the poly(urethane)urea by later incorporation of polyethylene glycol.[23, 24]

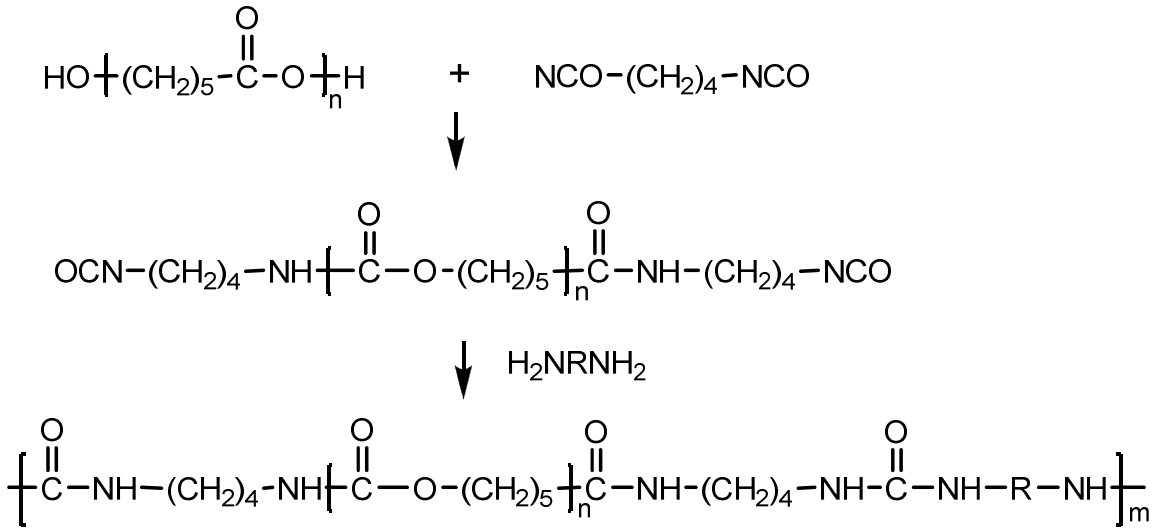

Figure 1-5. Synthesis of poly (ester urethane)urea (PEUU) by Guan *et al.*

As can be seen from the above examples, a wide variety of thermoplastic elastomers can be prepared by tuning the block composition and distribution. Since the elasticity of thermoplastic elastomers comes inherently from the phase separation of crystalline and amorphous regions. Once the elastomers are implanted inside body, the two regions will hydrolyze at different rates, and as such, the elastomers degrade heterogeneously resulting in a nonlinear loss of strength, which will deform the original designed structure.[19] However, completely amorphous thermoset elastomer materials will degrade more homogenously with a more linear degradation of physical properties, making them more desirable in tissue engineering scaffolds.[40]

1.1.2 Synthesis of biodegradable thermoset elastomers

The most common method used in the literature to fabricate biodegradable thermoset elastomers begins with prepolymer preparation with curable functional groups

that are located on the polymer backbone or on the chain ends. Three dimensional networks can be formed from these prepolymers using irreversible thermal curing or photocuring methods.[25-40]

1.1.2.1 Thermally crosslinked elastomers via ring-opening polymerization

Storey *et al.* synthesized a series of 3-arm poly(D,L-lactide-*co*-trimethylene carbonate) prepolymers (Figure 1-6).[36,37] The prepolymers were free radically crosslinked in the absence of reactive diluents to give amorphous, bioabsorbable networks with a broad range of thermal, mechanical and degradation properties. The sol content in the elastomers ranged from 2.87% to 6.17%. Tensile tests showed that the stress ranged from 3 to 60 MPa and strain was 5-55%. The degradation rate was dependent on the ratio of the two components, and the prepolymer of DLL:TMC = 40:60 gave the most uniform degradation rate in terms of strength loss with a mass loss of 4% after 119 days incubation in PBS at 37 ºC.

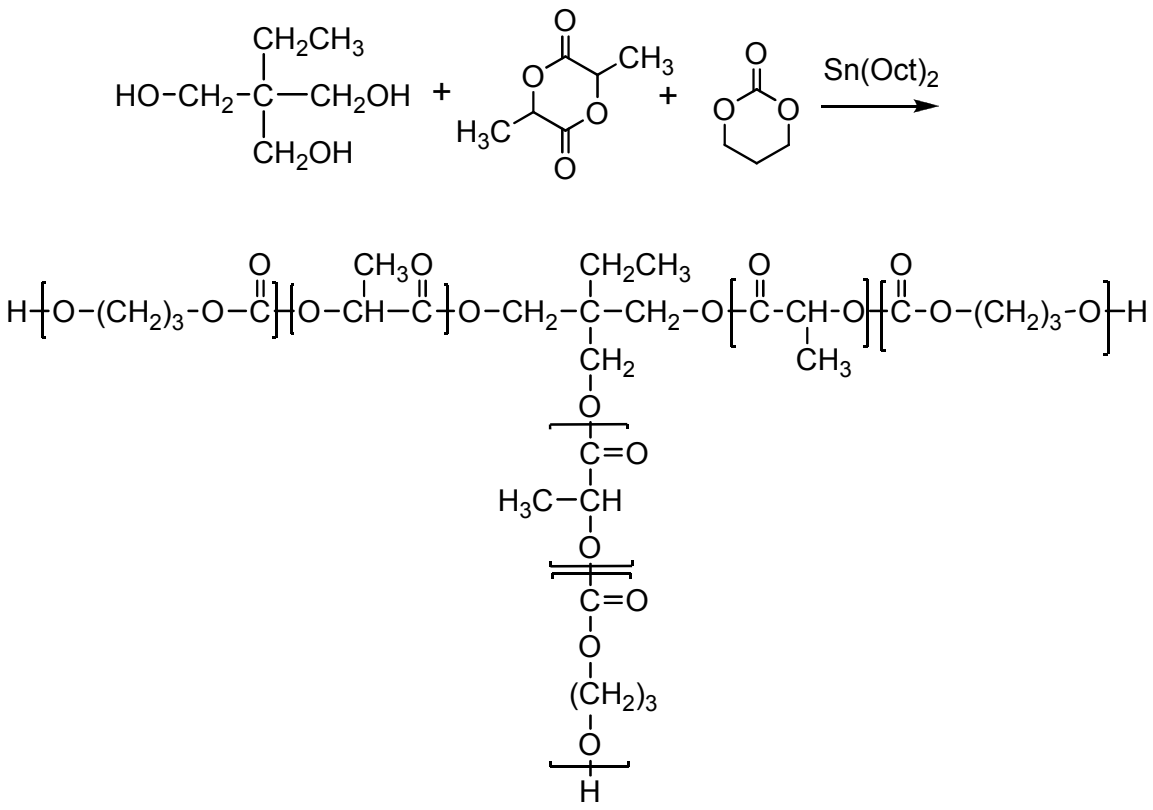

Figure 1-6. Synthesis of poly(D,L-lactide), poly(D,L-lactide-*co*-trimethylene carbonate) and poly(trimethylene carbonate) triols by Storey *et al.*

1.1.2.2 Thermally crosslinked elastomers via step growth polymerization

Another broadly used synthetic scheme to fabricate biodegradable thermoset elastomers is polycondensation of multifunctional carboxylic acids and polyols.[25,29,41,42] In this approach, small molecule by-products are produced and removed typically using high vacuum to drive the reaction forward. Compared with ring-opening polymerization, which suffers from a limited supply of cyclic monomers, making it more difficult to tune the properties for different application requirements, step growth polymerization can

easily incorporate a wide variety of monomers into the synthetic schemes, affording the ability to expand the properties of the elastomers.[43,44]

Multifunctional monomers are widely employed to fabricate thermally crosslinked elastomers. Kiyotsukuri *et al.* was one of the first to fabricate a thermally crosslinked network by using glycerol and a wide range of diacids at high temperatures (Figure 1-7) to prepare thermoset elastomers.[45] Prepolymers were first synthesized and successively post-polymerized to form the networks. The resultant films were transparent, flexible and insoluble in organic solvents. The Young's modulus ranged from 7-28 MPa with ultimate strains ranging from 13-30 %, and the T_g ranged from -50 ºC to -3 ºC.

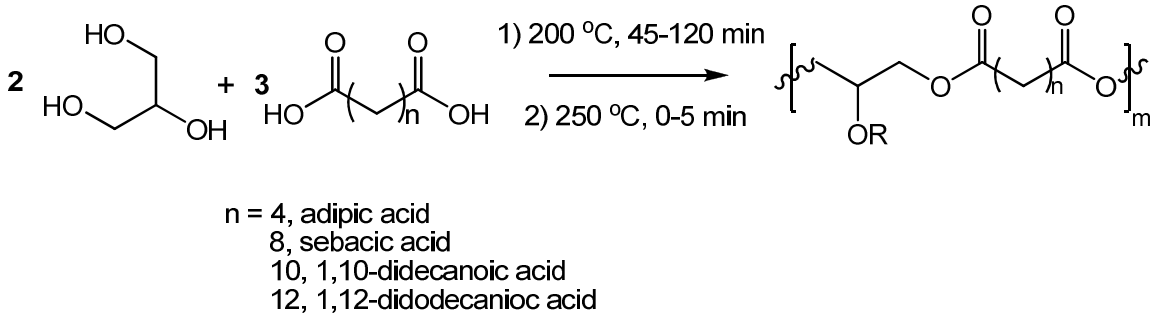

Figure 1-7. Elastomer preparation via polycondensation by Kiyotsukuri *et al.*

The same monomers were used by Langer's group to fabricate a softer biodegradable elastomer as scaffolds for soft tissue replacement.[25] They chose a lower reaction temperature (120 ºC) and a longer reaction time (24 h) to synthesize the prepolymer from sebacic acid and glycerol. An almost colorless elastomer was formed by further fabrication using heat and vacuum. DSC data showed two crystallization temperatures at -52.14 °C and -18.50 °C and two melting temperatures at 5.23 °C and 37.62 °C, respectively. The Young's modulus of the polymer is 0.282 ± 0.0250 MPa,

indicating a soft material with 267 ± 59.4 % strain and ultimate tensile strength > 0.5 MPa.

The multifunctional monomer methodology was improved by Ameer's group to prepare totally amorphous thermoset elastomers.[26,41] The synthesis was similar to Kiyotsukuri's approach but with citric acid used as the crosslinking agent instead of glycerol. Poly(diol citrate)s were synthesized by reacting citric acid with various diols to form a covalent crosslinked network via a polycondensation reaction without the use of a catalyst (Figure 1-8). The tensile strengths of the poly(diol citrate)s were as high as 11.15 ± 2.62 MPa, and Young's modulus ranged from 1.60 ± 0.05 MPa to 13.98 ± 3.05 MPa. Elongation was as high as 502 ± 16%. Glass transition temperatures (T_g) for all poly (diol citrate) thermosets were from −5 to 10 °C. No melting peaks or crystallization peaks were observed.

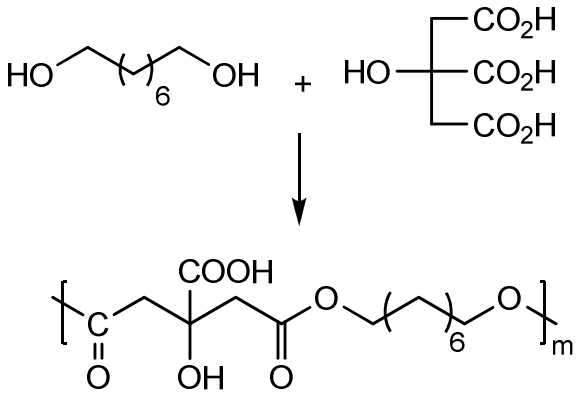

Figure 1-8. Poly(diol citrate)s preparation via polycondensation by Ameer *et al.*

However, multifunctional approaches suffer from a lack of ability to vary properties by controlling the crosslinking chemistry. Instead of the multifunctional monomer approach, many researchers chose free radical curing of the prepolymers to fabricate biodegradable elastomers. In this strategy, unsaturated groups are incorporated

in the prepolymers either on the backbone, as grafts or at the chain ends. Sheares *et al.* chose an unsaturated acid, hydromuconic acid, to react with poly(ethylene glycol) oligomers (Figure 1-9).[46] Completely amorphous, liquid poly (ester ether) prepolymers with number average molecular weights between 4 and 6 x 10^3 g/mol were prepared via condensation polymerization. These liquid prepolymers were then thermally crosslinked to form degradable elastomeric structures with glass transition temperatures below -30°C. Materials could be designed to completely degrade *in vitro* over a range of 30 days to 6 months, while the Young's modulus could be varied over 3 orders of magnitude (0.02-20 MPa). These prepolymers could not be photocured due to the low activity of the vinyl groups in the middle of the polymer backbones.

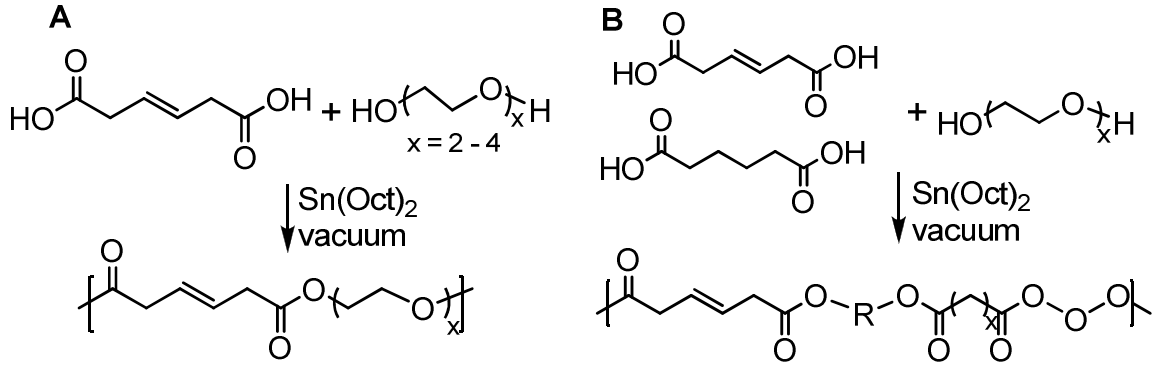

Figure 1-9. Synthesis of unsaturated poly(ester ether) A) prepolymers and B) copolymers by Sheares *et al.*

Although thermal crosslinking can afford totally amorphous thermoset elastomers, there are several disadvantages for this approach, as high temperatures (90–250 ºC) and long fabrication times (24 h to several days) are normally required. Another widely used approach to fabricate thermoset elastomers is to photo crosslink the network,

which leads to the material preparation in several minutes at room temperature with better spatial and temporal control.

1.1.2.3 Photocurable elastomers via ring-opening polymerization

Preparing unsaturated groups at the end of prepolymer chains is a broadly used method to make photocurable elastomers.[47-50] This strategy is popular because terminal double bonds are more reactive than those along the backbone, allowing more efficient network formation. And also, this method allows wide selection of monomers.

Anseth *et al.* prepared methacryloyl terminated poly(lactic acid-*co*-caproic acid) diethylene glycol based oligomers to explore new scaffold system for tissue engineering application by systematic chemical variations in the degradable block of the crosslinked network (Figure 1-10).[49] These macromers were then photo polymerized at 450 nm to produce crosslinked degradable networks. The prepolymer molecular weights ranged from 1.6-2.3 x 10^3 g/mol, and the methacrylation efficiency was 70-100%. They found the storage modulus was on the order of 10-10^3 MPa, and T_gs ranged from -30 to 56 °C. Complete degradation occurred in as short as 80 days to more than 6 months.

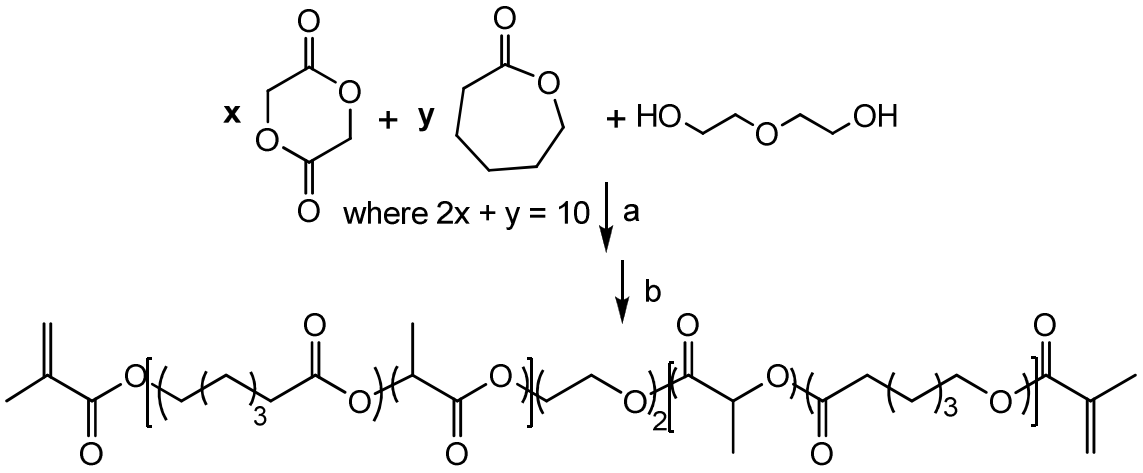

a: cat. $Sn(Oct)_2$, 130 °C, 6h
b: 2.4 eq. triethylamine, 2.2 eq. methacryloyl chloride (rel. to DEG, 0 °C), in CH_2Cl_2

Figure 1-10. Synthesis of diethylene glycol/α-hydroxy acid copolymer containing photo polymerizable end groups by Anseth *et al.*

The ring-opening polymerization approach was extensively explored by Amsden and his co-workers.[38-40] Star polyesters of ε-caprolactone-*co*-D,L-lactide were prepared by ring-opening polymerization, which was initiated by glycerol. After endcapping with acrylate groups, UV light was used to crosslink the system (Figure 1-11). The influence of the prepolymer molecular weight on the mechanical properties and thermal properties was determined. The glass transition temperature of the elastomers was independent of the prepolymer molecular weight and was from -6 to -8 ºC. The Young's modulus (G = 0.5-5.4 MPa) and stress at break (σ = 1.2-4.5 MPa) of the elastomers was inversely proportional to the prepolymer molecular weight, while the strain at break increased in a linear fashion with the prepolymer molecular weight.

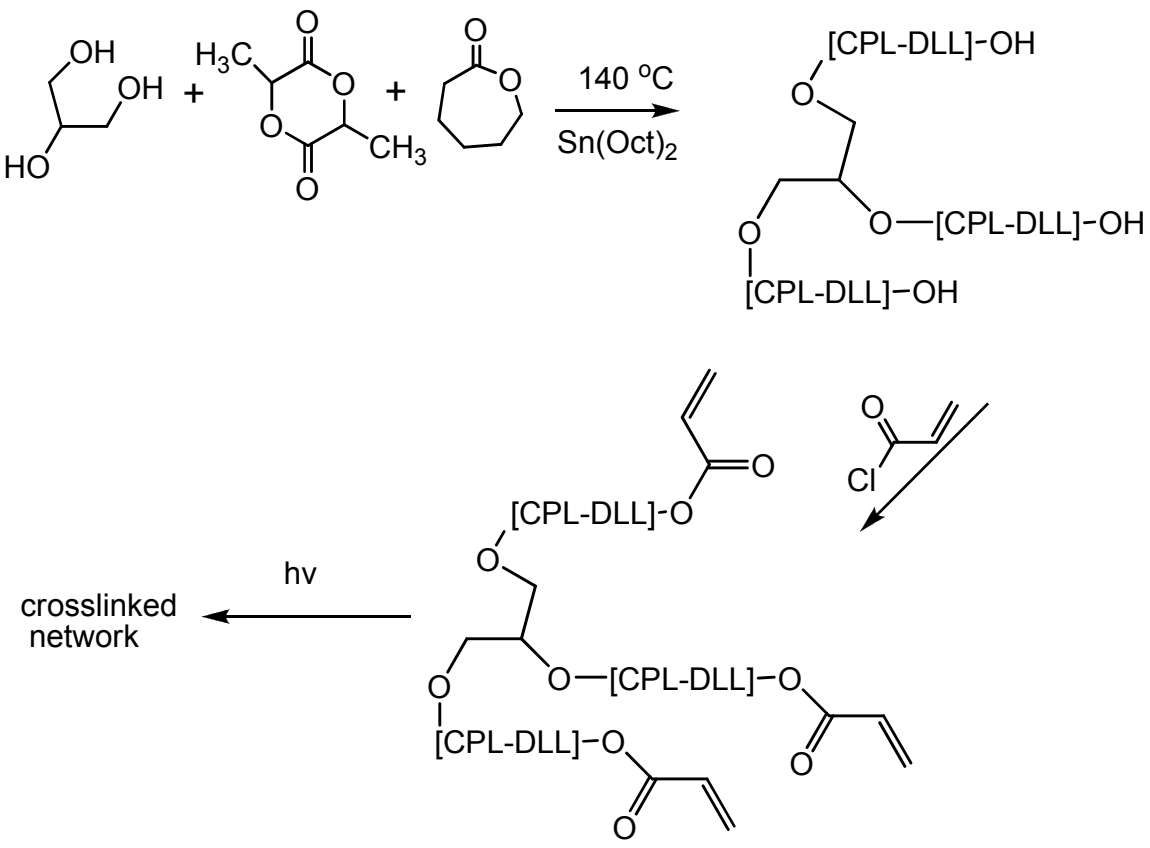

Figure 1-11. Synthesis of polyesters of ε-caprolactone-*co*-D,L-lactide by Amsden *et al.*

1.1.2.4 Photocurable elastomers via step growth polymerization

Minoru Nagata *et al.* reported photocurable and biodegradable multiblock copolymers by step growth polymerization of poly(ε-caprolactone) (PCL) diols and poly(ethylene glycol) (PEG) with 4,4'-(adipoyldioxy)dicinnamic dichloride as a chain extender (Figure 1-12). These copolymers were chosen to explore new shape memory materials with outstanding properties such as hydrophilicity, permeability, and degradability.[51,52] Glass transition temperatures ranged from -64 to -62 ºC, and melting temperature were from 34 to 48 ºC. The stress at break ranged from 3.1-4.7 MPa, and elongation at break ranged from 640-1500%. The materials recovered very rapidly to the

original size from 90-300% extension. The rate of degradation could be tuned by the ratio of PEG components. This approach needed long irradiation time to attain high crosslink density. Moreover, the elastomers were not fully amorphous.

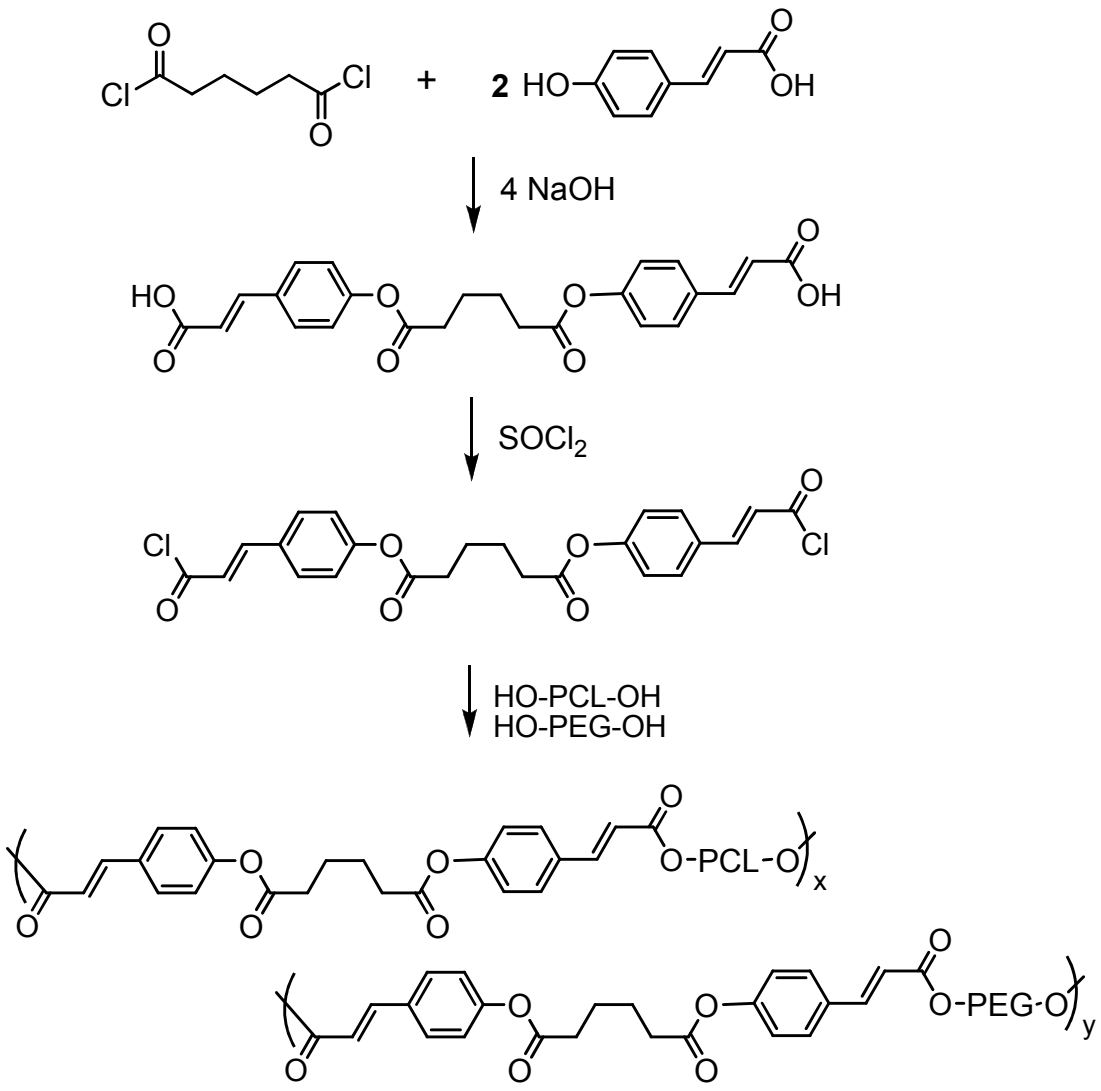

Figure 1-12. Preparation of polyesters derived from CAC, poly(ethylene glycol) diol and poly(ε-caprolactone) diol by Minoru Nagata *et al.*

1.1.3 General requirements for materials design

The previous examples described a wide variety of methods to develop biodegradable elastomers suitable for biomedical applications. While these elastomers have a wide range of properties and dramatically advanced the field of biomaterials science, there is still significant room for improvement. At this point, there are several properties that need to be further developed or optimized.

- *Soft materials:* Prepare materials that can be used for soft tissue replacement.
- *Totally Amorphous:* Prepare materials that can maintain the structural integrity over the use range.
- *Photocurable:* Prepare materials that with less energy consumption and better spatial and temporal control.
- *Synthetically Ease*: Prepare materials using a minimal number of synthetic steps and less post polymerization steps that can potentially degrade the material.
- *Tailorable Properties:* Develop synthetic methods that allow for the properties of the material to be easily modified with fine precision.
- *Biocompatibility:* Develop new materials with a reduced foreign body response.
- *Biodegradability:* Tailor the time span in which a material degrades over a broad range.

1.2 Biomedical applications of biodegradable elastomers

Biodegradable elastomers have received a great deal of interest in the biomedical field due to their suitable mechanical properties and degradation profiles. They have been extensively explored in the fields of tissue engineering and drug release systems.[30] The following discussion will focus on these two areas.

1.2.1 Biodegradable elastomers in tissue engineering

As the understanding of mechanical stimulation in the engineering of elastic soft tissues develops, appropriate biodegradable elastomers can be designed to meet these specifications (withstanding repeated dynamic loads, providing a cell attachment surface and limited irritation to the surrounding tissues). After a period of application, they can totally degrade without a second surgery requirement. When used in the tissue engineering field, the elastomers can be either serve as a functional coating[53,54] to modify other biomaterials or as scaffolds themselves.[55-58]

1.2.1.1 Modification for nondegradable materials

Yang *et al.* used poly(octanediol citrate)-based biodegradable elastomers (POC) to modulate expanded polytetrafluoroethylene (ePTFE) vascular graft, which is broadly used as large diameter blood vessels. They are not applicable to small diameter blood vessels (SDBV) due to the poor patency resulting from compliant mismatch to local tissues.[53] Due to the elastomeric nature of POC, POC coating on ePTFE (POC-ePTFE) significantly changed the surface energy of the ePTFE grafts without affecting graft compliance, which allows it to mobilize according to the expansion or contraction of the ePTFE fibrils when the graft is exposed to pulsatile flow conditions (Figure 1-13). POC

modification significantly improved the hemocompatibility and acute inflammatory response of ePTFE grafts implanted in a porcine iliac artery ePTFE bypass model.

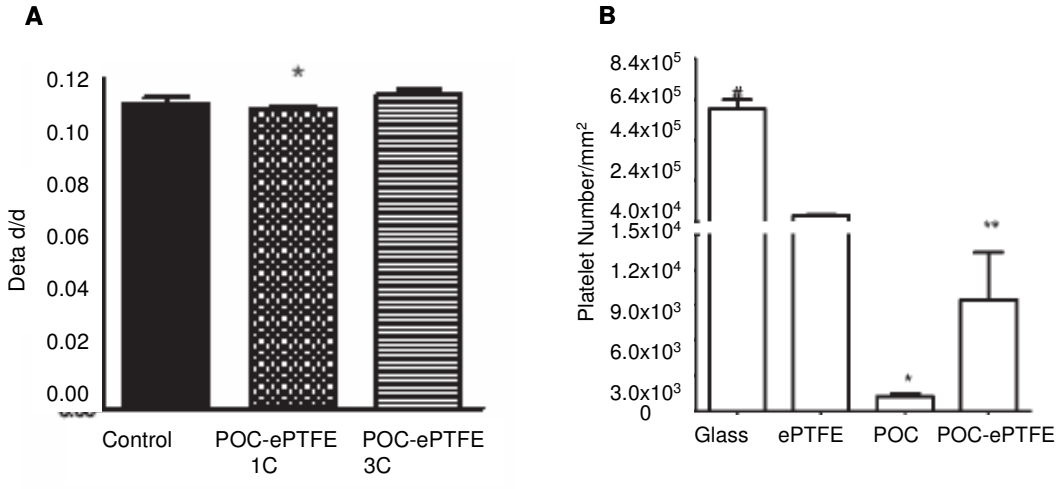

Figure 1-13. A) Effect of the POC coating on the compliance of graft. Compliance of the control ePTFE grafts and POC-ePTFE grafts with 1 coating (1 C) and 3 coatings (3 C). B) Platelet adhesion on ePTFE, POC, POC-ePTFE, and glass by Yang *et al.*

1.2.1.2 Nonporous Scaffolds

Biodegradable elastomers have been extensively studied as scaffolds in tissue engineering. Depending on their specific applications, the scaffolds can be fabricated to be nonporous or porous. Figure 1-14 shows some examples of nonporous scaffolds fabricated from poly(glycerol sebacate) based elastomers: microfluidic channels, grooved surface, micropatterned scaffolds and a block scaffold.[56,59-66] Different cell lines have been explored: primary baboon vascular cells, retinal progenitor cells, endothelial progenitor cells, Schwann cells, indicating the potential applications in nerve, cardiovascular, myocardium and vascular tissue engineering. The *in vitro* and *in vivo* degradation properties have been fully explored and it showed that the elastomers were

biocompatible and had better geometric stability than the commercial PLGA based biomaterials.

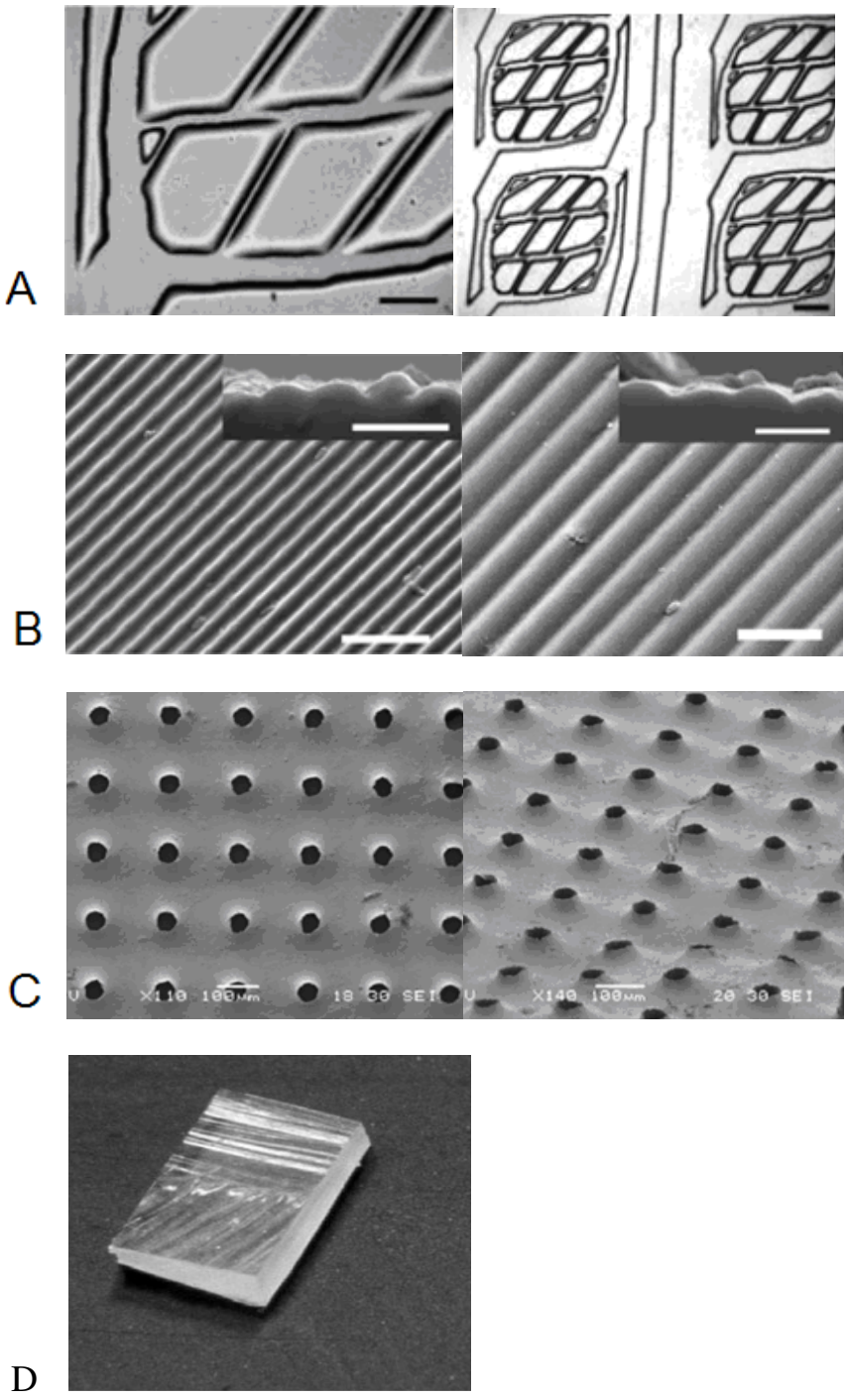

Figure 1-14. Poly(glycerol sebacate) based elastomers. A) PGS capillary networks, B) PGS grooved surface, C) PGS micropatterned scaffold, D) PGS block (*ref 56,59-66*)

Fujii *et al.* combined MEMS technology and biology together to fabricate microchambers and microchannels from acrylated poly(caprolactone-L-lactide) copolymers, which mimicked the *in vivo* microenvironment for cell behavior and explored their application in tissue engineering.[67] Various single and multistepwise microstructures were achieved by this soft lithography method (Figure 1-15). Microstructures down to 50 micron were fabricated for liver reconstructs. They investigated various mammalian cells growth and spreading in these implantable bioreactors. Static cultures of multiple cell lines could be successfully performed on single stepwise microstructures. Both cell culture and perfusion experiments suggested the possibility to use the present photosensitive polymer as microfluidic supports for biodegradable bioreactors for implantation applications.

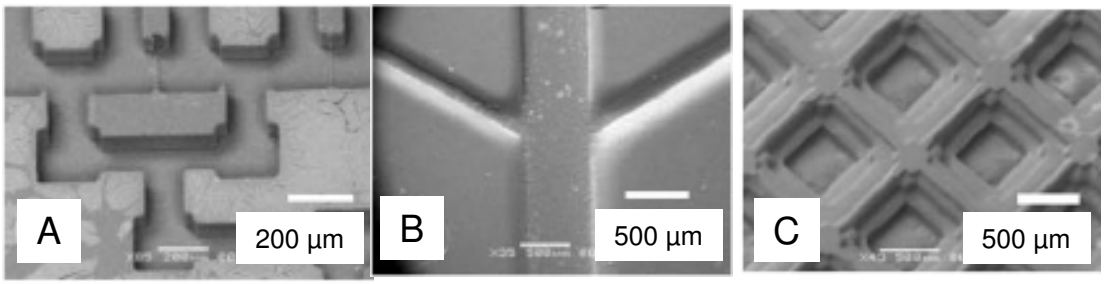

Figure 1-15. Various single and multistepwise microstructures were achieved by soft lithography method, A) single microstructure, scare bar = 200 µm, B) single microstructure, scare bar = 500 µm and C) multistepwise microstructure, scare bar = 500 µm by Fujii *et al.*

1.2.1.3 Porous Scaffolds

Porous tissue engineering scaffolds are more commonly designed than nonporous scaffolds since the interconnected pores can assure cell growth and the transport flow of nutrients and metabolic waste. Moreover, the porosity can be tuned to improve the mechanical match to the surrounding tissue without fundamental materials modification.[1, 56-58] Porous scaffolds can be fabricated by different techniques: salt leaching, gas foaming from a polymer melt, thermally induced phase separation or nonsolvent induced phase separation.[68, 69]

Wagner *et al.* fabricated two kinds of porous scaffolds by thermally induced phase separation using dimethyl sulfoxide as a solvent from biodegradable poly(urethane urea)s, namely poly(ester urethane)urea and poly(ether ester urethane)urea prepared from polycaprolactone, polycaprolactone-*b*-poly(ethylene glycol)-*b*-polycaprolactone, and 1,4-diisocyanatobutane.[70] By changing the polymer solution concentration or quenching temperature, scaffolds with random or oriented tubular pores were obtained (Figure 1-16). Smooth muscle cells were filtration seeded into the scaffolds, and it was shown that both scaffolds supported cell adhesion and growth.

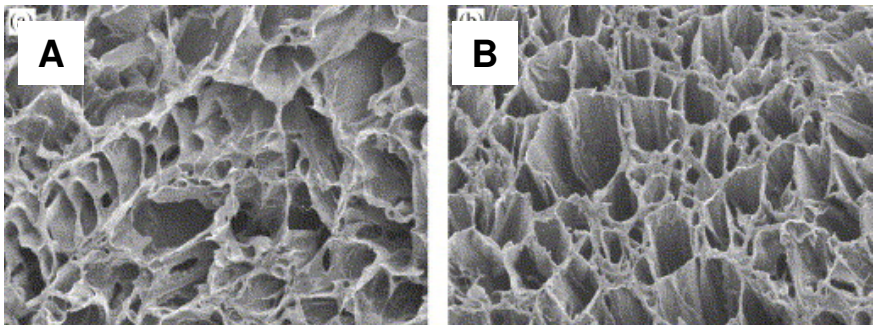

Figure 1-16. SEM of PEUU scaffolds prepared from different solution concentrations and quenching temperatures, A) 5% and -80 ºC and B) 8% and -20 ºC by Wagner *et al.*

Several techniques can be utilized together to design the specific structures.[71,72] Desai *et al.* developed porous micro-patterned poly(caprolactone) scaffolds using a novel technique that integrated soft lithography, melt molding and particulate leaching of polylactic-*co*-glycolic acid micro/nanoparticles.[71] Firstly, PLGA micro/nanospheres were prepared for use as a porogen. Secondly, micro-patterned PLGAs were embeded in PCL scaffolds with thicknesses on the tens of microns scale by a patterned PDMS mold. Lastly, the scaffolds were immersed in a basic solution to rapidly degrade the micro/nanospheres. The SEM images of the scaffolds are shown in Figure 1-17. The evaluation of nutrient diffusion through the porous scaffolds compared with nonporous PCL was conducted by using phenol red as a model. They found that PLGA-leached PCL scaffold had more phenol red passing through, indicating improvement for the nutrient diffusion. Vascular smooth muscle cells (VSMCs) were seeded on the scaffold to investigate the cell alignment on the porous patterned scaffolds. For unpatterned nonporous scaffolds, VSMCs showed unorganized and irregular shapes. In contrast, cells seeded on patterned PLGA-leached scaffolds appeared in an elongated and organized morphology, which indicated that patterned micro/nanospheres scaffolds helped maintain alignment. These findings are significant because micropatterning of VSMCs has been associated with promoting *in vivo* like VSMC morphology as well as enhanced ECM production and decreased proliferation.[73,74]

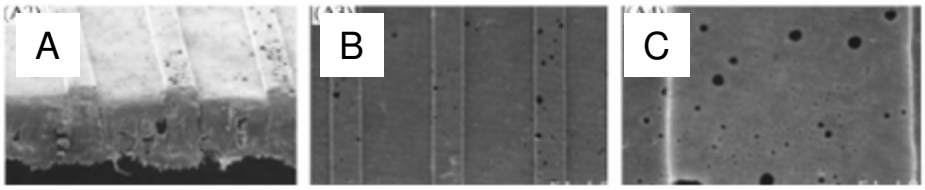

Figure 1-17. Porous micro-patterned polycaprolactone scaffolds by Desai *et al.*

As the understanding of the interaction between scaffolds and cells has progressed, more scaffolds have been fabricated to directly mimic the shape of target organs.[75-78] Sodian *et al.* fabricated a trileaflet heart scaffold from a polyhydroxyalanoate elastomer. The trileaflet heart valve scaffold consisted of a cylindrical stent containing three valve leaflets formed from a single piece of polyhydroxyalanoate (Figure 1-18).[77] The material was modified by a salt leaching technique to create a porous, three-dimensional structure. The leaflets opened and closed when tested in a pulsatile flow bioreactor, and cells formed a confluent layer after incubation. Later they used an advanced stereo lithography technique to fabricate a human aortic root scaffold and a pulmonary heart valve scaffold.[76]

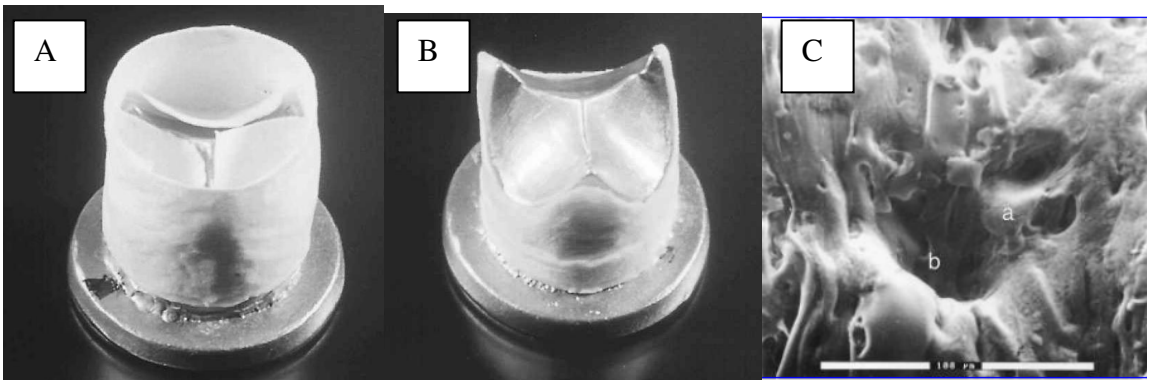

Figure 1-18. A) Crown like porous polyhydroxyalanoate construct, B) Trileaflet heart valve scaffold, C) Cell ingrowth into the pores by Sodian *et al.*

1.2.1.4 Biphasic Scaffolds made from nonporous and porous elastomers

Porous and nonporous structures can be combined together to fabricate more advanced scaffolds. An elastic biphasic scaffold was fabricated from POC based biodegradable elastomers to mimic small diameter blood vessels (Figure 1-19).[41,55] The

biphasic scaffold architecture was fabricated by sequential postpolymerization of concentric nonporous and porous layers of poly(diol citrate)s. The nonporous phase was designed to serve as a continuous surface for endothelial cell adhesion, proliferation, and differentiation and to provide mechanical strength and elasticity to the scaffold. The porous phase was expected to facilitate the three-dimensional expansion and maturation of smooth muscle cell and endothelial cells. Tensile tests, burst pressure, and compliance measurements confirmed that the nonporous phase created a "skin" connected to the porous phase and provided bulk mechanical properties that were similar to those of a native vessel. *In vitro* culture of tubular biphasic scaffolds seeded with human aortic smooth muscle cells and endothelial cells demonstrated the ability of this design to support cell compartmentalization, coculture, and cell differentiation.

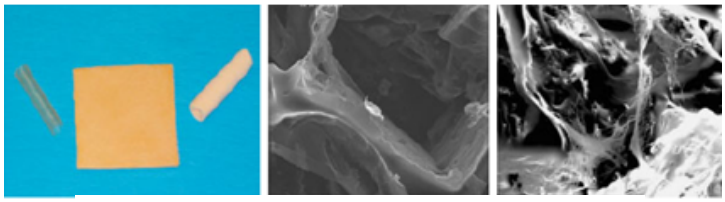

Figure 1-19. A) Photographs of POC scaffolds, B) SEM image of a porous scaffolds, and C) SEM of human aortic smooth muscle cell (HASMC) cultured within the porous POC scaffold (*ref 41,55*)

1.2.2 Biodegradable elastomers as drug carrier

There is significant interest in developing biodegradable elastomers as drug release systems since the materials are degradable, require no subsequent surgical

removal and lead to no accumulation inside body. Moreover, the materials are elastic, which has special advantages of osmotic pressure-driven in controlled release. Drugs can be chemically linked to the polymer chain (bioconjugation) or dispersed in the polymeric elastomer system (dispersion).[79,80]

1.2.2.1 Bioconjugate systems

Leong *et al.* designed drug-carrying elastomers based on poly(phosphoester-urethanes) (PPUs) (Figure 1-20).[81] The labile phosphoester linkage in the backbone of the PPU conferred biodegradability on the polymer. Using the reactive phosphite side chain in the PPUs, p-aminosalicylic acid and benzocaine (models of drugs) were attached pendantly to the polymer with or without a spacer. In contrast, ethambutol was incorporated into the backbone of the polymer. The drug release was studied from the two methods and also the cytotoxicity of the drug carrier. *In vitro* release of both drugs was completed in several hours, indicating the lability of the phosphoramidate bond (Figure 1-21). Particles of 1-5 μm size were fabricated from the elastomers, and the cytotoxicity was studied against a macrophage cell line. Results indicated healthy cell growth and particle uptake by cells.

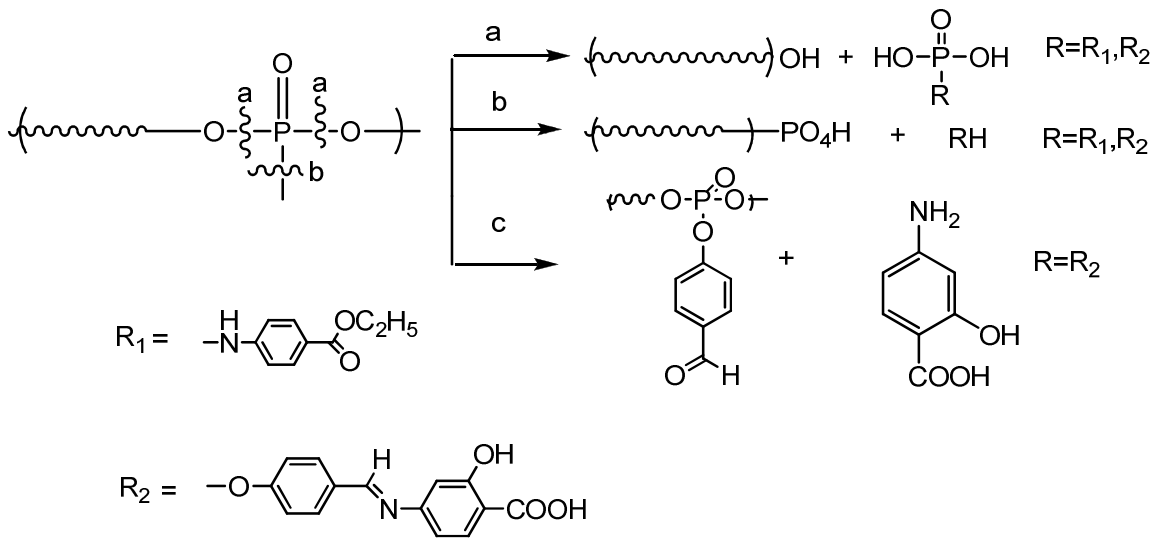

Figure 1-20. Synthesis of poly(phosphoester urethane)s (PPU) s by Leong *et al.*

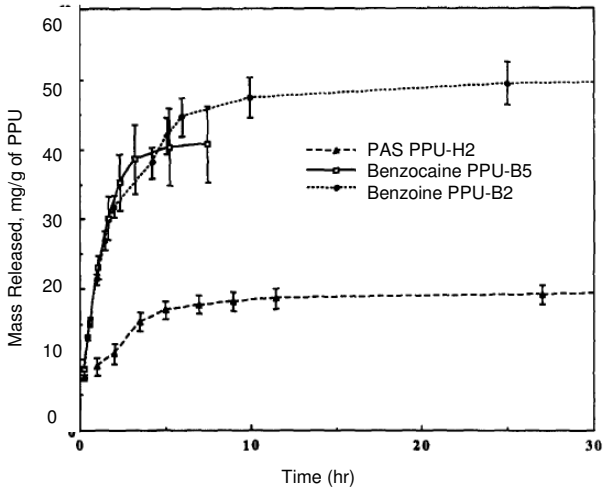

Figure 1-21. *In vitro* release of both drugs by Leong *et al.*

1.2.2.2 Dispersion systems

Although chemical grafting of drugs on the elastomers was useful for controlled drug release, there are limitations for the availability of drugs which can be grafted on the

polymer backbone. Moreover, to deliver different drugs, the polymer backbone has to be specially redesigned, which is synthetically difficult. The alternative is to directly disperse drugs inside the elastomer matrix where a wide selection of drugs and polymer systems can be used.

Drug dispersed elastomers have been broadly investigated for use in osmotic pressure-driven drug release. These materials help to provide a nearly constant release of drug for prolonged times because of the elastic properties from the elastomer matrix.[82-85]

For example, Ameer *et al.* fabricated slab-shaped or cylindrical elastomeric devices by photocrosslinking an acrylated star copolymer macromer of ε-caprolactone and D,L-lactide and tested the elastomer matrix as drug delivery vehicles for interferon-γ (IFN-γ), vascular endothelial growth factor (VEGF) and interleukin-2 (IL-2).[39,86,87] Under identical formulation conditions, these proteins were released at the same, nearly constant rate for a significant part of the release profile (until 70%–80% release depending on formulation characteristics). Decreasing the molecular weight of the acrylated macromers increased the rate of protein release, but did not alter the zero order nature of the release kinetics. The bioactivity of released proteins varied with VEGF at 57% bioactivity and IL-2 and IFN-γ at 80% bioactivity (Figure 1-22). The elastomer formulation has potential as a regiospecific protein delivery device.

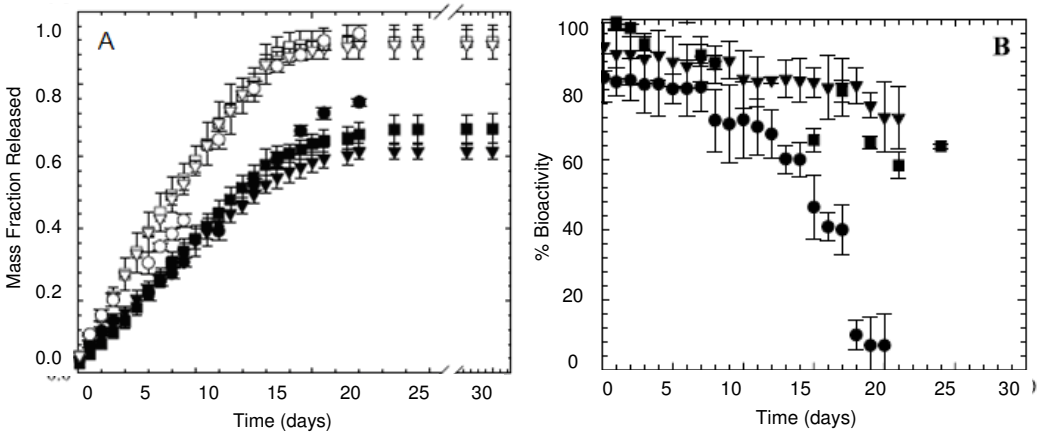

Figure 1-22. A) Release kinetics and B) percentage of bioactivity of vascular endothelial growth factor (VEGF; squares), interferon-γ (IFN- γ, triangles), and interleukin-2 (IL-2; circle) from elastomers by Ameer *et al.*

As can be seen from the above examples, biodegradable elastomers have been broadly investigated for biomedical applications and numerous advances have been made. However, there is still much room for improvement, such as maintaining the structural integrity upon degradation and controlled drug release responsive to the surrounding environment. Based on the requirements for scaffolds as soft tissue replacement, we designed completely amorphous, photocurable and biodegradable elastomers and explored their potential in tissue engineering. At the same time, we took advantage of the versatility of step growth polymerization and synthesized pH sensitive elastomers and further studied their applications as drug carrier systems.

1.3 Dissertation Organization

This dissertation is organized into five chapters.

1. The first chapter is the general introduction to biodegradable elastomers synthesis and application. In the first section, two major types of elastomers, biodegradable thermoplastic elastomers and biodegradable thermoset elastomers are discussed from various synthetic approaches with corresponding thermal and mechanical properties. In the second section, the applications of biodegradable elastomers are illustrated in the tissue engineering and drug delivery fields. This discussion is accompanied by fabrication methods and experimental results.
2. The second chapter describes the synthesis and characterization of new photocurable and biodegradable elastomers. The synthetic routes are explored and thermal, mechanical, surface and degradation properties as well as biocompatibility are studied.
3. The third chapter focuses on the *in vivo* study of the photocurable and biodegradable elastomers, including the mechanical change, surface morphology, and cell response.
4. The fourth chapter outlines the synthesis and characterization of amine functional biodegradable elastomers, fabrication of monodispersed particles and exploration of their applications as pH sensitive drug release carriers.
5. The fifth chapter summarizes and describes the future utility for this dissertation work. Each chapter is written in the style of a journal paper with its own supplemental materials.

1.4 Reference

1. Cordier, P.; Tournilhac, F.; Soulie-Ziakovic, C.; Leibler, L. *Nature* **2008**, 977-980.

2. Schweitzer, P. A. *Mechanical and Corrosion-resistant Properties of Plastics and Elastomers,* New York Marcel Dekker Inc., 2000.

3. Odian, G. *Principles of polymerization.* John Wiley & Sons, Inc.: Canada, 1981.

4. Hiki, S.; Miyamoto, M.; Kimura, Y. *Polymer* **2000***, 20,* 7369-7379.

5. Kissel, T.; Li, Y.; Unger, F. *Adv. Drug Delivery. Rev.* **2002***, 1,* 99-134.

6. Kim, J. H.; LEE, J. H. *Polymer J.* **2002**, 203-208.

7. Zhang, Z.; Grijpma, D. W.; Feijen, J. *J. Control. Release* **2006***, 2,* e29-e31.

8. Wanamaker, C. L.; O'Leary, L. E.; Lynd, N. A.; Hillmyer, M. A.; Tolman, W. B. *Biomacromolecules* **2007***, 11,* 3634-3640.

9. Kim, M. S.; Faust, R. *Polymer Bulletin* **2002***, 48,* 127-134.

10. Timbart, L.; Renard, E.; Langlois, V.; Guerin, P. *Macromolecular Bioscience* **2004***, 11,* 1014-1020.

11. Frick, E. M.; Hillmyer, M. A. *Macromol. Rapid Commu.* **2000***, 18,* 1317-1322.

12. Zini, E.; Scandola, M.; Dobrzynski, P.; Kasperczyk, J.; Bero, M. *Biomacromolecules* **2007***, 11,* 3661-3667.

13. Oprea, S.; Vlad, S.; Stanciu, A.; Ciobanu, C.; Macoveanu, M. *European Polymer J.* **1999***, 7,* 1269-1277.

14. Yeganeh, H.; Barikani, M.; Noei Khodabadi, F. *European Polymer J.* **2000***, 10,* 2207-2211.

15. Yeganeh, H.; Shamekhi, M. A. *Polymer* **2004***, 2,* 359-365.

16. Krijgsman, J.; Gaymans, R. J. *Polymer* **2004***, 2,* 437-446.

17. Tatai, L.; Moore, T. G.; Adhikari, R.; Malherbe, F.; Jayasekara, R.; Griffiths, I.; Gunatillake, P. A. *Biomaterials* **2007***, 36,* 5407-5417.

18. Kim, B. K.; Lee, J. C. *J. Polym. Sci. , Part A:Polym. Chem.* **1996***, 6,* 1095-1104.

19. Cohn, D.; Hotovely S.A. *Biomaterials* **2005***, 15,* 2297-2305.

20. Kozlowska, A.; Ukielski, R. *European Polymer J.* **2004***, 12,* 2767-2772.

21. Marcos-Fernández, A.; Abraham, G. A.; Valentín, J. L.; Román, J. S. *Polymer* **2006***, 3,* 785-798.

22. Guan, J.; Sacks, M. S.; Beckman, E. J.; Wagner, W. R. *J. Biomed. Mater. Res.* **2002***, 3,* 493-503.

23. Jiang, X.; Li, J.; Ding, M.; Tan, H.; Ling, Q.; Zhong, Y.; Fu, Q. *European Polymer J.* **2007***, 5,* 1838-1846.

24. Guan, J.; Sacks, M. S.; Beckman, E. J.; Wagner, W. R. *Biomaterials* **2004***, 1,* 85-96.

25. Wang, Y.D.; Ameer, G.A.; Sheppard, B.J.; Langer, R. *Nat. biotechnol.* **2002**, 602-606.

26. Yang, J.; Webb, A. R.; Pickerill, S. J.; Hageman, G.; Ameer, G. A. *Biomaterials* **2006***, 9,* 1889-1898.

27. Anderson, D. G.; Tweedie, C. A.; Hossain, N.; Navarro, S. M.; Brey, D. M.; Vliet, K. J.; Langer, R.; Burdick, J. A. *adv. mater.* **2006**, 2614-2618.

28. Helminen, A. O.; Korhonen, H.; Seppälä, J. V. *Macromol. Chem. Phys.* **2002***, 18,* 2630-2639.

29. Ding, T.; Liu, Q.; Shi, R.; Tian, M.; Yang, J.; Zhang, L. *Polym Degrad Stab* **2006***, 4,* 733-739.

30. Amsden, B. *Soft Matter* **2007**, 1335-1348.

31. Kamber, N. E.; Jeong, W.; Waymouth, R. M. *Chem. Rev.* **2007**, 5813.

32. Dechy-Cabaret, O.; Martin-Vaca, B.; Bourissou, D. *Chem. Rev.* **2004**, 6147-6176.

33. Nakayama, A.; Kawasaki, N.; Arvanitoyannis, I.; Iyoda, J.; Yamamoto, N. *Polymer* **1995***, 6,* 1295-1301.

34. Pitt, C. G.; Hendren, R. W.; Schindler, A.; Woodward, S. C. *J. Control. Release* **1984**, 3-14.

35. Lendlein, A.; Neuenschwander, P.; Ulrich W. Suter, U. W. *Macromol. Chem. Phys.* **2000**, 1067-1076.

36. Storey, R. F.; Warren, S. C.; Allison, C. J.; Puckett, A. D. *Polymer* **1997***, 26,* 6295-6301.

37. Palmgren, R.; Karlsson, S.; Albertsson, A. *J. Polymer Sci. Part A: Polymer Chem.* **1996**, 1635-1649.

38. Amsden, B. G.; Misra, G.; Gu, F.; Younes, H. M. *Biomacromolecules* **2004***, 6,* 2479-2486.

39. Gu,F.; Neufeld, R.; Amsden, B. . *Pharm. Res* **2006**, 23, 782-789.

40. Younes, H. M.; Bravo-Grimaldo, E.; Amsden, B. G. B. G. *Biomaterials* **2004***, 22,* 5261-5269.

41. Yang, J.; Webb, A. R.; Ameer, G. A. *Adv. Mater.* **2004**, 511.

42. Nijst, C. L. E.; Bruggeman, J. P.; Karp, J. M.; Ferreira, L.; Zumbuehl, A.; Bettinger, C. J.; Langer, R. *Biomacromolecules* **2007***, 10,* 3067-3073.

43. Albertsson, A.; Varma, I. K. *Adv. Polym. Sci* **2002**, 1-40.

44. Okada, M. *Prog. Polymer Sci.* **2002**, 87-133.

45. Kiyotsukuri, T.; Kanaboshi, M.; Tsutsumi, N. *Polym. Int.* **1994**, 1-8.

46. Olson, D. A.; Gratton, S. E. A.; DeSimone, J. M.; Sheares, V. V. *J. Am. Chem. Soc.* **2006***, 41,* 13625-13633.

47. John, G.; Morita, M. *Macromolecules* **1999***, 6,* 1853-1858.

48. Storey, R. F.; Warren, S. C.; Allison, C. J.; Wiggins, J. S.; Puckett, A. D. *Polymer* **1993***, 20,* 4365-4372.

49. Davis, K. A.; Burdick, J. A.; Anseth, K. S. *Biomaterials* **2003***, 14,* 2485-2495.

50. Shen, J. Y.; Pan, X. Y.; Lim, C. H.; Chan-Park, M. B.; Zhu, X.; Beuerman, R. W. *Biomacromolecules* **2007***, 2,* 376-385.

51. Nagata, M.; Sato, Y. *Polymer* **2004***, 1,* 87-93.

52. Nagata, M.; Kitazima, I. *Colloid & Polymer Sci.* **2006**, 380-386.

53. Yang, J.; Motlagh, D.; Allen, J. B.; Webb, A. R.; Kibbe, M. R.; Aalami, O.; Kapadia, M.; Carroll, T. J.; Ameer, G. A. *Adv. Mater.* **2006***, 12,* 1493-1498.

54. Ruane, P. H. US Patent 20070196423, Aug, 2007.

55. Yang, J.; Webb, A. R.; Ameer, G. A. *Tissue Eng.* **2005**, 1876-1885.

56. Motlagh, D.; Yang, J.; Lui, K. Y.; Webb, A. R.; Ameer, G. A. *Biomaterials* **2006***, 24,* 4315-4324.

57. Yang, S.; Leong, K.; Du, Z.; Chua, C. *Tissue Eng.* **2002**, 1-11.

58. Liu, T. V.; Bhatia, S. N. *Adv. Drug Delivery. Rev.* **2004***, 11,* 1635-1647.

59. Sales, V. L.; Engelmayr, G. C.; Johnson, J. A.; Gao, J.; Wang, Y.; Sacks, M. S.; Mayer, J. E. *Circulation* **2007***, 116,*55-63.

60. Webb, A. R.; Kumar, V. A.; Ameer, G. A. *J. Mater. Chem.* **2007***, 9,* 900-906.

61. Neeley, W. L.; Redenti, S.; Klassen, H.; Tao, S.; Desai, T.; Young, M. J.; Langer, R. *Biomaterials* **2008***, 4,* 418-426.

62. Chen, Q.; Bismarck, A.; Hansen, U.; Junaid, S.; Tran, M. Q.; Harding, S. E.; Ali, N. N.; Boccaccini, A. R. *Biomaterials* **2008***, 1,* 47-57.

63. Sundback, C. A.; Shyu, J. Y.; Wang, Y.; Faquin, W. C.; Langer, R. S.; Vacanti, J. P.; Hadlock, T. A. *Biomaterials* **2005***, 27,* 5454-5464.

64. Gao, J.; Crapo, P. M.; Wang, Y. *Tissue Eng.* **2006**, 917-925.

65. Gao, J.; Ensley, A. E.; Nerem, R. M.; Wang, Y. *J. Biomed. Mater. Res. Part A* **2007***, 4,* 1070-1075.

66. Bettinger, C. J.; Orrick, B.; Misra, A.; Langer, R.; Borenstein, J. T. *Biomaterials* **2006***, 12,* 2558-2565.

67. Leclerc, E.; Furukawa, K. S.; Miyata, F.; Sakai, Y.; Ushida, T.; Fujii, T. *Biomaterials* **2004***, 19,* 4683-4690.

68. Weigle, T.; Schinkel, G.; Lendlein, A. *Expert Rev. Med. Devices* **2006***, 3,* 835-851.

69. Pego, A. P.; Siebum, B.; Poot, A. A.; Grijpma, D. W.; Feijen, J. *Tissue Eng.* **2003***, 9,* 981.

70. Guan, J.; Fujimoto, K. L.; Sacks, M. S.; Wagner, W. R. *Biomaterials* **2005***, 26,* 3961-3971.

71. Sarkar, S.; Lee, G. Y.; Wong, J. Y.; Desai, T. A. *Biomaterials* **2006***, 27,* 4775-4782.

72. Radisic, M.; Park, H.; Chen, F.; Salazer-Lazzaro, J.; Wang, Y.; Dennis, R.; Langer, R.; Freed, L.; Vunjak-Novakovic, G. *Tissue Eng.* **2006**, 2077.

73. Thakar, R. G.; Ho, F.; Huang, N. F.; Liepmann, D.; Li, S. *Biochemical and Biophysical Research Communications* **2003***, 4,* 883-890.

74. Sarkar, S.; Dadhania, M.; Rourke, P.; Desai, T. A.; Wong, J. Y. *Acta Biomaterialia* **2005***, 1,* 93-100.

75. Mulder, M. M.; Hitchcock, R. W.; Tresco, P. A. *J. . Biomater. Sci. – Polym. Ed.* **1998***, 9,* 731.

76. Sodian, R.; Loebe, M.; Hetzer, R. *ASAIO J.* **2002***, 48,* 12-16.

77. Sodian, R.; Sperling, J. S.; Vacanti, J. P. *Tissue Eng.* **2000***, 6,* 183.

78. Lieshout, M. V.; Peters, G.; Rutten, M.; Baaijens, F. *Tissue Eng.* **2006***, 12,* 481.

79. Wada, R.; Hyon, S.; Nakamura, T.; andIkada, Y. *Pharm. Res.* **1991**, 1292-1296.

80. Guan, J.; Stankus, J. J.; Wagner, W. R. *J. Control. Release* **2007***, 1-2,* 70-78.

81. Dahiyat, B. I.; Posadas, E. M.; Iirosue, S.; Hostin, E.; Leong, K. W. *Reactive Polymers* **1995**, 101-109.

82. Malcolm, R. K.; McCullagh, S. D.; Woolfson, A. D.; Gorman, S. P.; Jones, D. S.; Cuddy, J. *J. Control. Release* **2004***, 2,* 313-320.

83. Woolfson, A. D.; Malcolm, R. K.; Gallagher, R. J. *J. Control. Release* **2003***, 3,* 465-476.

84. Malcolm, K.; Woolfson, D.; Russell, J.; Tallon, P.; McAuley, L.; Craig, D. *J. Control. Release* **2003***, 2,* 217-225.

85. Cussler, E. L. *J. Control. Release* **2003***, 3,* 399-320.

86. Gu, F.; Neufeld, R.; Amsden, B. *J. Control. Release* **2007***, 1,* 80-89.

87. Gu, F.; Younes, H. M.; El-Kadi, A. O. S.; Neufeld, R. J.; Amsden, B. G. *J. Control. Release* **2005***, 3,* 607-617.

CHAPTER 2

SYNTHESIS AND CHARACTERIZATION OF NEW PHOTOCURABLE AND BIODEGRADABLE ELASTOMERS

2.1 Introduction

Biodegradable elastomers have attracted a great deal of interest in recent years due to their potential applications in the biomedical field as scaffolds for tissue engineering[1-5]or drug delivery carriers[6-11]. Biodegradable elastomers resemble soft tissues in that they can readily recover from relatively large deformations while maintaining their proper function without mechanical irritation to the surrounding tissues.[12]

There are two classes of elastomers: thermoplastic elastomers[13-15] and thermoset elastomers.[5,12] Thermoplastic elastomers can be prepared from melt or solvent processings, and their elasticity comes from the phase separation of crystalline and amorphous regions. The two regions hydrolyze at different rates, and as such, the elastomers degrade heterogeneously resulting in a nonlinear loss of strength. Completely amorphous thermoset elastomer materials degrade more homogenously with a more linear degradation of physical properties.[16-17] Because of these differences, our interest is in the preparation of amorphous thermoset elastomers, since it is desired that the scaffolds maintain their structural integrity before the newly formed tissue reaches its fully functioning capacity.

There are two methods to prepare thermoset elastomers: thermal crosslinking and photocrosslinking. Thermal crosslinking conditions normally require high temperatures (90-130 ºC) and long fabrication times (24 h to several days).[12,18-19] Photocrosslinking methods have several advantages which include 1) production of elastomers in several minutes at room temperature, allowing for the loading of thermosensitive drugs or proteins,[20] 2) fabrication of elastomers with better spatial and temporal control,[21-23] 3) the

tuning of mechanical properties and degradation by controlling the crosslinking density and the composition.

To date, most of the photocured amorphous elastomers have been made from the copolymers of caprolactone with lactide and/or glycolide.[17, 24-25] Star prepolymers[26-27] (G = 0.59-5.3 MPa) and linear prepolymers[28] (G = 1.66-12.3 MPa) have been synthesized from these starting materials. These elastomers, prepared using ring-opening polymerization, presented several challenges. For example, there was a limited number of cyclic monomers suitable for this method. In addition, the ratio of monomers in the copolymers had to be precisely controlled to ensure the prepolymers were amorphous.[29] Finally, polycaprolactone took months to years under physiological conditions to degrade. These polymers had 3-6% weight loss in phosphate buffered saline (PBS) after 4 weeks degradation.[27-28]

An alternative to ring-opening polymerization for the fabrication of biodegradable thermoset elastomers is polycondensation polymerization. By this method, a wide variety of monomers can be easily incorporated, allowing for the expansion of the elastomer properties. Langer recently reported the synthesis of a photocurable poly(glycerol-*co*-sebacate) from polycondensation polymerization from multifunctional monomers.[30] The Young's modulus of the elastomers ranged from 0.05-1.38 MPa with degrees of acrylation ranging from 17-54%. A low degree of acrylation (17%) resulted in soft materials having high sol content (42%). This may be unfavorable for *in situ* polymerization as unreacted methacrylate functionalized macromers could diffuse into the surrounding tissues. In addition, the multifunctional approach suffers from the inability to vary properties by controlling the crosslinking chemistry. As such, it is more

desirable to have photocurable, biodegradable elastomers which can be prepared from polycondensation polymerization with high degrees of acrylation and better control of the polymer structures.

Our lab has successfully synthesized a series of completely amorphous linear prepolymer liquids from hydromuconic acid and ethylene glycol oligomers.[31,32] These amorphous prepolymers were prepared from facile polycondensation polymerization techniques, which can precisely control the composition of the resulting prepolymers and hence the network structure of the resulting elastomers. These elastomers were obtained by using thermal crosslinking conditions. Here, we expanded the scope of these materials to develop new linear amorphous prepolymers functionalized with photocurable groups. After UV irradiation, the fabricated elastomers present a wider mechanical property range and a faster degradation rate than the current available photocrosslinked amorphous elastomers. Because the prepolymers are liquid, they can be easily fabricated or molded into a wide array of devices and shapes.

2.2 Experimental

Materials. All chemicals were purchased from Sigma-Aldrich unless otherwise noted. 2,2-Diethoxyacetophenone (DEAP) was purchased from Acros. Poly(lactic-glycolic acid) (PLGA) was purchased from Boehringer Ingelheim with relative molecular mass 15,000. Adipic acid (AA) was recrystallized from distilled water prior to use. Diethylene glycol (DEG) was dried overnight over calcium hydride and distilled.

Preparation of hydroxyl endcapped poly(diethylene glycol adipate). A 50 mL round-bottom flask was charged with the calculated amount of adipic acid and diethylene

glycol. The contents of the flask were placed under a nitrogen atmosphere. The mixture was stirred at 130 ºC using magnetic stirring until a homogeneous melt was formed. Stannous 2-ethylhexanoate (1.0 mol %) was added to the melt. The mixture was stirred for 1 h, and the pressure was reduced to 20 mmHg. The reaction was allowed to proceed at 20 mmHg for 23 h, for a total reaction time of 24 h. Polymerization was terminated by precipitating the polymer into cold methanol (-78 ºC).

Preparation of methacrylate endcapped poly(diethylene glycol adipate). A 25 mL round-bottom flask was charged with 3 g of hydroxyl endcapped prepolymer. The flask was sealed, flame-dried, and purged with nitrogen. This procedure was repeated 3 times. Under the flow of nitrogen and stirring, 15 mL of fleshly distilled methylene chloride and triethylamine (4.2 mole equiv) were injected into the flask. The flask was cooled to 0 ºC using an ice-water bath. Methacryloyl chloride (4.2 mole equiv) was added dropwise into the flask. The reaction proceeded overnight and was terminated by washing with 1 N hydrochloric acid twice, sodium bicarbonate solution (3%) twice, distilled water once and saturated sodium chloride solution once. The collected fraction was dried over magnesium sulfate. Magnesium sulfate was removed by filtration, and the solvent was removed under reduced pressure. The residue was precipitated in cold methanol (-78 ºC).

Preparation of hydroxyl endcapped poly(tetraethylene glycol adipate) and preparation of methacrylate endcapped poly (tetraethylene glycol adipate). The procedures were the same as above.

Elastomer fabrication. Elastomer films (50 mm x 15 mm x 0.5 mm) were prepared by spreading a mixture of the liquid prepolymer (0.25 g) and photoinitiator (DEAP) (0.1-5 wt %) on a glass mold. The mixture was put inside of a UV oven chamber

(ECL-500), purged with N_2 for 10 min, and subjected to 30 mW/cm^2 UV irradiation (365 nm) for the prescribed time (1-10 min).

Porous scaffold fabrication. To the mixture of methacrylated prepolymer and photoinitiator (DEAP), three weight equiv of sodium chloride (90-150 μm) was added. The mixture was then transferred to a 20 mm x 20 mm square mold and subjected to UV exposure as above. After the radiation, the mold was immersed in distilled water for 24 h and was peeled from the mold while in water. The distilled water was changed every 24 h for 4 days. After drying in a fume hood for several days, the photographs of the prepared scaffolds were taken.

Bilayer scaffold fabrication. For the nonporous phase, a glass rod (~ 5 mm in diameter) was coated with mixture of prepolymer and photoinitiator. The rod was subjected to UV exposure for 2 min without N_2 purge. After the irradiation, the glass rod was coated with the mixture of salt, prepolymer and photoinitiator. The glass rod was put inside the UV oven again, purged with N_2 for 10 min, and subjected to irradiation for 10 min. The cured bilayer scaffold was slowly removed from the glass rod after immersion in distilled water for half an hour. The pores were produced after leaching away the salt in distilled water for 4 days with water changed every day. After drying in a fume hood for several days, the photographs of the prepared scaffolds were taken. The cross section image of the scaffold was taken by SEM.

2.3 Characterization

^{1}H NMR spectra were acquired in deuterated chloroform on a Bruker 400 AVANCE. A Waters Gel Permeation Chromatography (GPC) system was used to

measure polymer molecular weights relative to polystyrene standards. The measurements were taken at 40 ºC with THF as the mobile phase in four columns. Fourier transform infrared spectroscopy (FTIR) spectra were acquired on a PerkinElmer Spectrum BX. Thermogravimetric analysis (TGA) was performed using a Perkin-Elmer thermogravimetric analyzer with a heating rate of 10 ºC/min in a N_2 atmosphere. Glass transition temperatures and melting points were measured on a Seiko 220C differential scanning calorimeter (DSC) using the second heat at a heating rate of 10 ºC/min. Water-in-air contact angles were measured at room temperature using a KSV instrument and imaging system using the sessile drop method. Four independent measurements at different sites were averaged. The contact angle was monitored with time from 0 to 5 min. Scanning electron microscopy (SEM) was performed on a Hitachi S-4700 SEM.

Sol content analysis was conducted by swelling a 0.15 g elastomer film in methylene chloride for 24 h at 25 ºC. The solvent was removed and the percent soluble fraction (Q_s) was determined according to the following equation,

$$Q_s = 100 \times (m_i - m_f) / m_i$$

where m_i and m_f represent the initial and final masses. Each measurement was performed on three separate samples. The value was reported as the average of the three measurements.

***In vitro* degradation studies and mechanical property measurements.** Dumb bell shaped elastomer samples were immersed in 20 mL of phosphate buffered saline (PBS) (pH 7.4 and 37 ºC) in a 20 mL scintillation vial. At each sampling time point, the elastomers were removed, blotted dry, and measured. The slabs were then subjected to a tensile measurement while hydrated. The mechanical data were collected on an Instron

5566 at a crosshead speed of 10 mm/min at 25 ºC. The Young's modulus (G) was calculated using the initial linear portion of the stress/strain curve (0-5% of strain). The pieces from the tensile measurement were collected and dried under mild heat in a vacuum oven for 24 h. The dried mass was then measured. All measurements were made in triplicate.

***In vitro* biocompatibility.** An NIH 3T3 fibroblast cell line was used. Glass Petri dishes (60 mm diameter) were soaked in ethanol overnight, wiped dry, etched with HF solution (5%) for 1 min, rinsed with distilled water and wiped dry. To the dish was added 2 mL of methylene chloride solution of the prepolymer (1%) with 1 wt% of DEAP. The dishes were transferred into a UV chamber after evaporation of the solvent in air. The elastomer was formed after 10 min N_2 purge and 2 min UV irradiation of the prepolymer mixture. The control used for this study was the dish covered by PLGA (1 wt% in CH_2Cl_2, solvent evaporated for 24 h in air and sterilization by UV radiation for 15 min). The dishes were rinsed with sterile water and PBS 3 times and incubated at 37 ºC for 2 h in cell growth medium (Eagle minimal essential medium (EMEM) + 10 v/v% fetal bovine serum (FBS) + penicillin (100 IU/mL) + streptomycin (100 μg/mL)) to remove any residuals. Each dish was seeded with fibroblast cells and 5 mL of growth medium. The cells were incubated at 37 ºC with 5% CO_2. The morphology of attached cells was observed after 24 h incubation and recorded with an inverted microscope (Zeiss Axiovert 200) equipped with a Dage 240 digital camera.

2.4 Results and discussion

2.4.1 Synthesis and characterization of liquid prepolymer

A series of polyesters made from the polycondensation polymerization of adipic acid and ethylene glycol dimers (DEG) or tetramers (TEG) are shown in Figure 2-1. By controlling the feed ratio of the two monomers, hydroxyl endcapped prepolymers with number average molecular weights from 1 x 10^3 g/mol to 7 x 10^3 g/mol were easily prepared. The methacrylate endcapped prepolymers were achieved by using methacryloyl chloride to react with the endcapped hydroxyl groups. The glass transition temperatures for the methacrylate functionalized prepolymers were near -50 ^oC, while the glass transition temperatures for photocured elastomers were -59 ^oC to -31 ^oC with the EG oligomer length and molecular weight not having a significant effect on the thermal properties (Table 2-1).

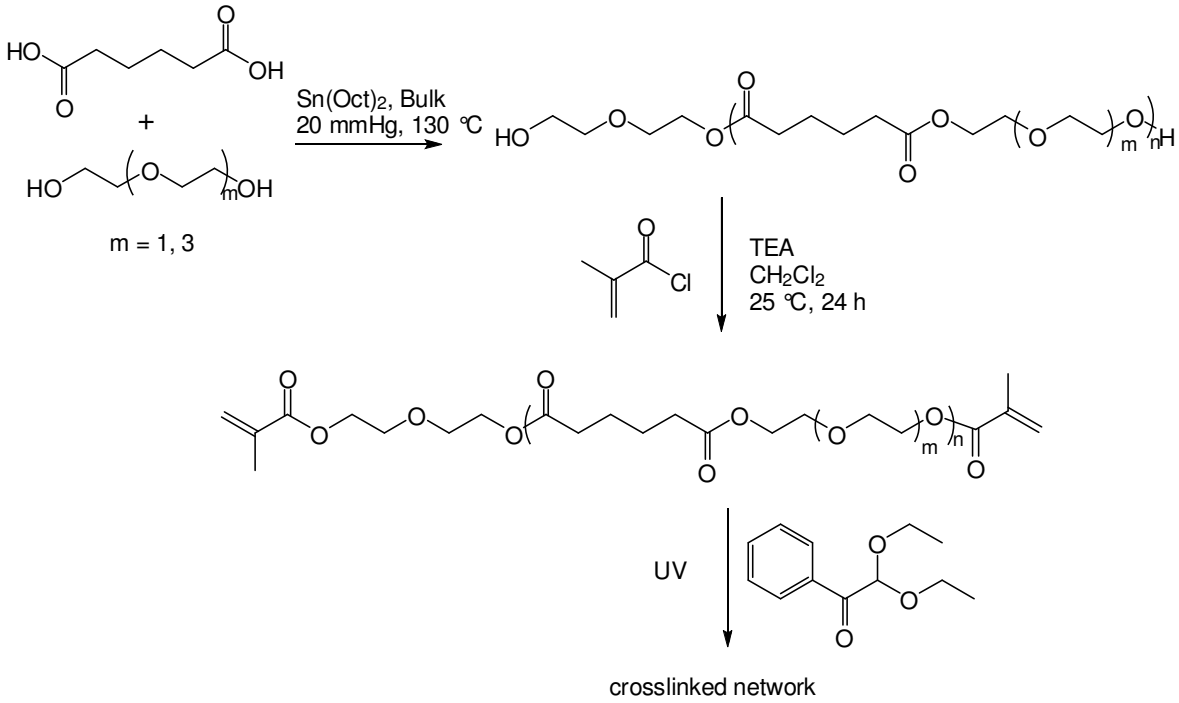

Figure 2-1. Synthesis of photocurable polyester dimethacrylate and elastomer formation

Table 2-1. Characterization of the prepolymer liquids and prepared elastomers

Sample	‹M_n› x 10^{-3} g/mol[a]	PDI[a]	Degree of acrylation[b]	Elastomer sol content (%)[c]	T_g prepolymer (°C)[d]	T_g elastomer (°C)[d]
DEG-1K	1.2	1.9	85	1.7	-42.0	-36.5
DEG-2K	2.3	1.5	80	7.9	-55.3	-48.8
DEG-4K	4.1	1.4	94	16.3	-51.7	-58.9
DEG-7K	6.9	1.4	80	14.5	-42.1	-45.6
TEG-1K	1.1	1.8	83	1.4	-31.3	-42.6
TEG-2K	2.1	1.6	81	2.6	-53.0	-59.2
TEG-4K	4.3	1.4	86	13.3	-49.9	-54.5
TEG-7K	7.2	1.4	87	14.5	-46.3	-45.5

[a] Determined by GPC; [b] Determined by ^{1}H NMR ; [c] Extracted in methylene chloride for 24 h at 25 °C;

[d] Determined by DSC, second heat, 10 °C/min

Figure 2-2 shows the ^{1}H NMR spectra of a representative hydroxyl endcapped prepolymer (A) and a methacrylate endcapped prepolymer (B) (DEG-4K), with all the peaks assigned.[27] The methacrylation of the end termini of the prepolymer was confirmed by the spectrum. ^{1}H NMR of the methacrylate group endcapped prepolymer (B) clearly showed peaks at δ = 5.52 and 6.1 ppm, corresponding to the vinyl protons of the methacrylate group, and δ = 1.9 ppm corresponding to the methyl protons of the methacrylate group. The removal of unreacted methacryloyl chloride in the final prepolymer was confirmed by the absence of peaks at δ = 6.59, 6.25 and 2.43 ppm corresponding to the vinyl and methyl protons of methacryloyl chloride. The degree of methacrylation was consistent in most methacrylate endcapped prepolymers, and ranged from 80% to 90%, as calculated according to the literature from the integration ratio of peaks at M and N (Figure 2-2 (B)).[26,33] Finally, methacrylation did not significantly alter the molecular weight or polydispersity of the prepolymers, which can be seen clearly by the GPC chromatograms of the hydroxyl endcapped prepolymer and methacrylate endcapped prepolymer in Figure 2-3.

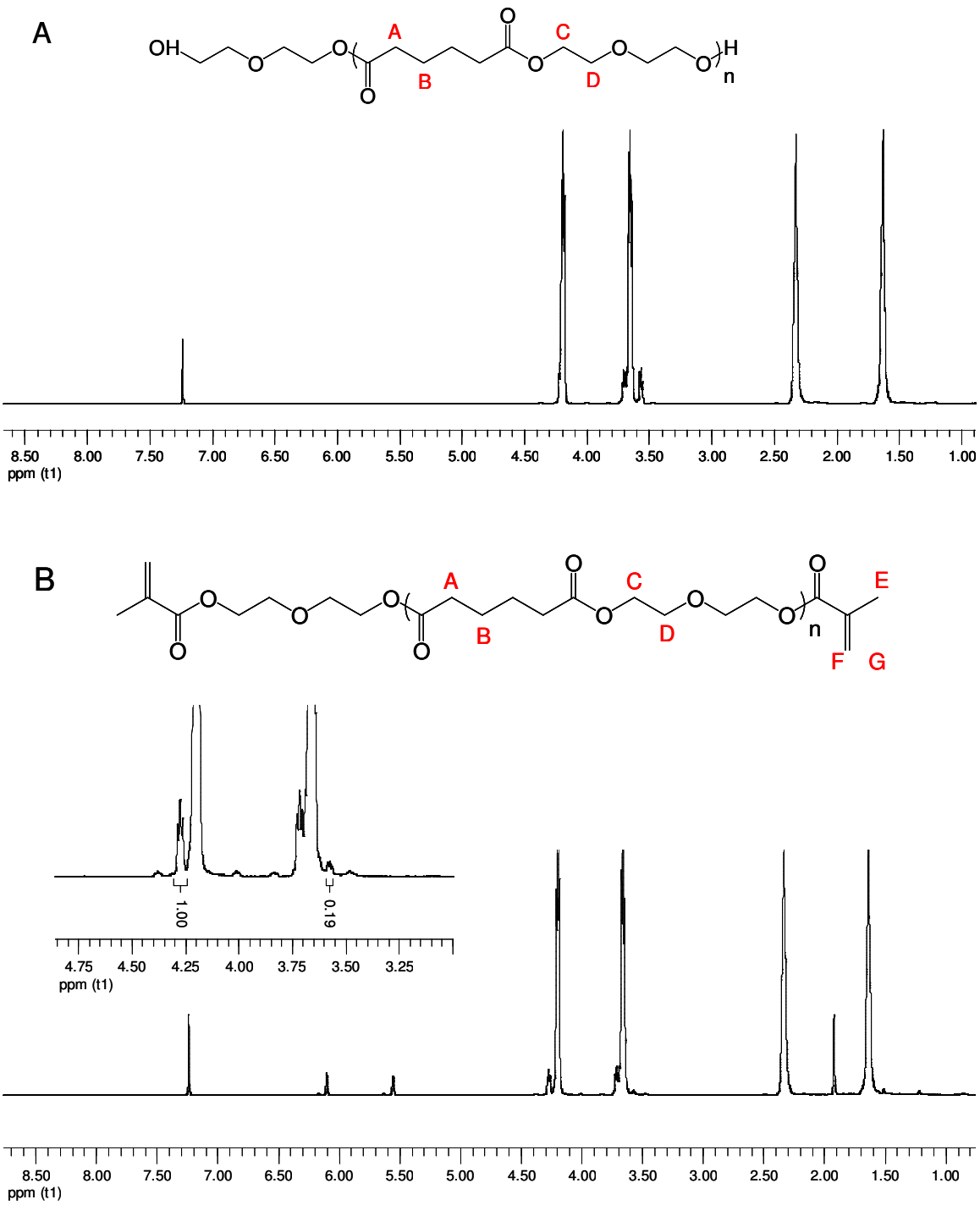

Figure 2-2. A) ^{1}H NMR spectra of a hydroxyl endcapped prepolymer, B) a methacrylate endcapped prepolymer

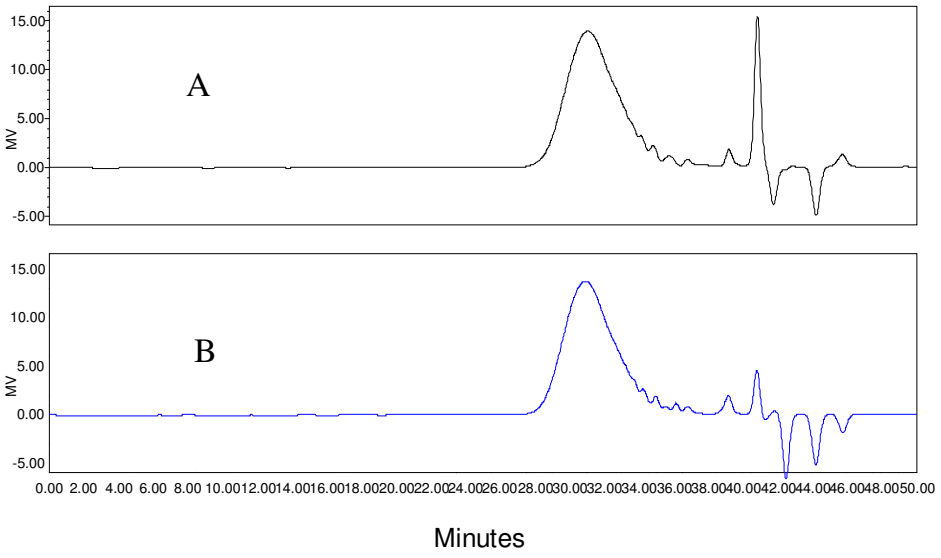

Figure 2-3. GPC chromatograms of A) a hydroxyl endcapped prepolymer and B) a methacrylate endcapped prepolymer (DEG-7K)

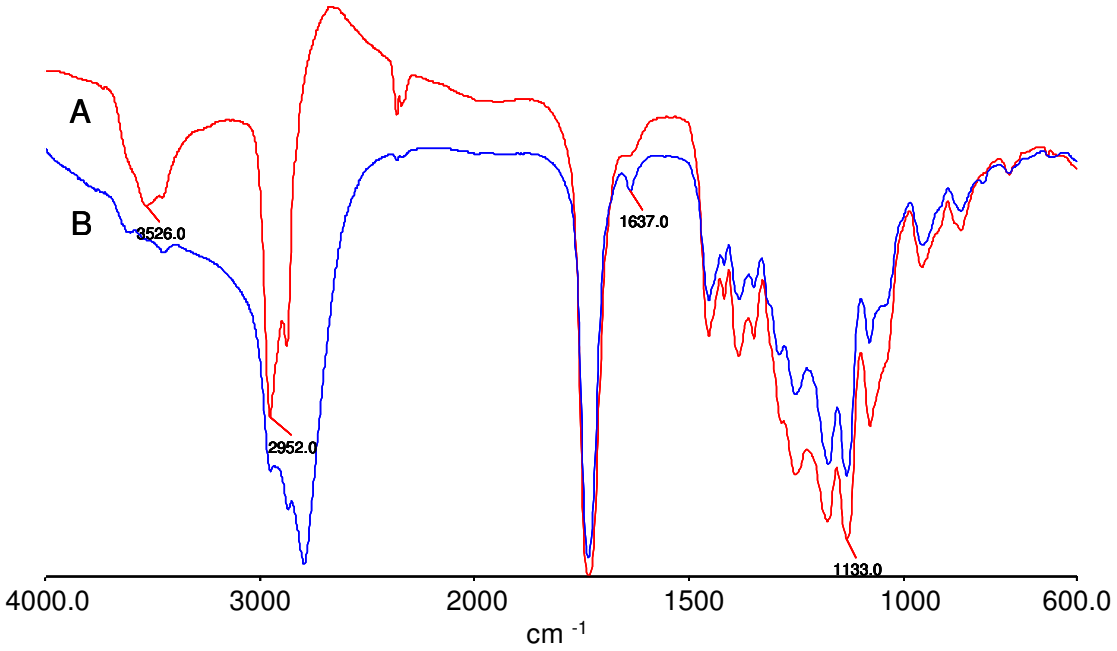

Figure 2-4. FTIR spectra of A) a hydroxyl endcapped prepolymer and B) a methacrylate endcapped prepolymer (DEG-4K)

The FTIR spectra of hydroxyl endcapped prepolymer (A) and methacrylate endcapped prepolymer (B) are shown in Figure 2-4. The FTIR spectrum of (A) showed an absorption band at 3526 cm^{-1} due to the terminal hydroxyl group. This band almost disappeared in (B) due to methacrylation. The bands at 2952 cm^{-1} and 1133 cm^{-1} were attributed to the C-H stretch and ether stretch, respectively, and were present in both polymers. The peak at 1637 cm^{-1} in (B) was ascribed to the vinyl group signals due to the methacrylate functionality.[29]

2.4.2 Characterization of photocured elastomers

The methacrylate endcapped prepolymers were crosslinked using 365 nm UV radiation and 2,2-diethoxyacetophenone (DEAP) as the photoinitiator. The crosslinking conditions were optimized with regard to UV exposure time and photoinitiator concentration. The representative methacrylate endcapped prepolymer used here was DEG-2K. In one set of experiments, the photoinitiator concentration was kept at 1 wt% while UV radiation times were changed from 1 min to 10 min. The prepared elastomers were weighed, immersed into 20 mL of methylene chloride overnight at 25 ^{o}C, dried under vacuum and reweighed. The sol content was determined from the weight loss, and its relationship to exposure time is shown in Figure 2-5 (A). After 1 min exposure, the sol content in all of the elastomers was consistently near 8%. This indicated that photocuring is a fast process and that 1 min exposure is sufficient to fully cure the elastomers. Figure 2-5 (B) illustrates the effect of the photoinitiator concentration to the sol content, with the exposure time kept at 1 min. At 0.1 wt% photoinitiator, the sol

content of the elastomer was already minimized. Therefore, the optimized crosslinking conditions were 0.1 wt% photoinitiator and 1 min UV exposure time, suitable for the incorporation of sensitive drugs or proteins, such as vascular endothelial growth factor.[9,10]

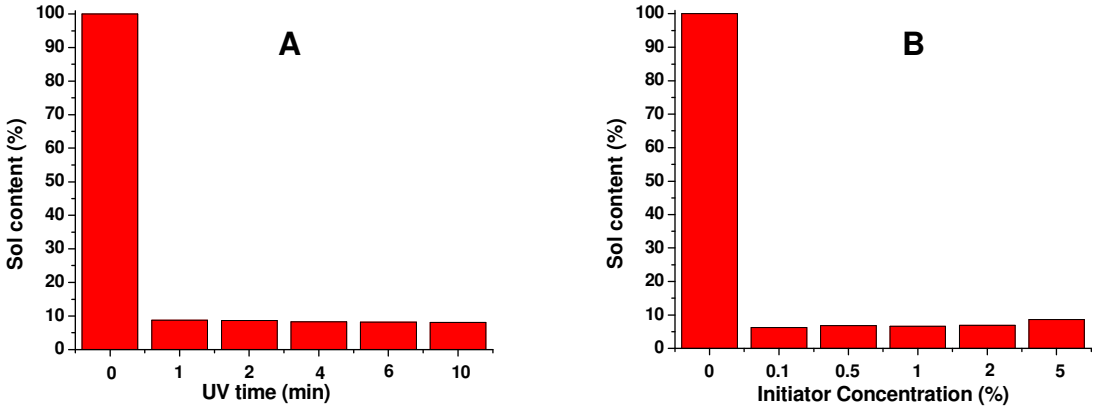

Figure 2-5. Sol content values versus A) exposure time and B) photoinitiator concentration

To be desirable as scaffolds in tissue engineering, a combination of properties is necessary that include suitable strength, biodegradability, surface hydrophilicity, nontoxicity. In the following text, the mechanical, degradation, surface properties and biocompatibility of our elastomers are discussed.

The mechanical properties of the fabricated elastomers were examined first. Dumb bell shaped samples were mounted for stress-strain test in triplicate. We studied the influences of different ethylene oxide oligomers and prepolymers of different molecular weight on the mechanical properties. Figure 2-6 (A) shows typical stress-strain

curves of the elastomers. As can be seen from Figure 2-6 (B), the mechanical properties of the DEG and TEG based elastomers followed similar trends as the prepolymer molecular weights increased. Elastomers made from prepolymers of lower molecular weight presented higher Young's modulus and shorter extension. While prepolymers of higher molecular weight led to the elastomers with lower Young's modulus and longer extension. Since the elastomers are a crosslinked network, the crosslinking density depends on the density of available photocurable groups (methacrylate groups). For prepolymers with lower molecular weights, the density of methacrylate groups is higher than the density of methacrylate groups in prepolymers of higher molecular weight. As such, prepolymers of lower molecular weight lead to stronger elastomers. Overall, Young's modulus ranged from 0.12-10.3 MPa for elastomers made from prepolymers of molecular weights ranging from 1K to 7K. It is in the mechanical range for some soft tissues inside of the body, such as the knee articular cartilage (G = 2.1-11.8 MPa), and the cerebral vein (G = 6.85 MPa). There are only a few photocurable elastomers in the literature that show this wide mechanical property range.[16,30]

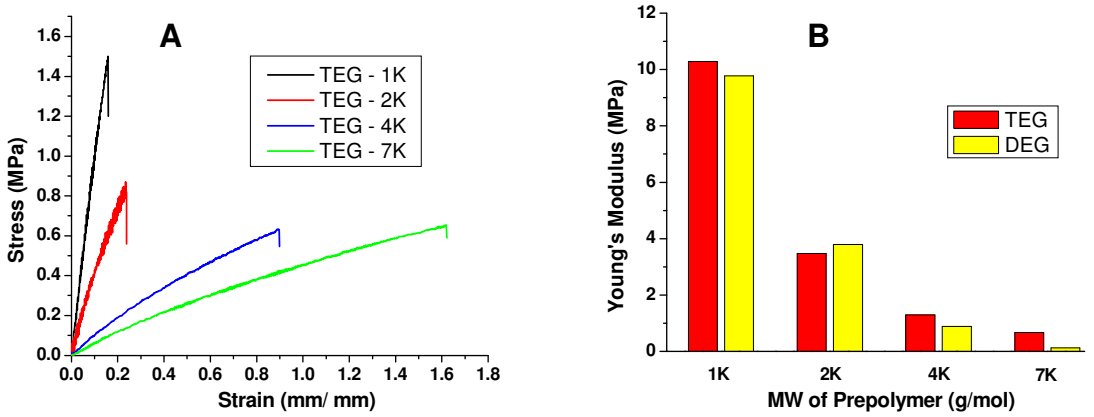

Figure 2-6. A) Typical stress-strain curves of the elastomers, B) Young's modulus of elastomers versus prepolymer molecular weight

Next, we studied the degradation properties of the photocured elastomers. *In vitro* mass loss of elastomers in PBS over 5 weeks was measured (Figure 2-7). Both sets of elastomers prepared from diethylene glycol and tetraethylene glycol with molecular weights ranging from 1K to 7 K were used. During week one, the elastomers degraded at a rather fast rate with the highest loss of approximately 10% of its original weight, seen for the TEG-7K sample. In the following weeks, the elastomers presented stable degrading profiles. At 5 weeks, the fastest degradation was seen in the DEG-7K sample with 16% of its original weight lost. Also, the degradation rate changed slightly with the molecular weights of the prepolymers. Elastomers fabricated from higher molecular weight prepolymers (such as 7K) degraded faster than the elastomers prepared from lower molecular weight prepolymers (such as 1K). This can be explained in the same manner as above. The former has less photocurable density in the elastomer, so the network is not as tight as the later. It is easy for water molecules to enter the network and increase the exposure of the elastomer with the medium. At the same time, it is also easy for the degraded products to diffuse out of the matrix.[27]

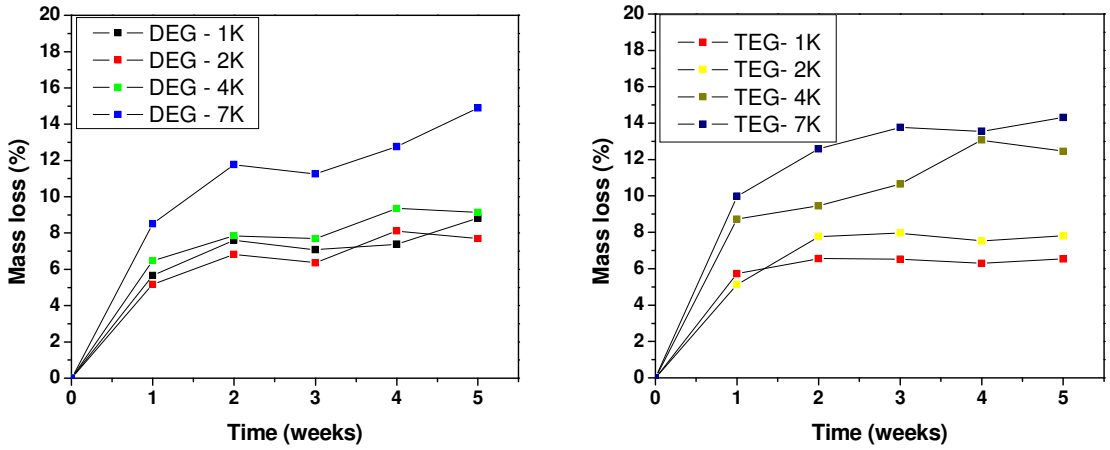

Figure 2-7. Percentage of weight loss of DEG and TEG based elastomers with different molecular weights during *in vitro* degradation in PBS (pH 7.4) at 37 ºC

When a scaffold is used to support cell growth, it is expected that the scaffold will maintain sufficient strength before the formed tissues can fully function. Since the materials are degrading during the application, it is important to know the influence of degradation on the mechanical properties. Figure 2-8 shows the change of Young's modulus as the degradation progressed in PBS. Elastomers made from DEG and TEG prepolymers with different molecular weights were investigated for 5 weeks. After each week, three samples from each group were taken out, blotted dry, and mounted for Instron tension testing. Both sets of elastomers showed similar trends for the change of Young's modulus, decreasing as the degradation proceeded. When further examined, the percentage of Young's modulus loss after 5 weeks of degradation versus the molecular weight of prepolymers showed an interesting trend (Figure 2-8 (C)), which can be explained by the balance of diffusion and auto-catalysis effects. For elastomers made from prepolymers of low molecular weight (such as 1K), the crosslinking density is high, making it difficult for water molecules to penetrate into the matrix and slowing degradation. At the same time, the degraded acidic by-products have difficulty diffusing out of the network, causing an auto-catalysis effect. In this case, the auto-catalysis is dominant, leading to an accelerated degradation and increased chain scission with significant Young's modulus loss of 40%. For elastomers made from prepolymers of high molecular weight (7K), the crosslinking density is low and the network is loose. As such, water molecules can easily enter the network and the degradation products easily diffuse out of the network. The loss of Young's modulus after 5 weeks immersion in PBS is similar to the elastomers made from 1K molecular weight prepolymers, also about 40%.

Here, the diffusion is clearly dominant. Elastomers made from prepolymers with a molecular weight of 2K allowed for limited exposure of the network to penetrating water molecules and for degraded acidic by-products to diffuse out of the network, cancelling the auto-catalysis effect. Balanced by these two main factors, the loss of Young's modulus was the smallest seen at only 6% after 5 weeks of degradation. This is one of the first reports of this trend of Young's modulus loss versus the molecular weights of prepolymers.

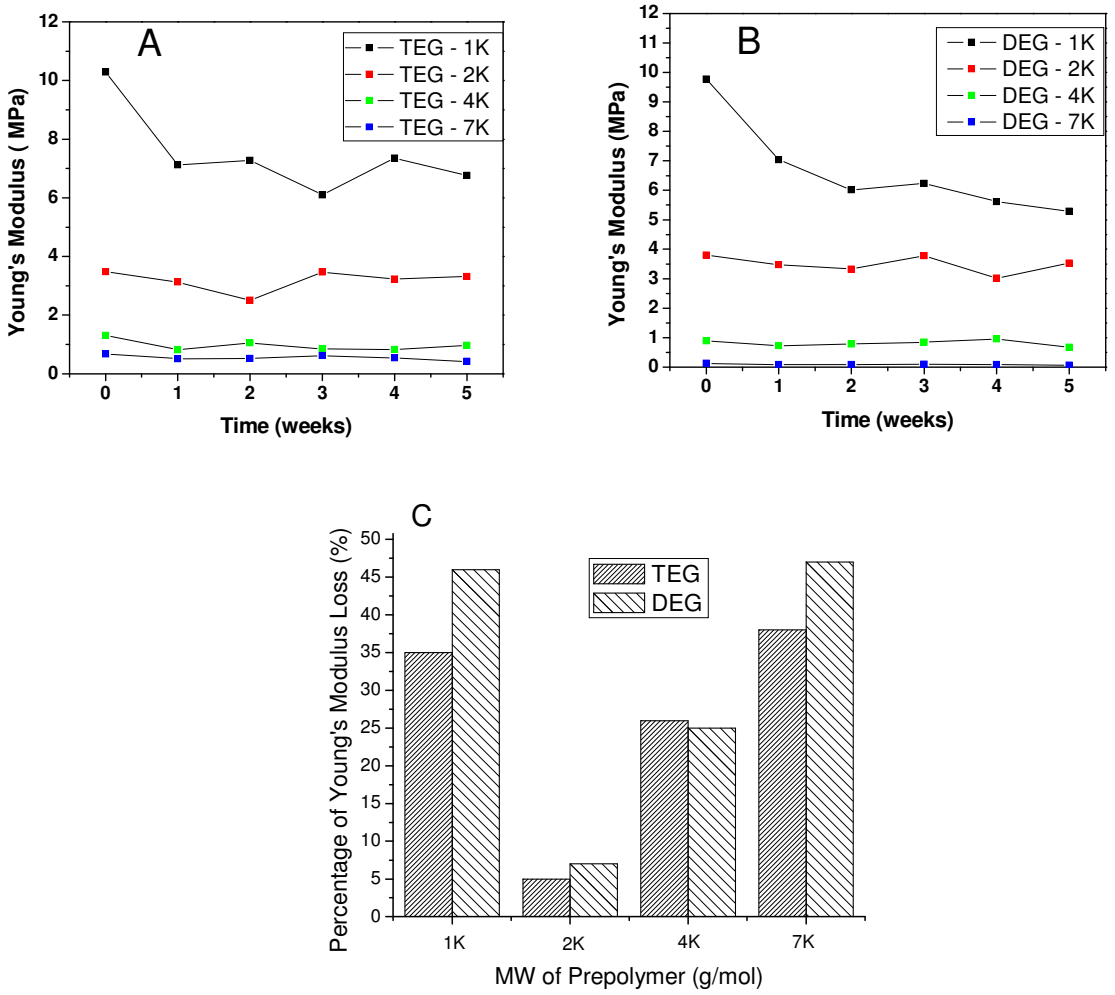

Figure 2-8. Changes of Young's moduli of elastomers during *in vitro* degradation study in PBS (pH 7.4). A) TEG based elastomers with different molecular weights, B) DEG based elastomers with different molecular weights, C) Percentage of Young's modulus loss after 5 weeks for all elastomers

The hydrophilicity of the surface should be suitable for cells be able to attach to the scaffold surface and grow. As a first probe of the hydrophilicity, we studied the

surface properties of our elastomers using advancing water-in-air contact angle measurement. While the mechanical and degradation properties of elastomers made from diethylene glycol (DEG) and tetraethylene glycol (TEG) were similar, the surface properties of the two sets of elastomers differed significantly (Figure 2-9). The elastomers made from diethylene glycol were more hydrophobic (contact angle stabilized at ~ 50 θ after 5 min) than the elastomers made from tetraethylene glycol (contact angle stabilized at ~ 20 θ after 5 min). To be a good candidate for cell attachment, the optimal contact angle range for biomaterials is 30-60 θ[23], placing our materials in a suitable contact angle range to support cell growth.

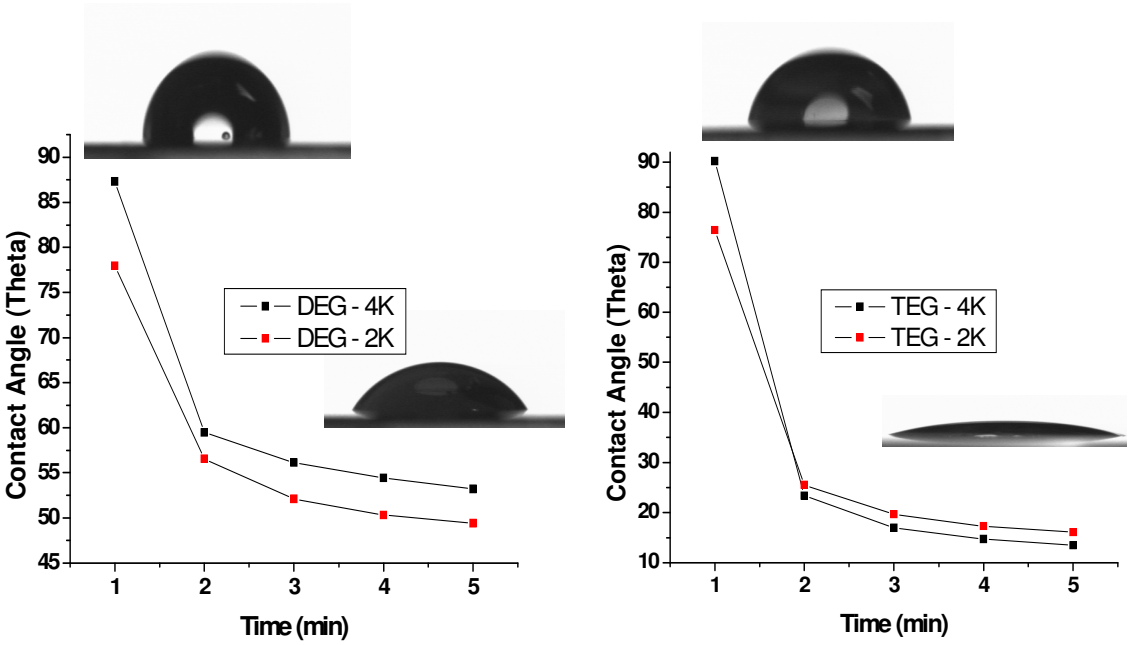

Figure 2-9. Water-in-air contact angle profiles of elastomers of DEG and TEG after 5 min

We also examined the cytotoxicity of our elastomers. The photocured elastomers appeared to be biocompatible *in vitro*. NIH 3T3 fibroblast cells were seeded homogeneously on elastomer-coated glass Petri dishes with the biocompatible PLGA-coated dishes as controls. Before the experiment, the dishes were rinsed with sterile water and phosphate buffered saline and incubated for 2 h in cell growth medium to sterilize the surfaces and remove any residuals. The fibroblast cells were transferred to all dishes with the cell growth medium. Figure 2-10 shows the cell morphology on elastomer DEG - 4K and PLGA after 24 h culture. The fibroblast cells on the elastomer surface showed normal morphology comparable to PLGA, a commercially used biomaterial.

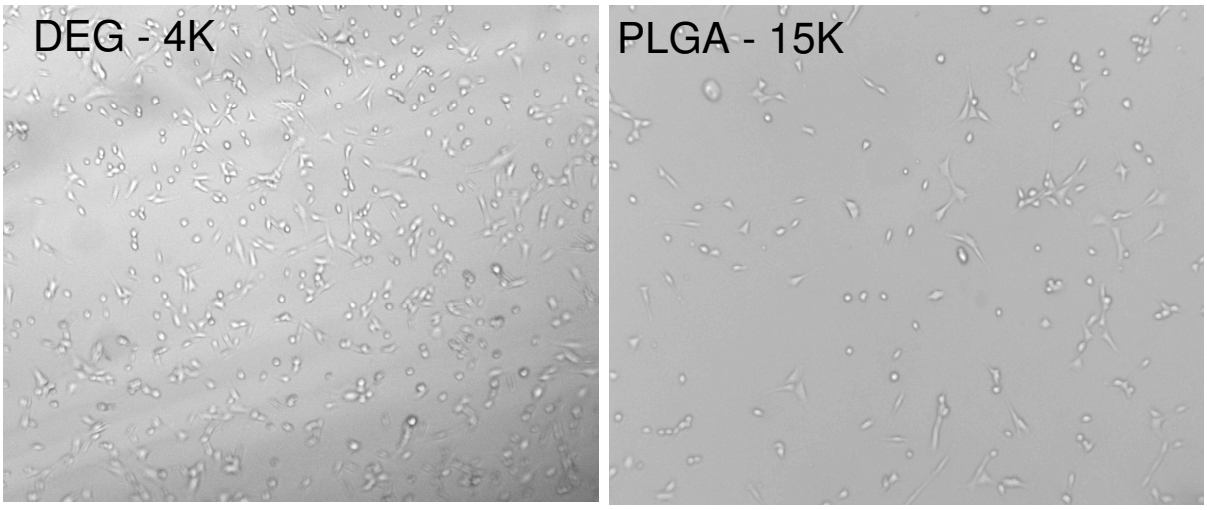

Figure 2-10. NIH 3T3 fibroblast cells grown on DEG - 4K (left) and PLGA (right) after 24 h culture

Lastly, we tried to fabricate different scaffolds from our elastomers. Since our photocurable prepolymers are completely amorphous liquids, they can be easily fabricated into different structures. Figure 2-11 shows the components of the bilayer scaffold (TEG-7K) that was fabricated to mimic the small diameter blood vessel.

Compared to materials in the literature[7], which took about 1 week, high temperature (120 ºC) and high vacuum (4 mmHg), we can prepare the scaffold at room temperature and pressure in 15 minutes.

At the same time, examples of a solid scaffold and a porous scaffold (TEG-7K) were fabricated (Figure 2-11 (B), (C)). Porous scaffolds are broadly used in tissue engineering since the interconnected pores can assure cell growth and the transport flow of nutrients and metabolic waste. Moreover, the porosity can be tuned to improve the mechanical match to the surrounding tissue without fundamental materials modification.[34,35] As can be seen from the above examples, our photocurable elastomers can be easily designed to be nonporous, porous or biphasic structures without using high temperature and high pressure.

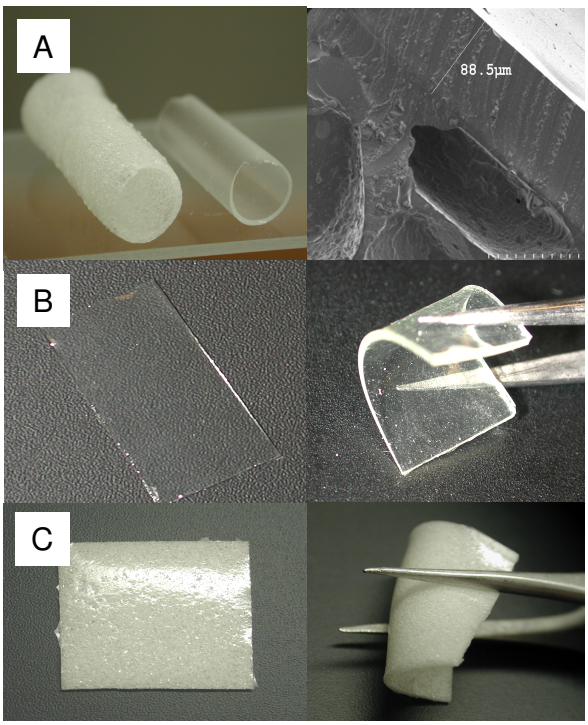

Figure 2-11. Scaffolds fabricated from photocured elastomers. A) a bilayer scaffold, B) a solid scaffold, C) a porous scaffold

2.5 Conclusions

New photocurable prepolymer liquids were successfully prepared from adipic acid and ethylene glycol oligomers by condensation polymerization. At room temperature and pressure, the liquids were easily fabricated into completely amorphous elastomers by using 0.1 wt% of photoinitiator and 1 min UV exposure. By tuning the molecular weights of the prepolymers or compositions, the mechanical properties, degradation rates and surface properties were easily controlled. Initial *in vitro* cell studies showed that the elastomers were not cytotoxic. These studies indicate that these photocured, biodegradable elastomers show great potential as a new class of biomaterials. The *in vivo* biocompatibility of these elastomers will be discussed in Chapter 3.

2.6 References

1. Chem, R.; Mooney, D. *Pharm. Res.* **2003**, 20, 1103-1112.
2. Guan, J.; Stankus, J.; Wagner, W. *J. Control. Release* **2007**, 120, 70-78.
3. Jong, W.; Bergsma, J.; Robinson, J.; Bos, R. *Biomaterials* **2005**, 26, 1781-1791.
4. Sarkar, S.; Lee, G.; Wong, J.; Desai, T. *Biomaterials* **2006**, 27, 4775-4782.
5. Gross, R.; Kalra, B. *Science* **2002**, 297, 803-807.
6. Yang, J.; Webb, A. R.; Ameer, G. A. *Adv. Mater.* **2004**, 16, 511-516.
7. Yang, J; Motlagh, D.; Webb, A.; Ameer, G. *Tissue Eng.* **2005**, 11, 1876-1885.
8. Gu, F.; Neufeld, R.; Amsden, B. *European J. Pharm. and Biopharm.* **2007**, 66, 21-27
9. Gu, F.; Neufeld, R.; Amsden, B. *Pharm. Res.* **2006**, 23, 782-789.
10. Amsden, B. *J. Pharm. Pharmaceut. Sci*. **2007**, 10, 129-143

11. Yang, J.; Webb, A. R.; Pickerill, S. J.; Hageman, G.; Ameer, G. A. *Biomaterials* **2006**, *27*, 1889-1898.

12. Wang, Y.; Ameer, G. A.; Sheppard, B. J.; Langer, R. *Nat. Biotechnol.* **2002**, 20, 602-606.

13. Frick, E.; Zalusky, A.; Hillmyer, M. *Biomacromolecules* **2003**, 4, 216-223

14. Ba, C.; Yang, J.; Hao, Q.; Liu, X.; Cao, A. *Biomacromolecules* **2003**, 4, 1827-1834.

15. Cohn, D.; Hotovely-Salomon A. *Polymer* **2005**, 46, 2068-2075

16. Younes, H.; Bravo-Grimaldo, E.; Amsden, B. *Biomaterials* **2004**, 25, 5261-5269

17. Brown, A.; Sheares, V. *Macromolecules* **2007**, 40, 4848-4853.

18. Liu, Q.; Tian, M.; Ding, T.; Shi, R.; Zhang, L. *J. Applied Polym. Sci.* **2005**, 98, 2033-2041.

19. Ding, T.; Liu, Q.; Shi, R.; Tian, M.; Yang, J.; Zhang, L. *Polym. Degr. Stab.* **2006**, 91, 733-739.

20. Brandl, F.; Sommer, F.; Goepferich, A. *Biomaterials* **2007**, 27, 134-146

21. Tsang, V.; Bhatia, S. *Adv. Drug Delivery Rev.* **2004**, 56, 1635-1647.

22. Anderson, D.; Tweedie, C.; Hossain, N.; Navarro, S.; Brey, D.; Vliet, K.; Langer, R.; Burdick, J. *Adv. Mater.* **2006**, 18, 2614-2618.

23. Leclerc, E.; Furukawa, K.; Miyata, F.; Sakai, Y.; Ushida, T.; Fujii, T. *Biomaterials* **2004**, 25, 4683-4690.

24. Helminen, A.; Korhonen, H.; Seppala, J. *Macromol. Chem. Phys*. **2002**, 203, 2630-2639.

25. Huang, M.; Li, S.; Vert M. *Polymer* **2004**, 45, 8675-8681.

26. Amsden, B. G.; Tse, M. Y.; Turner, N. D.; Knight, D. K.; Pang, S. C. *Biomacromolecules* **2006**, 7, 365-372.

27. Amsden, B.; Misra, G.; Gu, F.; Younes, H. *Biomacromolecules* **2004**, 5, 2479-2485.

28. Shen, J.; Pan, X.; Lim, C.; Chan-Park, M.; Zhu, X.; Beuerman, R. *Biomacromolecules* **2007**, 8, 376-385.

29. Nagata, M.; Sato, Y. *Polymer* **2004**, 45, 87-93

30. Nijst, C.; Bruggeman, J.; Karp, J.; Ferreira, L; Zumbuehl, A.; Bettinger, C.; Langer, R. *Biomacromolecules* **2007**,8, 3067.

31. Olson, D.; Gratton, S.; DeSimone, J.; Sheares, V. *J. Am. Chem. Soc.* **2006**, 128, 13625-13633.

32. Olson, D.; Sheares, V. *Macromolecules* **2006**, 39, 2808-2814.

33. Xiao, Y.; Cummins, D.; Palmans, A.; Koning, C.; Heise, A. *Soft Matter* **2008**, 4, 593–599

34. Motlagh, D.; Yang, J.; Liu, K. Y.; Webb, A. R.; Ameer, G. A. *Biomaterials* **2006***, 24,* 4315-4324.

35. Liu, T. V.; Bhatia, S. N. *Adv. Drug Delivery. Rev.* **2004***, 11,* 1635-1647.

CHAPTER 3

IN VIVO STUDY OF BIODEGRADABLE ELASTOMERS

3.1 Introduction

Biodegradable elastomers have been explored extensively for applications in the bioengineering field, especially as scaffolds in tissue engineering.[1-14] These materials are particularly suitable for situations where the biomaterial mechanical properties need to be similar or close to the target organs or tissues, with no irritation to the surrounding environment.[4]

A number of biodegradable elastomers have been fabricated, and generally they belong to two categories: thermoplastic elastomers and thermoset elastomers. Thermoplastic elastomers normally phase separate into amorphous and crystalline phases. Because these two phases have different solvent behaviors, the degradation *in vitro* or *in vivo* is heterogeneous with no shape integrity.[7] Completely amorphous thermosets have better structural stability upon degradation.[15] To fabricate scaffolds with long term shape unity, amorphous thermoset elastomers are more desirable.

For biodegradable polymers to be used as scaffolds in tissue engineering, an essential requirement is the biocompatibility of the fabricated scaffolds and also of the degraded by-products. After the *in vitro* biocompatibility evaluation, the *in vivo* evaluation is the most direct method to test the material performance. A widely used approach is to subcutaneously implant the fabricated scaffolds to the back or fermur of animals, such as rabbits[1,2], rats[3-10], mice[11,12], sheep[13] and pigs[14].

We recently synthesized new photocurable and biodegradable elastomers. All the *in vitro* studies focusing on the mechanical, degradation, cytotoxicity and surface properties, demonstrated that these elastomers are good candidates for tissue engineering scaffolds. Herein, we further investigated the *in vivo* performance of these elastomers by

subcutaneous implantation on the dorsal parts of rats. The degradation, mechanical, surface properties and inflammatory response are discussed.

3.2 Experimental

Photocurable prepolymer synthesis. The synthesis of methacrylate prepolymers have been described in Chapter 2. Herein, poly(diethylene glycol-adipate) based elastomers were used for the entire experiment with poly(lactic-glycolic acid) (PLGA) as the control.

Elastomer fabrication. The methods of preparation and characterization of the elastomers were as described previously in Chapter 2. Briefly, the calculated amounts of adipic acid and diethylene glycol were polymerized with stannous 2-ethylhexanoate catalyst at reduced pressure at 130 ºC for 24 h to get hydroxyl endcapped prepolymers. These hydroxyl groups then reacted with methacrylol chloride at room temperature overnight to prepare methacrylate endcapped prepolymers. The vinyl endcapped liquids (around 200 mg) were mechanically mixed with 1 wt% of photoinitiator (2,2-diethoxyacetophenone) in a 2 cm x 2 cm square mold and subjected to UV exposure for 10 min to fully cure. The cured films were evenly cut into 4 pieces, each with a size of 1 cm x 1 cm.

Control samples used in this experiment were square blocks made from PLGA, purchased from Boehringer Ingelheim with relative molecular mass 15,000 (50:50, carboxyl ended). PLGA solutions in CH_2Cl_2 (20 wt%) were cast into a PTFE mold. After

the evaporation of the solvent in air for 2 days, the formed blocks were carefully cut into square pieces (1 cm x 1 cm) and were dried in the fume hood for another 2 days.

Subcutaneous implantation. Elastomers made from diethylene glycol based prepolymers with $\langle M_n \rangle$ = 2 x 10^3, 4 x 10^3 and 6 x 10^3 g/mol were used (DEG-2K, DEG-4K, DEG-6K). To sterilize the surfaces, 70% ethanol was used. The PLGA pieces were sterilized with ethylene oxide. DEGs and PLGA were implanted subcutaneously in 15 nine-week-old female Sprague-Dawley rats (Charles River Laboratories, Wilmington, MA). During the surgery, rats were anesthetized using isoflurane and O_2. While under a surgical plane of anesthesia (monitored for adequate anesthesia by monitoring wakefulness and response to handling and toe pinch), the rats were shaved off all hair on the dorsal portions of the right and left sides. The surgical areas were prepared with alternating applications of a 10% povidone-iodine solution and 70% ethanol. Four 1 cm longitudinal incisions were made to allow the implantation of 3 pieces of DEGs (each from elastomer prepared from prepolymer with $\langle M_n \rangle$ = 2 x 10^3, 4 x 10^3 and 6 x 10^3 g/mol) and 1 piece of PLGA. The incisions were closed using sterile 5-0 surgical suture, and an injection of 0.33% locaine was given at each injection site. The implantation sites were marked by tattoo marks 2 cm away from the implanted center. At each sampling point (1, 2, 5, 6, 7 weeks), 3 rats were sacrificed, and tissue samples surrounding the implants were harvested with the intact implants, total of 12 samples. Two groups of polymer samples were retrieved for mechanical and surface studies, and one group was fixed with 10% formalin for 24 h. After extensive washing with distilled water, the samples were immersed in 70% ethanol and embedded in paraffin. The slices were stained with

hematoxylin and eosin stain (H&E) and Masson's Trichrome stain (MTS) for routine histological examination.

Water uptake and degradation studies. Immediately after explantation, all the elastomers were blotted dry, weighed and subjected to mechanical tests. After the tests, the pieces were collected and thoroughly dried in a vacuum oven. The water uptake was measured by the weight difference before and after drying:

$$Q_s = 100 \times (m_w - m_d) / m_d$$

where m_w and m_d represent the wet mass and dry mass.

The degradation rate was measured by weight difference after drying and the original weight before implantation:

$$Q_s = 100 \times (m_i - m_f) / m_i$$

where m_i and m_f represent the initial mass and final mass.

Mechanical properties. The mechanical properties of the explants were measured on an Instron 5566 at a crosshead speed of 10 mm/min at 25 ºC. The Young's modulus (G) was calculated using the initial linear portion of the stress/strain curve (0-5% of strain).

Surface morphology. First, photographs of both original samples and explants were taken by regular camera. Then, these materials were mounted on aluminum sample holders, and subjected to observation by atomic force microscopy (AFM). They were scanned in tapping mode with a Nanoscope III AFM (Digital Instruments, Inc., Santa

Barbara, CA) using silicon probes. Through Digital Instruments software, the images were processed with a second-order flattening routine. Roughness data were calculated by the contrast intensity on the images and 3-dimensional surface morphologies were produced.

3.3 Results and Discussion

3.3.1 Explant comparison

Previously in Chapter 2, new completely colorless and amorphous elastomers were fabricated by UV exposure with Young's modulus (G) ranging from 0.1-10 MPa and strain (ε) from 30-170%. These values are in the mechanical range for several soft tissues inside of the body, such as knee articular cartilage (G = 2.1-11.8 MPa), and cerebral vein (G = 6.85 MPa and ε = 83%). The degradation studies showed that these elastomers were fast degrading materials with weight loss up to 16% after 5 weeks incubation in PBS at 37 ºC. The water-in-air contact angle demonstrated that these elastomers were hydrophilic, and cytotoxicity studies indicated that these elastomers were nontoxic at the test conditions. All of these data implied that our elastomers could be good scaffold candidates for soft tissue replacement in tissue engineering.

In this chapter, we further investigated the *in vivo* performance of these elastomers by subcutaneously implanting to the dorsal parts of 9-week old female rats. Poly(lactic-glycolic acid) (PLGA) was employed as the control to examine the biocompatibility of our elastomers, which is a FDA approved biomaterial, and has been

utilized broadly in tissue engineering[2,5,9]. However, this material is hydrophobic and crystalline, which makes it less favorable for cell attachment and spread.[10] In this set of experiments, elastomers made from diethylene glycol based polyesters were used. The molecular weights for the prepolymers were $\langle M_n \rangle$ = 2 x 10^3, 4 x 10^3, and 6 x 10^3 g/mol (DEG-2K, DEG-4K, DEG-6K). Each week, samples were harvested from each rat.

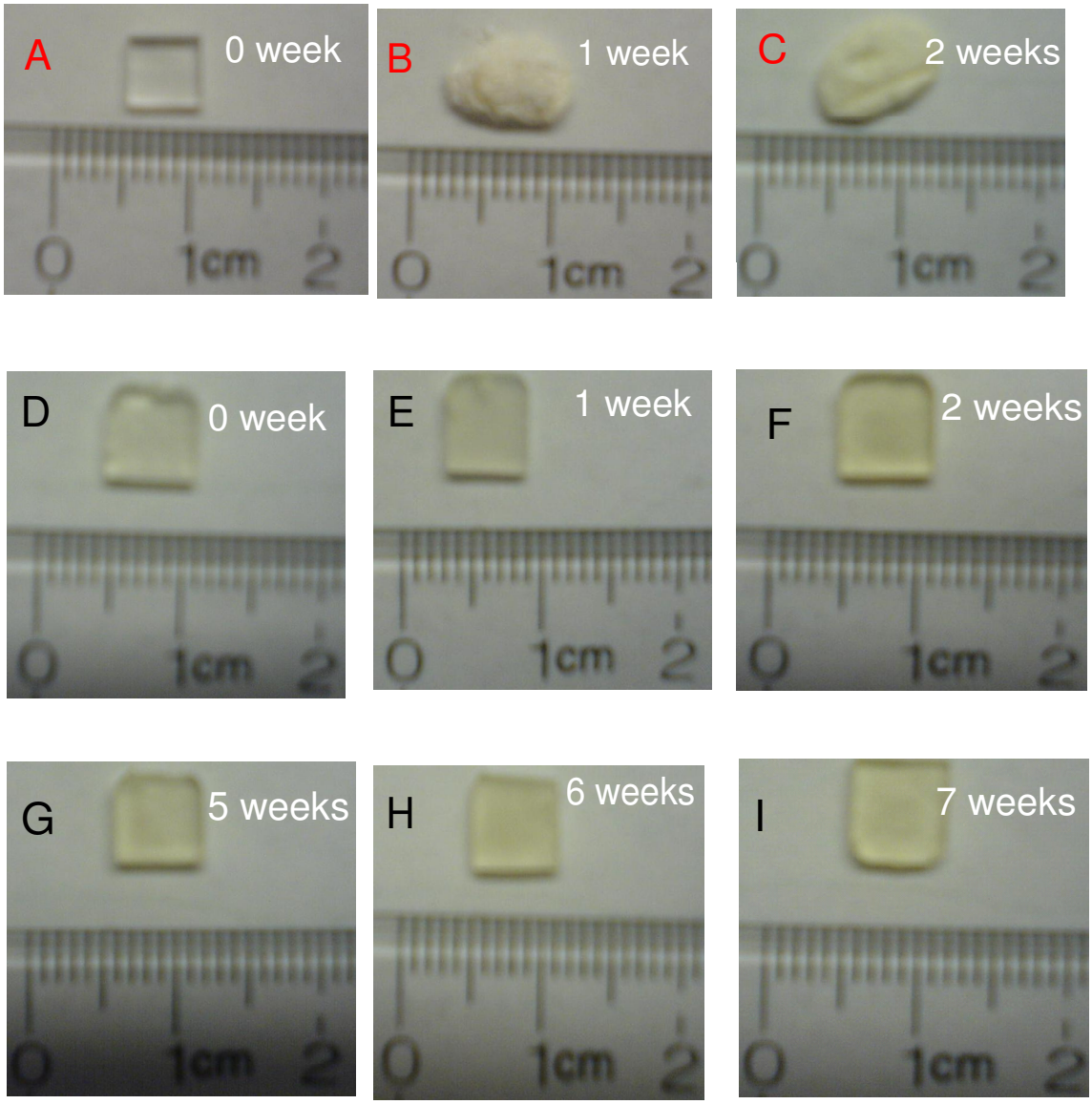

Figure 3-1. Photographs of explants: PLGA (A,B,C) and elastomers (D, E, F, G, H, I). The elastomers shown here prepared from DEG-4K

Photographs were taken when these materials were explanted from rats every week, as shown in Figure 3-1. Samples made from PLGA (A, B, C), after one week implantation inside rats, lost their original shape, changing from transparent square blocks to opaque porous lumps with rounded edges. This trend continued at the second week. After 5 weeks of implantation, PLGA based materials totally deformed inside of the rat and disappeared from the incision sites.

For DEG based elastomers (D, E, F, G, H, I), the structural stability was clearly evidenced by the photographs in Figure 3-1. Even after 7 weeks of implantation inside rats, the samples maintained their original shapes without noticeable difference among the samples prepared from prepolymers of different molecular weights. These photographs shown here are elastomers made from prepolymer with $\langle M_n \rangle = 4 \times 10^3$ g/mol. The same structural properties were seen in all DEGs. These elastomers were lightly colored after implantation inside rats, but the integrity of the elastomers was consistent throughout the entire 7 week study.

These results are comparable to the literature. Langer *et al.* fabricated thermally crosslinked poly(glycerol sebacate) (PGS) as tissue engineering scaffolds for soft tissue replacement.[10] It took 48 h at 120 ºC and 30 mTorr to fabricate the elastomer with Young's modulus of 0.282 MPa. PGS was implanted into rats with PLGA as the control, and similar phenomena were observed. PLGA distorted within 14 days and disappeared beyond 3 weeks. PGS maintained its integrity, but the surface roughened significantly as the experiment progressed.

3.3.2 Surface morphology

Atomic force microscopy (AFM) was utilized to quantitatively study the surface morphology of explants, as well as the contoured features simulated by 3-D images (Figure 3-2). As can be seen from the images, there were cracks (about 0.5 μm) formed on the surface of the explants. As the experiments progressed, the cracks connected with each other and more small cracks (about 0.2 μm) formed in between. In addition, the roughness of the surface increased with time, which can be easily seen from the 3-D image simulations (Figure 3-2). The highest roughness could be observed by explants after 6 weeks, around 77 nm compared to roughness of the original surface around 1nm. At 7 weeks, the surface roughness decreased to 40 nm. This can be explained that the elastomers continued degradation inside of the rat with the roughest tips being worn away by the surrounding medium. The roughness data are summarized in Table 3-1. Root mean square roughness (RMS) and arithmetic roughness (Ra) were used to quantitatively describe the surfaces. Compared with PGS, which roughened significantly and was easily noticeable with cracks as large as 40 μm observed from SEM,[10] our elastomers maintained a smoother surface with significantly smaller cracks (0.5 μm). This result indicated that our elastomers had better shape maintaining capacity than PGS.

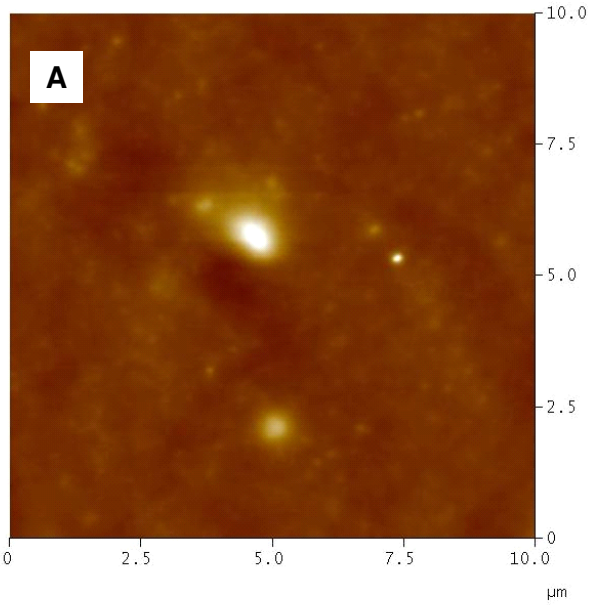
A
10.0
7.5
5.0
2.5
0
0
2.5
5.0
7.5
10.0
µm

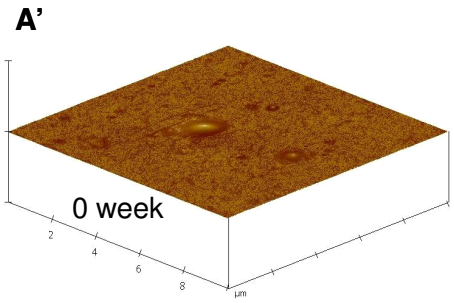
A'
0 week
2
4
6
8
µm

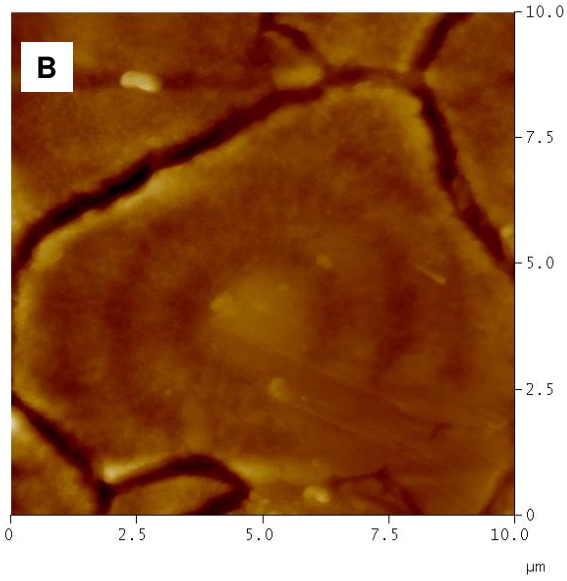
B
10.0
7.5
5.0
2.5
0
0
2.5
5.0
7.5
10.0
µm

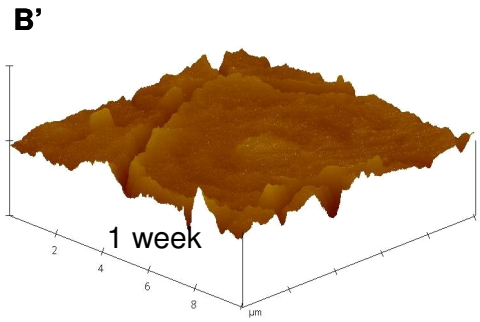
B'
1 week
2
4
6
8
µm

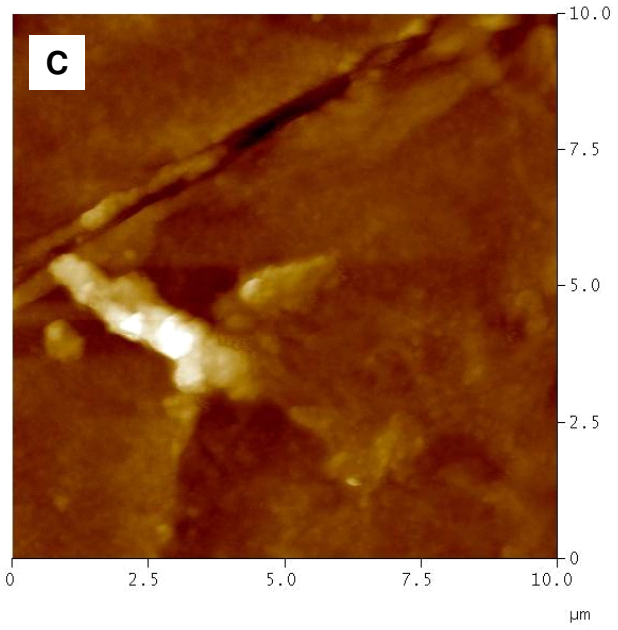
C
10.0
7.5
5.0
2.5
0
0
2.5
5.0
7.5
10.0
µm

C’

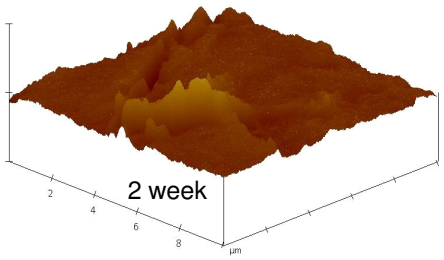
2 week

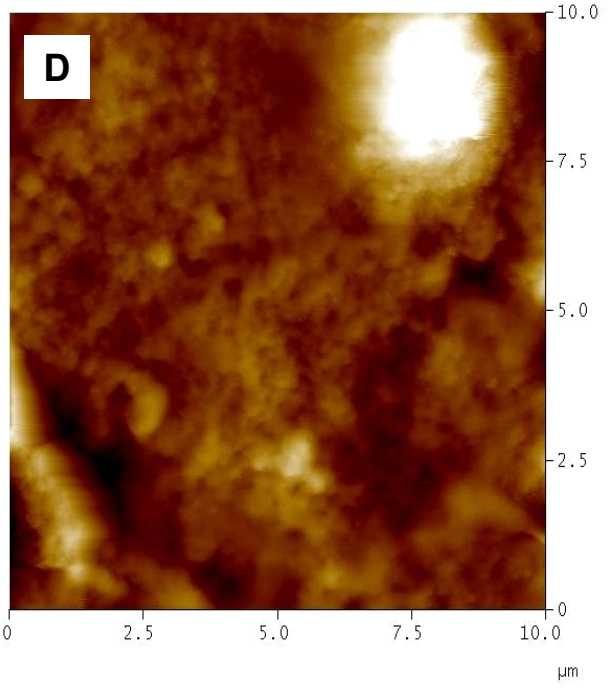
D
10.0
7.5
5.0
2.5
0
0
2.5
5.0
7.5
10.0
µm

D’

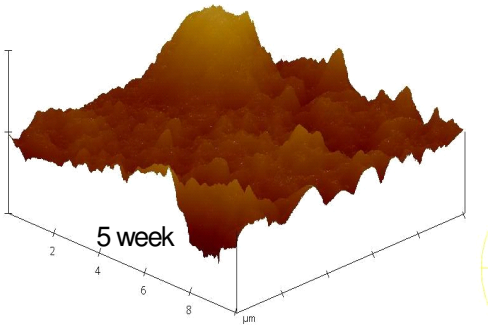
5 week

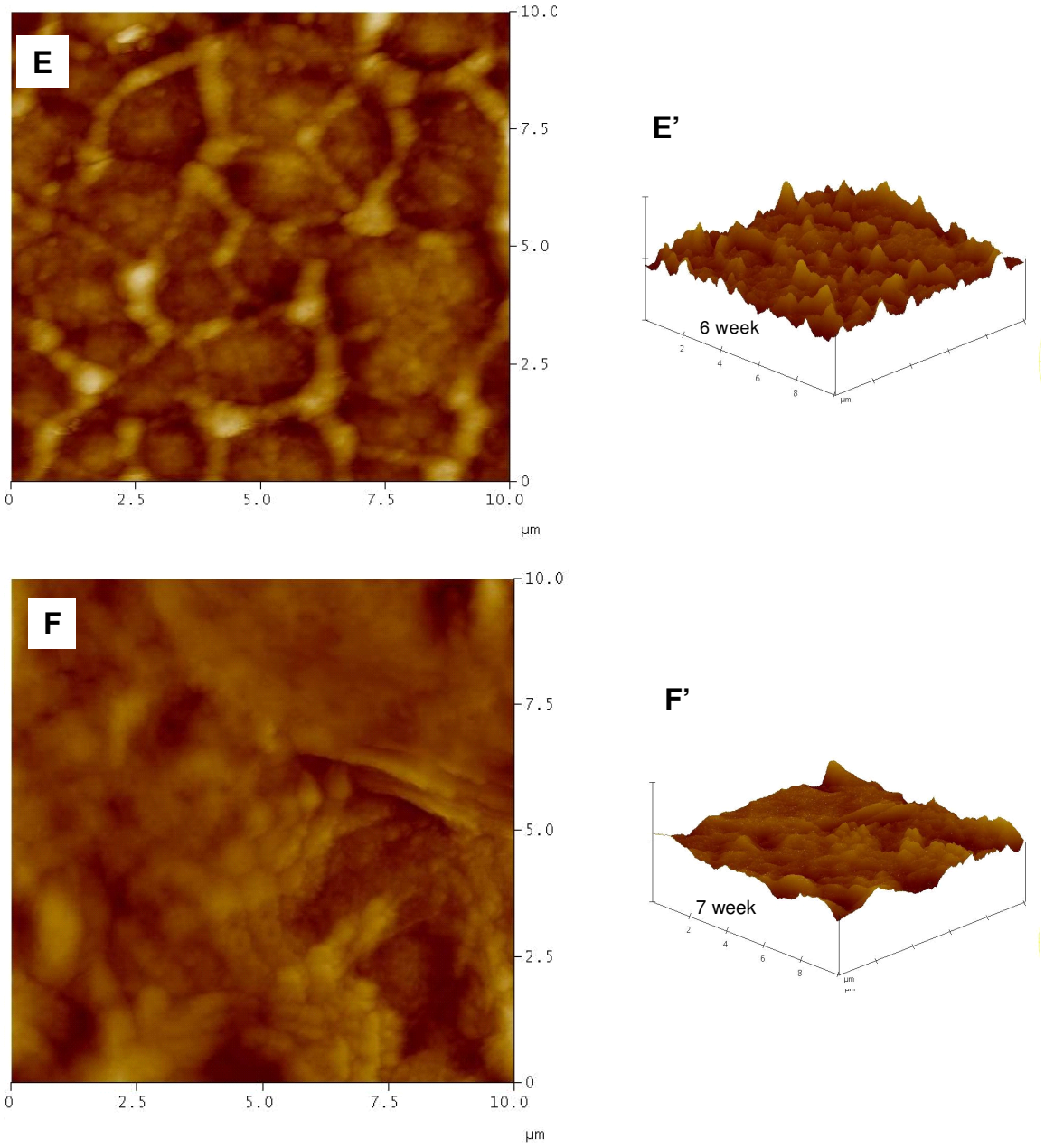

Figure 3-2. AFM images of elastomers at various time points of explantation with corresponding 3-D surface simulation (the images were processed with a second-order flattening routine), A) 0 week, B) 1week, C) 2 weeks, D) 5 weeks, E) 6 weeks, F) 7 weeks

Table 3-1. Surface roughness of explants during the implantation study

Week	RMS (R_q) (nm)	R_a (nm)
0	0.98	0.71
1	23.45	18.33
2	32.57	24.73
5	60.01	48.01
6	77.46	62.70
7	39.36	29.99

3.3.3 Water uptake and degradation rate

To better understand the performance of the elastomers *in vivo* and to assess their potential as cell-supporting scaffolds, water uptake was investigated to determine the swelling of the implants. The degree of swelling of degradable polymers *in vivo* is a key parameter for proper implant materials. Excessive swelling is usually undesirable for an implant, as it distorts the shape of the implant and softens the polymer.[10] Figure 3-3 shows the percentage of water uptake versus the study time for DEG based elastomers. As can be seen, after 1 week implantation inside of the rats, three sets of elastomers showed different amounts of water uptake, with higher water uptake for elastomers made from prepolymers of higher molecular weight. For DEG-2K, water uptake was 5%; for DEG-4K, water uptake was 9%; for DEG-6K, water uptake was 16%. After 2 weeks, the percentage of water uptake began to stabilize at 15% for DEG-4K and DEG-6K, and at

10% for DEG-2K. It is interesting to see that for DEG-2K and DEG-4K based implants, the percentage of water uptake did not fluctuate significantly during the following studies. But for DEG-6K based elastomers, the percentage of water uptake increased consistently after 5 weeks of implantation with the highest water uptake of 27% after 7 weeks of implantation. The water uptake of DEG-4K was close to the PGS implant, which had water content at 15% after 7 weeks of implantation.[10] DEGs and PGS had less water uptake than PLGA did, which took up 67% water after only 2 weeks of implantation.

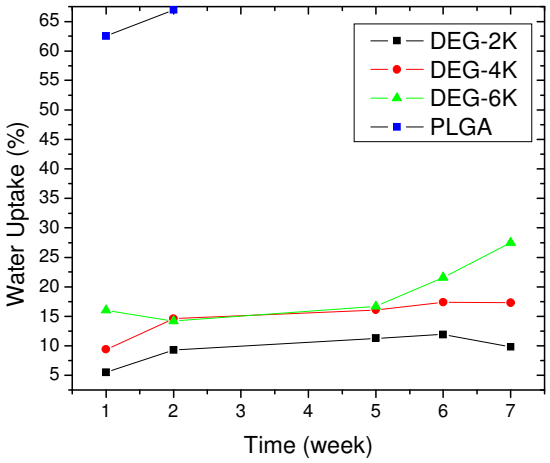

Figure 3-3. Water uptake studies of DEG based elastomers prepared from prepolymers of different molecular weights

The rate of mass loss is of fundamental importance in studying the degradation characteristics of a biodegradable polymer. The degradation rates of the elastomers were studied, and *in vivo* mass loss was faster than in PBS buffer at 37 ºC. As shown in Figure 3-4, elastomers made from prepolymers of molecular weight 6K degraded fastest, followed by elastomers made from 4K and then 2K. After 7 weeks of implantation, DEG-6K degraded 27%, DEG-4K degraded 16% and DEG-2K degraded 14%. For the PLGA

implant, the degradation was not significant at the first week. But it lost mass dramatically at the second week at 53%. After that time, PLGA could not be harvested from the implantation site. This phenomenon was observed previously in the literature.[16] While for the PGS implant, 70% of its original mass was lost after 7 weeks.[10] These data indicated that our elastomers could maintain their designed structure longer inside body. The dependence of degradation rate *in vivo* on prepolymer molecular weight is similar to the *in vitro* degradation, where elastomers prepared from prepolymers of higher molecular weight degraded faster than the elastomers made from prepolymers of lower molecular weight. The difference for *in vivo* degradation and *in vitro* degradation is that the same elastomers tended to degrade faster in the physiological environment than in PBS solutions. Because the elastomers were subcutaneously implanted, the aqueous surroundings were significantly different from the *in vitro* experiments. There was not only hydrolyzed degradation happening, but enzymes were contributing to degradation as well. In this complex *in vivo* environment, we observed about twice faster degradation rate than *in vitro* experiments.

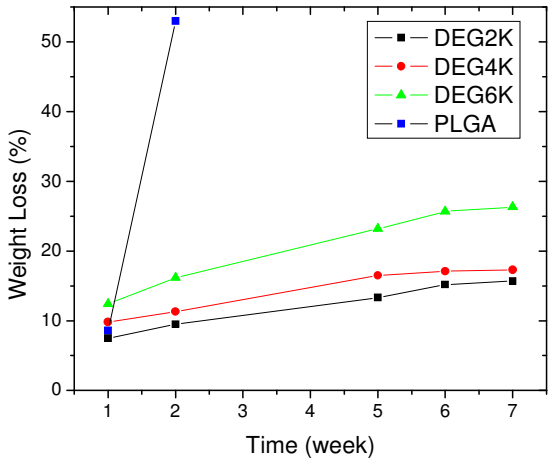

Figure 3-4. *In vivo* degradation of DEG based elastomers prepared from prepolymers of different molecular weights

3.3.4 Mechanical properties

As the degradation progressed, the mechanical properties of explants changed (Figure 3-5). It is desired that the elastomers maintain sufficient mechanical strength while new tissue is formed.[5] Elastomers of DEG-2K had an original Young's modulus of G = 3.4 MPa, and it decreased to 1.14 MPa after 5 weeks of implantation. The percentage of Young's modulus loss was 67%. For elastomers of DEG-4K, the percentage of Young's modulus loss was 21%, decreasing from 0.9 MPa to 0.7 MPa. Elastomers of DEG-6K had the medium percentage of Young's modulus loss, about 48% after 5 weeks. While for PGS implant, at day 35, the modulus is about 50% of the original.[10] Once again, it indicated that our elastomers, especially DEG-4K, showed better sustained mechanical strength. The dependence of the percentage of Young's modulus loss on prepolymer molecular weight after the *in vivo* study was not the same trend as we observed during the *in vitro* study, where DEG-2K had the smallest Young's modulus loss of 6% after 5 weeks. So the best way to evaluate the mechanical properties of a new biomaterial is to carry out *in vivo* study, while the *in vitro* study will give some clues about this material.

Since the surface of the explants roughened gradually as the implantation progressed, accompanied with the Young's modulus loss, it is hypothesized that the degradation mechanism for these sets of elastomers can be the combination of surface erosion and bulk degradation.[17] The medium surrounding the materials diffused into the elastomer matrix and degradation happened inside of the bulk. Meanwhile, the elastomer surface degraded because of the extensive interaction with the media.

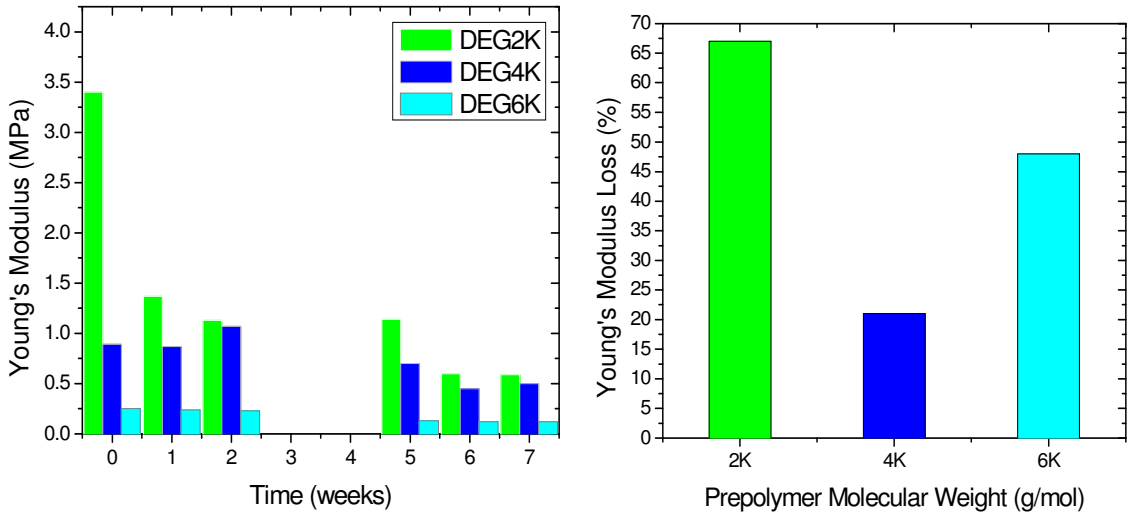

Figure 3-5. A) Young's modulus of explants changed with the implantation time, B) Percentage of Young's modulus loss after 5 weeks implantation versus the prepolymer molecular weight

3.3.5 Cell response

Figure 3-6 depicts the histological examination of cell response to the elastomeric specimens after 1 week of implantation. H&E (Figure 3-6 (A)) staining confirmed that there was loose connective tissue with minimal collagen fibers and evenly scattered plump spindle cells with oval nuclei (interpreted as fibroblasts). There were a few areas of minimal fibrin deposition on the inner surface of the rim. MTS (Figure 3-6 (B)) staining indicated that the formation of collagen after 1 week implantation. As the study progressed, it was difficult to collect good sections of specimens. It could result from the nature of the section preparation. Further study is needed to verify these results. But from the outside skin of the rats, we could not observe any difference from the elastomer side and the PLGA side.

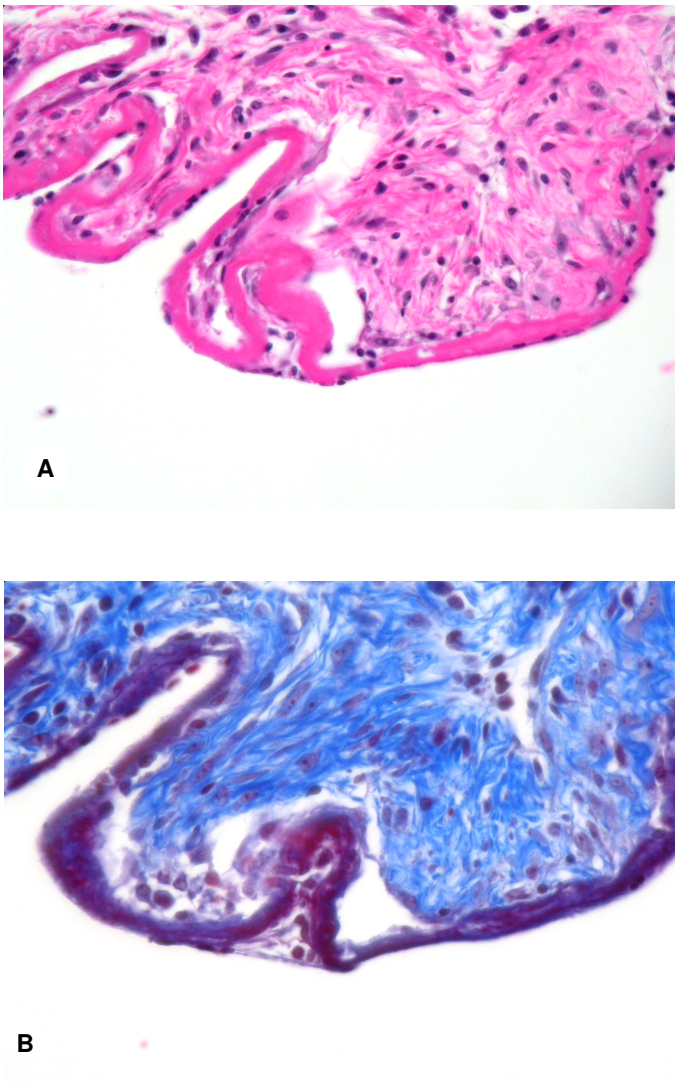

Figure 3-6. A) H&E stained sample, B) MTS stained sample

3.4 Conclusions

Photocured elastomers (DEGs) were studied *in vivo* with the commercial biomaterial PLGA by subcutaneous implantation to the dorsal parts of rats. PLGA lost structural integrity inside rats after 1 week of implantation. DEG implants preserved their implant geometry and showed good retention of mechanical strength. The implant surfaces were studied by AFM. These results indicated that the degradation of our elastomers could be the combination of bulk degradation and surface erosion. Our elastomers may prove useful in the biomedical field where the implant integrity is highly emphasized.

3.5 Reference

1. Guo,D; Sun, H.; Xu,K.; Han, Y. *J. Biomed. Mat. Res. Part B: Appl. Biomat.* **2007***,* 82B, 533-544.

2. Hedberg, E. L.; Kroese-Deutman, H. C.; Shih, C. K.; Crowther, R. S.; Carney, D. H.; Mikos, A. G.; Jansen, J. A. *Biomaterials* **2005***,* 22, 4616-4623.

3. Bölgen, N.; Menceloğlu, Y. Z.; Acatay, K.; Vargel, İ; Pişkin, E. *J.Biomat. Sci.-Polym. Ed.* **2005***,* 12, 1537-1555.

4. Wang, Y.; Ameer,G.; Sheppard, B.J.; Langer, R. *Nat. biotechnol.* **2002**, 602-606.

5. Grayson, A. C. R.; Voskerician, G.; Lynn, A.; Anderson, J. M.; Cima, M. J.; Langer, R. *J. Biomat. Sci.-Polym. Ed.* **2004***,* 10, 1281-1304.

6. Sun, H.; Mei, L.; Song, C.; Cui, X.; Wang, P. *Biomaterials* **2006***,* 9*,* 1735-1740.

7. Amsden, B. G.; Tse, M. Y.; Turner, N. D.; Knight, D. K.; Pang, S. C. *Biomacromolecules* **2006***,* 1*,* 365-372.

8. Deschamps, A. A.; Van-Apeldoorn, A. A.; Hayen, H.; De-Bruijn, J. D.; Karst, U.; Grijpma, D. W.; Feijen, J. *Biomaterials* **2004***,* 2*,* 247-258.

9. Cao, Y.; Mitchell, G.; Messina, A.; Price, L.; Thompson, E.; Penington, A.; Morrison, W.; O'Connor, A.; Stevens, G.; Cooper-White, J. *Biomaterials* **2006***,* 14, 2854-2864.

10. Wang, Y.; Langer, R. *J. Biomed. Mater. Res. Part A* **2003***,* 66A, 192-197.

11. Jeong, S. I.; Kim, B. -.; Lee, Y. M.; Ihn, K. J.; Kim, S. H.; Kim, Y. H. *Biomacromolecules* **2004***,* 4*,* 1303-1309.

12. Jeong, S. I.; Kim, B.; Kang, S. W.; Kwon, J. H.; Lee, Y. M.; Kim, S. H.; Kim, Y. H. *Biomaterials* **2004***,* 28*,* 5939-5946.

13. Sun, Y.; Peng, Y.; Aksornkoae, N.; Johnson, J. R.; Boring, J. G.; Scruggs, D.; Cooper, R. C.; Laizure, S. C.; Shukla, A. J. *J. Control. Release* **2002***,* 1-3, 125-134.

14. Warfvinge, K.; Kiilgaard, J. F.; Lavik, E. B.; Scherfig, E.; Langer, R.; Klassen, H. J.; Young, M. J. *Arch Ophthalmol.* **2005***,* 10, 1385-1393.

15. Yang, J; Motlagh, D.; Webb, A.; Ameer, G. *Tissue Eng.* **2005**, 11, 1876-1885.

16. Lu, L.; Peter, S.J.; Langer, R.; Mikos, A.G. *Biomaterials* 2000, 21, 1837-1845.

17. Doi, Y.; Steinbuchel, A. *Biopolymers, 4, Polyesters 3,* 154-157. Wiley-VCH,**2002**.

CHAPTER 4

SYNTHESIS OF PHOTOCURABLE AND BIODEGRADABLE AMINE-CONTAINING ELASTOMERS AND INVESTIGATION OF THEIR APPLICATIONS AS DRUG CARRIERS

4.1 Introduction

Biodegradable polymers with hydrolyzable chemical bonds have been extensively studied in the biomedical field, especially as drug release carriers. These labile chemical bonds include esters, anhydrides, ortho esters, acetals and related groups.[1,2] Among them, polyester-based materials are one of the most widely investigated systems due to their availability and well-defined characterization.[3] In this field, a controlled drug release system is more desirable.[1] Recent work demonstrated that controlled drug delivery was possible with degradable elastomers due to their special osmotic pressure-driven release.[4-6]

In addition, biodegradable polymers have been shown to respond to environmental stimuli such as pH change and enzymatic, offering many benefits as drug release systems.[7-15] A significant amount of research has been done in this field and several new materials developed, such as poly(β-amino ester)s[7-11], poly(hydroxyproline) esters[1,12], pullulan-histidine conjugates[13], and branched polyesters[14,15]. Most approaches have primary amine, secondary amine and/or tertiary amine groups incorporated into the polymer backbone or side chain to endow pH sensitivity to the drug release system. The tunability of these amine groups allows the pH buffering capacity of the polymer to span a wide range according to the desired functionalites.[11]

Besides ester groups, disulfides stand as another class of biodegradable groups. With the help of reducing agents, disulfides can be cleaved to the corresponding thiols.[16] Disulfide groups bring several advantages to the design of biodegradable polymers such as rapid cleavage by glutathione and thioredoxin reductases in the cytoplasm, which are

naturally present within cells at millimolar concentrations.[17,18] Also, cytotoxicity can be decreased by avoiding the high charge density that is common in amine concentrated polymers. Disulfide-containing polyesters[19], polyamines[20-22], and polyamides[23] have been developed and explored in applications as environmentally sensitive carriers. Besides the incorporation into the polymer backbone, disulfide-functionalized dimethacrylate crosslinkers have also been employed as bridges to connect two polymer chains.[18, 24, 25]

Generally drug release systems are micro/nano sized polymeric particles, and are prepared by heterogeneous polymerization methods, either emulsion or inverse (mini)emulsion polymerization[7], or by controlled radical[26] or atom transfer radical polymerization (ATRP)[18, 24], or by conjugate self organization[13]. Herein, we utilized a newly developed technology, called PRINT (*P*article *R*eplication *I*n *N*on-wetting *T*emplates), which enables the fabrication of monodispersed particles with excellent control over size and shape, which plays an important role during the interaction of particles with the target cells.[27]Moreover, the fabrication process is highly reproducible, and the payload of drugs can be concisely controlled during the process. Finally, PRINT is compatible with a wide variety of raw materials.[28]

Based on the advantages of PRINT technology and the promising properties of biodegradable elastomers, we synthesized a series of photocurable amine-containing polyesters. We chose to prepare elastomers fabricated from prepolymers made via polycondensation polymerization for several reasons: 1) a broad array of monomers available, 2) the ease of functionalization of the polymer backbone, and 3) the ease of synthetic control. As well, we chose a photocuring method to crosslink the network as it is significantly faster than thermal fabrication with better control over the entire structure

and shape of the final material. Using these photocurable liquids and a disulfide crosslinker, we fabricated monodispersed amine-disulfide containing particles via PRINT, and studied the cytotoxicity and intracellular uptake. Furthermore, we examined the possibility of these particles as environment sensitive drug carriers against the release of a hydrophobic drug (Doxorubicin) and a hydrophilic drug (Minocycline hydrochloride).

4.2 Experimental

Materials. All chemicals were purchased from Sigma-Aldrich unless otherwise noted. 2,2-Diethoxyacetophenone (DEAP) was purchased from Acros. Fluorocur™, the perfluoropolyether used as the molding material in the PRINT process, was purchased from Liquidia Technologies. Poly (ethylene glycol) monomethyl ether monomethacrylate (M_n=1000 g/mol) was purchased from Polysciences. Adipic acid (AA) was recrystallized from distilled water prior to use. Diethylene glycol was dried over calcium hydride overnight and distilled. 1,4-bis (2-hydroxyethyl)piperazine (PIP) was recrystallized from ethanol prior to use. Poly(ethylene glycol) methacrylate (M_n= 526 g/mol) was dissolved in distilled water, and purified by extraction from diphenyl ether twice (collecting the aqueous layer), heptane twice, cyclohexane twice, and extraction from the cosolvent of dichloromethane/hexane (3:1) (v/v) (collecting the organic layer) twice to get rid of poly(ethylene glycol) dimethacrylate component and poly(ethylene glycol) component.[29]

Preparation of hydroxyl endcapped poly(diethylene glycol-piperazine-adipate). A 50 mL round-bottom flask was charged with calculated amounts of adipic acid, 1,4-bis (2-hydroxyethyl)piperazine and diethylene glycol. The contents of the flask were then placed under a nitrogen atmosphere. The mixture was stirred at 130 ºC using magnetic stirring until a homogeneous melt was formed. Stannous 2-ethylhexanoate (1.0 mol %) was added to the melt. The mixture was stirred for 1 h, and the pressure was reduced to 20 mmHg. The reaction was allowed to proceed at 20 mmHg for 23 h for a total reaction time of 24 h. Polymerization was terminated by precipitating the polymer into cold methanol (-78 ºC).

Preparation of methacrylate endcapped poly(diethylene glycol-piperazine-adipate). A 25 mL two-neck round-bottom flask equipped with a condenser was charged with 3 g of hydroxyl endcapped prepolymer. The entire apparatus was sealed, flame-dried, and purged with nitrogen. This procedure was repeated 3 times. Under the flow of nitrogen and stirring, 15 mL of fleshly distilled methylene chloride was injected into the flask followed by heating of the flask to 50 ºC using an oil bath. 2-Isocyanatoethyl methacrylate (4.2 mole equiv) was added dropwise into the flask with 2 drops of stannous 2-ethylhexanoate. The reaction proceeded for 2 h under reflux, and was terminated by precipitation in cold methanol (-78 ºC) after removal of all solvent.

Synthesis of the disulfide crosslinker: dithiopropionyl poly(ethylene glycol) dimethacrylate. Clean PEG-monomethacrylate (10 g) was dissolved in 60 mL dry CH_2Cl_2 with 3.9 g dicyclohexyl carbodiimide (DCC) and 0.5 g dimethylaminopyridine (DMAP). 3,3'-Dithiopropionic acid (2.3 g) in 30 mL dry THF was added dropwise to

the above mixture in an ice bath at 0 °C over 20 min. The resulting mixture was allowed to stir at room temperature overnight. The formed solids were removed by vacuum filtration, and the combined solvents were removed by rotary evaporation. The resulting oily residue was dissolved in CH_2Cl_2 (100 mL), and was washed with aqueous $NaHCO_3$ solution three times to remove excess diacid. After CH_2Cl_2 was removed, the resulting yellow oily residue was dissolved in THF (5 mL), and refrigerated at -5 °C for 12 h. The insoluble solids were removed by vacuum filtration, THF was removed by rotary evaporation, and the product dried in a vacuum oven at 35 °C for 12 h to form a yellow oily residue in 50 % yield.

Preparation of drug loaded particles. Cylindrical particles with feature sizes of 2 x 2 μm were fabricated by PRINT technology. First, a patterned Fluorocur™ mold was fabricated as the methods described elsewhere.[28] Briefly, an 8 inch patterned silicon wafer (with feature sizes of 2 μm), which was set up inside an enclosed UV chamber, was covered with 20 mL of Fluorocur™ resin containing 0.1 wt% of 2,2-diethoxyacetophenone. The system was then purged with nitrogen for 2 min and exposed to UV irradiation (λ =365 nm, power > 20 mW/cm^2) for 1 min to cure the Fluorocur™ resin. The cured elastomeric mold was then gently peeled away from the surface.

For a representative formula, the PRINT particles were derived from a mixture composed of 77 wt% methacrylate endcapped polyester liquid, 20 wt% PEG monomethyl ether monomethacrylate, 1 wt% 2,2-diethoxyacetophenone, and 2 wt% fluorescein. Drops of the mixture were randomly dispersed on the patterned elastomeric mold. A poly(ethylene) sheet (American Plastics Co.) was then placed over the mold, evenly

pressed by a roller and peeled off. The mold was covered by the same sheet again but in different directions, and the above procedures were repeated several times until a uniform coverage of the mixture on the patterned mold. Finally this poly(ethylene) sheet was peeled back at a rate of approximately 3.0 cm/min with heating. Following this, the mold was placed in the UV curing chamber. The chamber was purged with nitrogen for 2 min and UV irradiation was applied (λ =365 nm, power >20 mW/cm^2) for 1 min. A physical means was used to harvest the particles. A Drop of acetone (filtered through a 0.22 μm PTFE filter) was placed on the particle-filled mold, and this drop of acetone was gently moved along the surface of the mold using a glass slide. The collected acetone suspension was ultrasonicated for 10 min, and was centrifuged at 3200 rpm for 30 min using an IEC CENTRA CL2 Centrifuge (Thermo Electron Corporation). The supernatant was removed via aspiration, and the particle pellet was redispersed in 50 mL of fresh acetone by unltrasonication for 10 min followed by centrifugation for an additional 30 min. This process was repeated 3 times and at the last time, the particle pellet was dispersed in a minimal amount of acetone and was transferred into an eppendorf tube and centrifuged in a microfuge (Fisher Scientific) for 20 min. After removal of the supernatant, the tube was dried in a vacuum oven overnight. The weight changes for the eppendorf tube were recorded as the weight of the particles.

Elastomer fabrication. Elastomer films (20 x 20 x 0.5 mm) were prepared by spreading a mixture of the liquid prepolymer (0.25 g) and 1 wt% photoinitiator (DEAP) on a glass mold. The mixture was put inside of the UV oven chamber (ECL-500), and

purged with N_2 for 10 min, and then was subjected to UV irradiation (365 nm) for the prescribed time (2 - 10 min).

4.3 Characterization

^{1}H NMR spectra were acquired in deuterated chloroform on a Bruker 400 AVANCE. A Waters Gel Permeation Chromatography (GPC) system was used to measure polymer molecular weights relative to polystyrene standards. The measurements were taken at 40 ºC with THF as the mobile phase in four columns. Fourier transform infrared spectroscopy (FTIR) spectra were acquired on a Perkin-Elmer Spectrum BX. Thermogravimetric analysis (TGA) was performed using a Perkin-Elmer thermogravimetric analyzer with a heating rate of 10 ºC/min in a N_2 atmosphere. Glass transition temperatures and melting points were measured on a Seiko 220C differential scanning calorimeter (DSC) using the second heat at a heating rate of 10 ºC/min. Scanning electron microscopy (SEM) was performed on a Hitachi S-4700 SEM. The mechanical data were collected on an Instron 5566 at a crosshead speed of 10 mm/min at 25 ºC. The Young's modulus (G) was calculated using the initial linear portion of the stress/strain curve (0-5% of strain).

Surface charge analysis. The zeta potential of PRINT microparticles was measured using a ZetaPlus Zeta Potential Analyzer (Brookhaven Instruments Corporation). The microparticles were dispersed in distilled water at a concentration of 0.3 mg/mL and the zeta potential was measured.

Sol content analysis. Sol content analysis was conducted by swelling a 0.15 g elastomer film in methylene chloride for 24 h at 25 ºC. The solvent was removed and the percent soluble fraction (Q_s) was determined according to the following equation,

$$Q_s = 100 \times (m_i - m_f) / m_i$$

where m_i and m_f represent the initial mass and final mass. Each measurement was performed on three separate samples. The value was reported as the average of the three measurements.

pKa buffering study. pK_a value of amine-containing polyesters was determined via a classical acid-base titration. The polyester liquid was dissolved in 0.1 M HCl with pH of 2. The solution was then titrated with 0.1 M NaOH solution in a stepwise manner in order to obtain the titration curves. The pK_a value was calculated from the derivative of the curves.

In vitro **degradation studies.** About 100 mg bulk elastomer samples were immersed in 20 mL of phosphate-buffered saline (PBS) (pH 7.4 and 37 ºC) in a 20 mL scintillation vial. At each sampling time point, the slabs were taken out, washed with distilled water and dried under mild heat in a vacuum oven for 24 h. The dried mass was then measured. All measurements were made in triplicate.

Another set of particle degradation was proceeded by suspending 1 mg particles in 1 mL pH 5(FIXANAL, $C_6H_8O_7$/NaOH) buffer and pH 7.4 buffer (phosphate buffered saline) (PBS) in eppendorf tubes, respectively. The tubes were incubated at 37 ^oC. Everyday, the tubes were shaken manually to get evenly dispersed solutions. A small drop of solution was taken out from each tube and sprayed on a glass slide for the optical microscopy study.

***In Vitro* drug release from particles**. Freshly made pH 5 and pH 7.4 buffers were used. Particle suspensions (1.5 mL) (2 mg/mL) in different buffers were put into dialysis tubes (Fisher, Regenerated cellulose tubular membrane, MWCO 6,000-8,000). The bags were sealed and immersed into 20 mL of pH 5 and pH 7.4 buffers. The release medium was stirred at 250 rpm at 37 ºC. At the predetermined sampling time, 0.25 mL release mediums were taken out and the amount of DOX in the solution was determined via UV spectroscopy at 500 nm.

Particle cellular uptake. Hela cells were used for cellular uptake. The day before the experiment, Hela cells were seeded at $2.0x10^4$/100 µL SMEM (5% Fetal bovine serum + 5% Horse serum, 2 mM L-glutamine)/well in a 96-well plate (Costar 3595 clear), and incubated overnight at 37 ºC. Next day Hela cells were about 95% confluence. The media was aspirated from cells, and washed once with Opti-MEM I/GlutaMAX I. A 50 µL graded particle solution in Opti-MEM I/GlutaMAX I was added to each well. The wells were incubated at 37 ºC for 3 h. At the end of incubation, the medium was aspirated off, and washed once with DPBS. Cells were trypsinized with 50 µL/well of 1x Trypsin-EDTA at 37 ºC for 5 min. Trypsin was neutralized with 150 µL of DMEM-10/well and cells were transferred to a 96 well round bottom plate. The plates were centrifuged at 1200 rpm for 5 min and the supernatants were poured off. Trypan blue (50 µL of 0.1%) was added, and left at room temperature for 10 min to quench fluorescence of particles on cell surfaces. Dulbecco's Phosphate Buffers Saline (DPBS) (200 µL) was added and centrifuged at 1200 rpm for 5 min and the supernatants were removed. Cells were washed once with DPBS, resuspended in 200 µL DPBS and transferred into 1.1 mL microtubes for flow analysis (Cyan ADP analyzer, Dako Cytomation). All events were collected and

the percentage of cellular uptake represents the fluorescein positive cells against all cells collected.

Cytotoxicity test. Hela cells were used for cytotoxicity test. The procedures were similar to the beginning procedures of cellular uptake. The day before the experiment, Hela cells at 2.0 x 10^4/100 μL SMEM were seeded and incubated overnight at 37 ºC, and particles were added to each well. The wells were incubated at 37 ºC for 3 h. At the end of incubation, particles were replaced with 100 μL of fresh medium and 20 μL of cell proliferation assay reagent (Promega G3582) were added to each well. The wells were incubated at 37 ºC for about 1 h to develop colors. The optical density at 492 nm was measured using a BioRad Model 3550 microplate reader (BioRad Laboratories). Cell viability was expressed as percentage of living cells against the cells in control which contained medium only.

4.4 Results and discussion

4.4.1 Synthesis and characterization of photocurable elastomers

Amine-containing biodegradable polymers have been investigated extensively in gene delivery and drug release applications because of the cationic properties of the amine functional group, which can condense anionic DNA or load anionic drugs at physiological pH.[17,30-32] The buffering capability from primary amine, secondary amine and tertiary amine groups can help to mediate the gene transfer effects as well as control drug release. Some of these cationic polymers bear the pendant amines in the polymer side chains and some contain tertiary amines in the polymer backbone, such as the

poly(β-amino ester) library prepared from Michael addition of bifunctional amines to bisacrylamides.[11,33]

Herein, we report a simple polycondensation polymerization method to synthesize new secondary and tertiary amine containing polyesters. The synthetic scheme is shown in Figure 4-1. The first step was to incorporate the tertiary amine into the polymer backbone by using 1,4-bis(2-hydroxyethyl)piperazine (PIP) as the donor. By controlling the feed ratio of PIP to diethylene glycol (DEG) and also the feed ratio of the two diols to adipic acid, hydroxyl endcapped polyester liquids with various number average molecular weights were easily prepared. Secondary amines were then added into the polymer backbone by using urethane chemistry. The strategy was to react the endcapped hydroxyl groups with 2-isocyanatoethyl methacrylate. The reaction was run at 50 ^{o}C for two hours. This process was monitored by FTIR spectroscopy.[34]

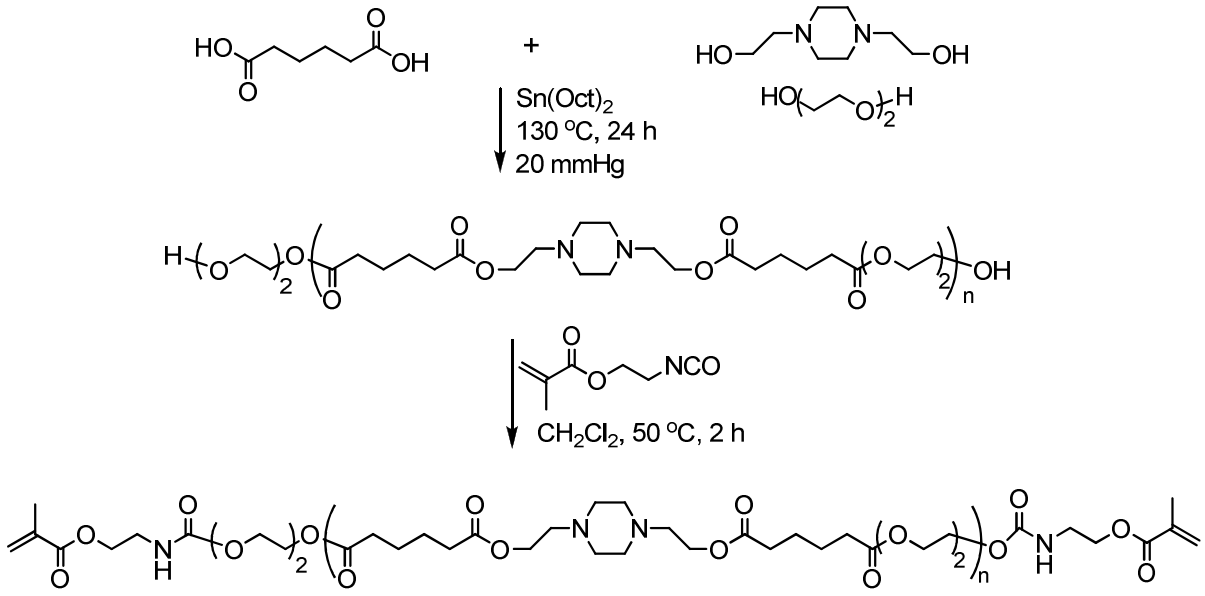

Figure 4-1. Synthesis of methacrylate endcapped prepolymers

Two series of methacrylate endcapped prepolymers were synthesized. As shown in Tables 4-1 and 4-2. Table 4-1 includes samples (1-4) with different feed ratios of PIP: DEG prepared with a targeted prepolymer number average molecular weight near 5 x 10^3 g/mol. The results of DSC analysis of the materials showed that when the feed ratio of PIP:DEG was less than 20:30, totally amorphous prepolymers were made. Table 4-2 is the summary of samples (3, 5, 6, 7) with prepolymer molecular weights ranging from 1 x 10^3 g/mol to 6 x 10^3 g/mol at similar reaction conditions with the constant feed ratio of PIP:DEG = 20:30. DSC studies did not show any melting peaks, and the glass temperatures for all samples were near -30 ºC. The sol content of the fabricated elastomers ranged from 7-15%, indicating high degrees of endcapping.

Table 4-1. Characterization of amine containing photocurable prepolymers at varying diol feed ratios

Sample	PIP:DEG ratio		‹M_n›	PDI[b]	T_g[c]	T_m[c]	Sol content (%)[d]
	feed	observed[a]	x 10^{-3} (g/mol)[b]				
1	40:10	40:11	4.3	1.6	-34	57	8.3
2	30:20	30:22	5.2	1.7	-28	53	12.1
3	20:30	20:26	6.2	1.5	-30	*f*	5.6
4	10:40	10:38	6.5	1.5	-32	*f*	14

[a] Determined by NMR; [b] determined by GPC; [c] determined by DSC, second heat, 10 ºC/min; [d] extracted in methylene chloride for 24 h at 25 ºC; [f] materials were amorphous

Table 4-2. Characterization of amine containing photocurable prepolymers at a constant diol feed ratio

Sample	PIP:DEG ratio		‹M_n›	PDI[b]	T_g[c]	Sol content (%)[d]
	feed	observed[a]	x 10^{-3} (g/mol)[b]			
3	20:30	20:26	6.2	1.5	-36	5.6
5	20:30	20:27	1.1	1.9	-34	12.3
6	20:30	20:27	2.1	1.7	-31	1.7
7	20:30	20:28	3.3	1.6	-42	1.6

[a] Determined by NMR; [b] determined by GPC; [c] determined by DSC, second heat, 10 ºC/min; [d] extracted in methylene chloride for 24 h at 25 ºC

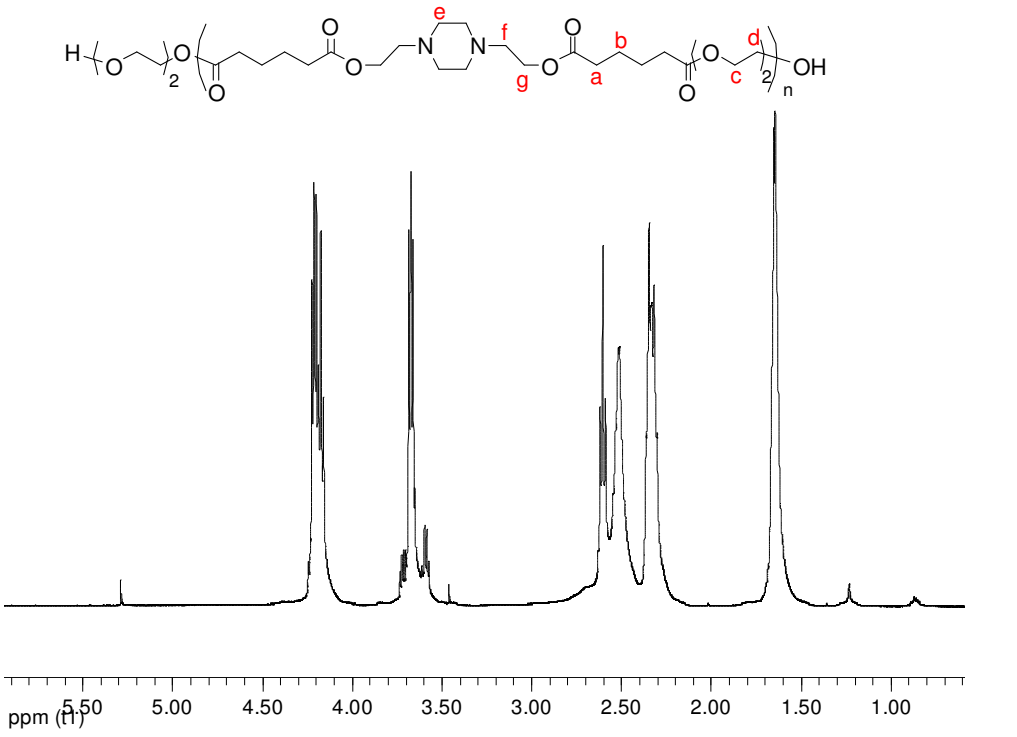

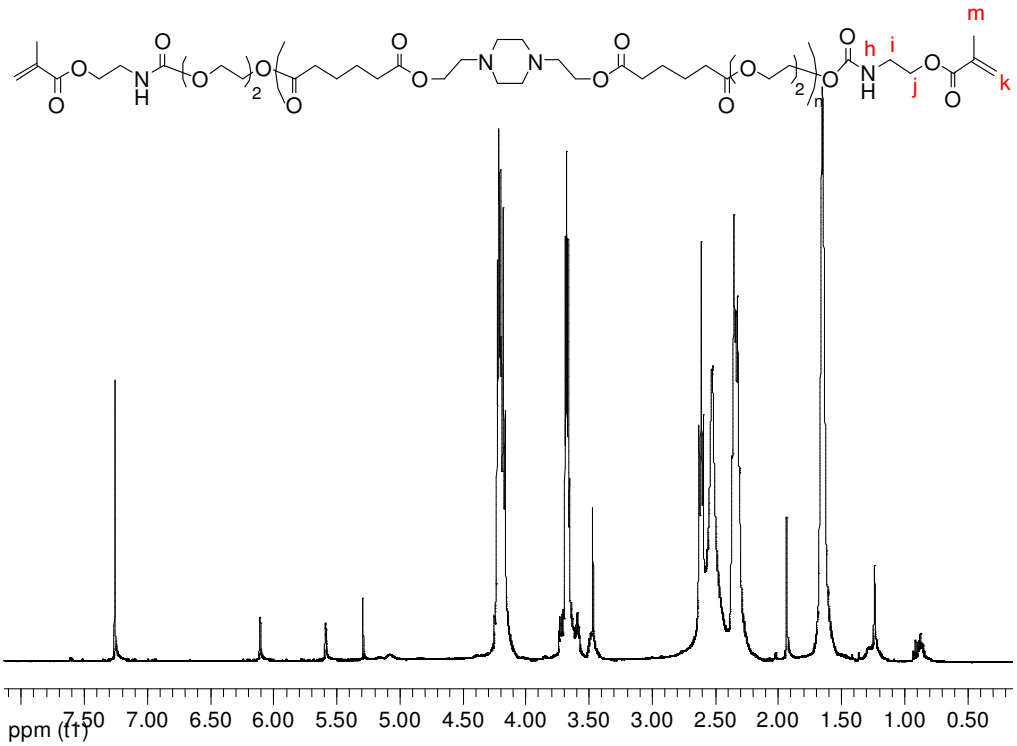

Figure 4-2. ^{1}H NMR spectra of A) hydroxyl endcapped prepolymer and B) methacrylate endcapped prepolymer

Figure 4-2 shows the ^{1}H NMR spectra of a representative hydroxyl endcapped prepolymer (A) and a methacrylate endcapped prepolymer (B), with all the peaks assigned. The methacrylation of the end termini of the prepolymer was confirmed by the spectra. ^{1}H NMR of the methacrylate endcapped prepolymer (B) clearly showed peaks at δ = 5.3, 5.6 ppm, corresponding to the vinyl protons of the methacrylate group, and δ = 1.9 ppm corresponding to the methyl protons of the methacrylate group. The methylene groups (marked as *i* and *j* from spectrum (B)) from the 2-isocyanatoethyl methacrylate end group overlapped with the methylene groups from diethylene glycol. The degree of methacrylation (calculated by the same method from Chapter 2) was consistent in most methacrylate endcapped prepolymers, with the methacrylation conversion ranging from 80% to 90%. The component ratio of piperazine versus diethylene glycol was found from the integration ratio of the peaks at 2.6 ppm and 4.2 ppm. These calculated ratios were close to the feed ratios of the two components. Finally, GPC studies showed that the endcapping of methacrylate groups onto the polyester prepolymer did not degrade the polymer backbone (shown in Appendix C).

Amine groups have solution buffering capacity. Since amine groups were incorporated onto the prepolymer backbone, the solubility of the prepolymers differed in pH 5 and pH 7.4 buffers. In titration studies, the pKa value of Prepolymer 3 was found at 6.2 (titration curve shown in Appendix C). Figure 4-3 depicts the solubility of Prepolymer 3 in pH 5 and pH 7.4 buffers. Instead of the clear solution seen in pH 5 buffer, an opaque solution was observed for Prepolymer 3 in pH 7.4 buffer. This could result from the quaternization of the amine groups on the polymer backbone at pH 5 that

improved the solubility of this prepolymer. This pH sensitivity has been illustrated by other amine containing polymers.[8]

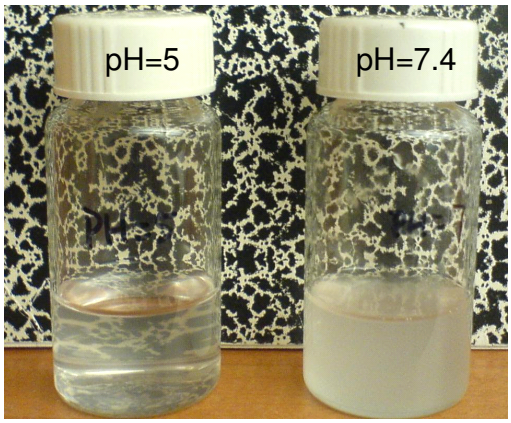

Figure 4-3. Polymer 3 in pH 5 and pH 7.4 buffers

4.4.2 Mechanical properties, water uptake and degradation properties

In the following discussion, the mechanical, degradation and water uptake properties will be the focus to study the potential of these biodegradable elastomers as drug release carriers.

The mechanical properties of the fabricated elastomers were examined first. To possess osmotic pressure-driven release capacity, the materials have to be designed to be elastic. 2,2-Diethoxyacetophenone (DEAP) was used to photo initiate the amine containing polyester liquids. The photocuring conditions were consistent for all the fabricated elastomers: 1 wt% DEAP, 10 min exposure with N_2 flow to ensure full network formation. Herein, we examined two elastomers made from Prepolymer 3 ($\langle M_n \rangle$ = 6.2 x 10^3 g/mol) and Prepolymer 7 ($\langle M_n \rangle$ = 3.3 x 10^3 g/mol). The dependence of mechanical properties and degradation properties on the prepolymer molecular weights

was explored. As can be seen from the stress-strain curves (Figure 4-4), both of the materials exhibited elastic properties, as indicated by the long extension up to 62%. Young's modulus (G) was calculated from the data of 0-5% strain and ranged from G= 2.4 MPa to G= 0.6 MPa for Elastomer 7 and Elastomer 3, respectively. These results were similar to our previous results from Chapter 2, where elastomers fabricated from low molecular weight prepolymers were tougher than the elastomers made from higher molecular weight prepolymers

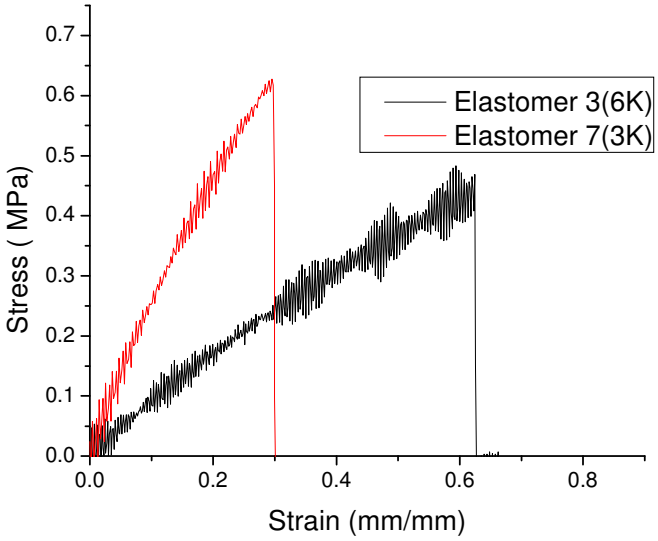

.

Figure 4-4. Tensile test of elastomers made from Prepolymer 3 (‹M_n› = 6.2 x 10^3 g/mol) and Prepolymer 7 (‹M_n› = 3.3 x 10^3 g/mol)

Next, the kinetics of our elastomer degradation was also investigated using a pH 5 buffer and a pH 7.4 buffer, since amine containing polyesters showed pH sensitive degradation and used for pH sensitive drug release.[7,8] The degradation was monitored by the weight loss of elastomers over the time at 37 ^oC. Elastomers weighing 100 mg were used and the buffer solutions were change weekly. At each sampling point, the

elastomers were washed with distilled water and dried in a vacuum oven overnight at 40 ^{o}C. The weight loss was taken as the difference of dried sample weight over the original sample weight. Figure 4-5 shows the degradation profiles of elastomers as a function of time. As the degradation progressed, all elastomers lost weight significantly. Elastomer 3 degraded faster than Elastomer 7, indicating prepolymer molecular weight dependence consistent with previous results from Chapter 2. In general, the elastomers degraded faster at pH 7.4 than at pH 5. This result is consistent with the pH-degradation profiles of other amine-containing polyesters, including poly(4-hydroxy-L-proline ester), which contains mainly primary amine groups[1,12], linear poly(β-amino ester)s, which contains tertiary amine groups [7, 8, 35], and hyperbranched poly(ester amine)s[15], which contains primary, secondary and tertiary amine groups. It is hypothesized that the amine group on the polymer chain, either in the primary, secondary or tertiary status, acts as an intramolecular nucleophilic catalyst and contributes to the slow degradation at pH 5. At pH 7.4 a higher fraction of unprotonated amino groups in the polymer catalyze the hydrolysis of the ester groups in the polymer. It was noticed that for elastomers at pH 7.4 buffer, the degradation profiles were rather linear after initial burst degradation. While for elastomers at pH 5 buffer, the degradation was slower after the initial burst degradation, and after 4 weeks, the degradation increased. These fast initial and slow following phenomena were similar to the reported research by Lim's group[1,12], who observed a slower degradation rate after initial rapid degradation, which was contributed the different buffering capacity of the primary amine groups with the secondary and tertiary amine groups. In all, the degradation of these cationic elastomers was fast, with the fastest one losing 83% of its original weight after 5 weeks in pH 7.4 buffer. Similar

elastomers without the cationic compositions lost 15% of original weight after 5 weeks in PBS (from Chapter 2). The degradation rates of the fabricated elastomers depend not only on the prepolymer molecular weight, but also the pH value of the medium.

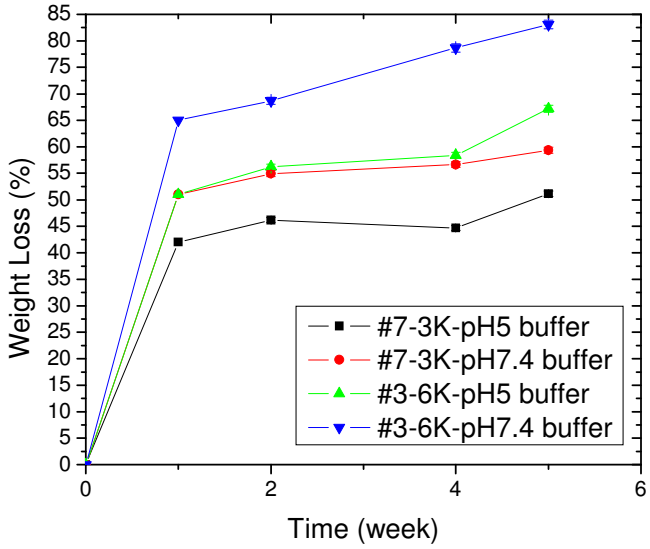

Figure 4-5. Degradation study of elastomers made from Prepolymer 3 (‹M_n› = 6.2 x 10^3 g/mol) and Prepolymer 7 (‹M_n› = 3.3 x 10^3 g/mol)

Along with the degradation studies, water uptake was also examined. It is an important parameter to indicate the interaction of the elastomer network with the medium. The common strategy used for water uptake is to compare the weights of hydrated samples with the weights of original samples. But for our experiment, the elastomers degraded rapidly, and it was more reasonable to compare the weights of hydrated samples with the weight of dried samples after hydration, as has been previously described for rapidly degrading materials.[14] The water uptake measurement ran for 3 days, and at the same time the degradation was monitored. Herein, we compared two sets of elastomers, one set made from DEG based prepolymers with ‹M_n›= 6 x 10^3 g/mol and the other set made from tetraethylene glycol (TEG) based prepolymers. These studies

were carried out at pH 5 and pH 7.4 buffers. It is clearly seen from Figure 4-6, TEG based elastomers showed a higher degree of water uptake and faster degradation rates to their DEG counterparts. It is not surprising to see this phenomenon since tetraethylene glycol is more hydrophilic than diethylene glycol, and this trend has been reported for different TEG and DEG containing polyesters previously.[36] The water uptake and degradation for the same materials in different pH buffers were also compared. DEG based materials took up more water at pH 5 buffer than pH 7.4 buffer, but the degradation was faster in pH 7.4 buffer than in pH 5 buffer. The same trend could be seen by TEG based elastomers. It is likely that when the elastomers were immersed in pH 5 buffer, they were protonated, making it easier for water to penetrate into the network. The difference in degradation rates can be explained by the same phenomenon. At pH 7.4, a higher fraction of unprotonated amino groups in the polymer catalyze the hydrolysis of the ester groups in the polymer backbone. In all, the interaction of the elastomers with buffer is a complicated process, multiple factors can contribute and intertwine, and it is important to carefully to determine which one is dominant and significant.

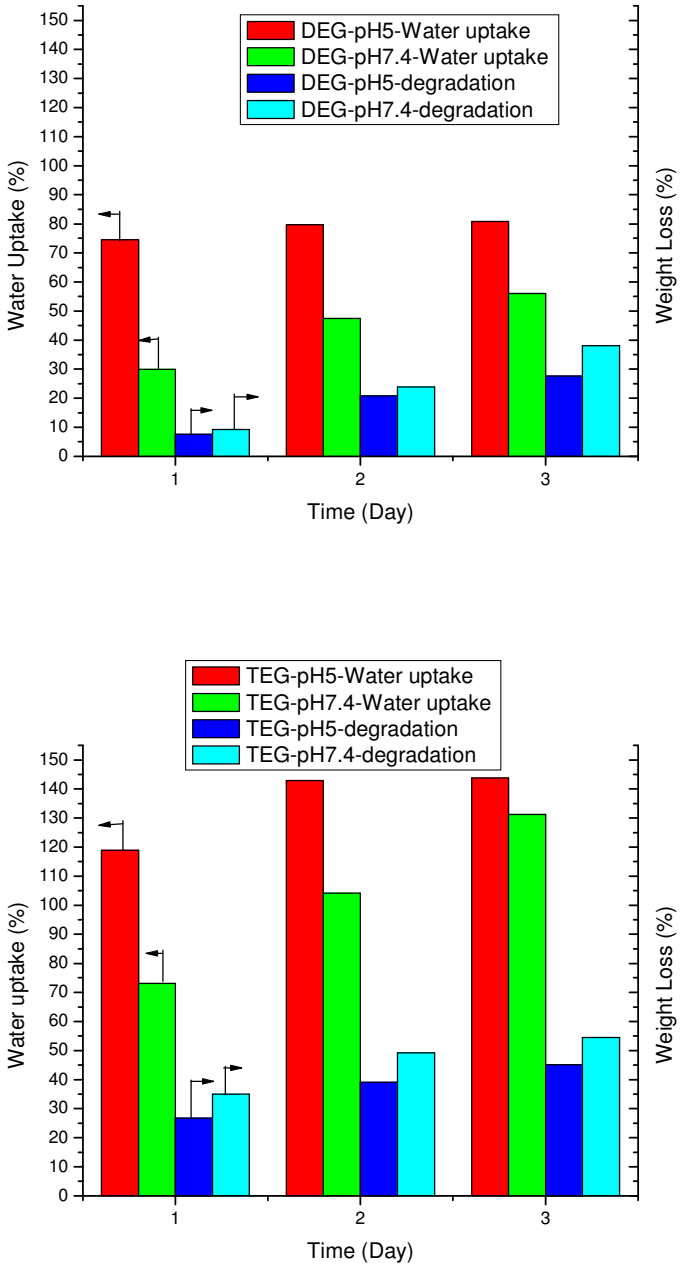

Figure 4-6. Water uptake and degradation studies for DEG and TEG based elastomers; 3 day study, $\langle M_n \rangle = 6 \times 10^3$ g/mol for all prepolymers

4.4.3 PRINT particle fabrication and properties

Based on the understanding of these cationic elastomers, we were interested in exploring their applications as drug release carriers. There are numerous reported approaches to prepare micro- to nano- sized polymeric particles by emulsion[7], self organization[13], ATRP[18], *etc*. Herein, we chose a novel imprint lithographic technique, PRINT (*P*article *R*eplication *I*n *N*on-wetting *T*emplates), to take advantage of its capacity to produce monodispersed particles in a wide range of shapes and sizes, two factors reported to significantly affect the interaction of particles and their targets.[28] PRINT is also easy to utilize with excellent reproducibility.

We fabricated 2 micron and 200 nm sized cylindrical particles using the following formulation: 77 wt% methacrylate endcapped prepolymers, 20 wt% PEG monomethyl ether monomethacrylate (known to increase the circulation of particles inside body),[33] 1 wt% 2,2-diethoxyacetophenone, and 2 wt% fluorecein *o*-acrylate (for fluorescent effect). These monodispersed particles were fabricated by the method as described previously.[28] Figure 4-7(A) shows the fluorescent image of particles with 2 wt% of fluorecein *o*-acrylate incorporation, which can be used for particle tracking. Figure 4-7(B) depicts the optical image of particles without fluorecein, and Figure 4-7(C) shows the SEM image of particle size of 200 nm. As can be seen from these images, monodispersed particles with different size and formulation can be easily fabricated by PRINT technology. These particles maintained their individual stable sizes and shapes after several hours in water, with no observed aggregation.

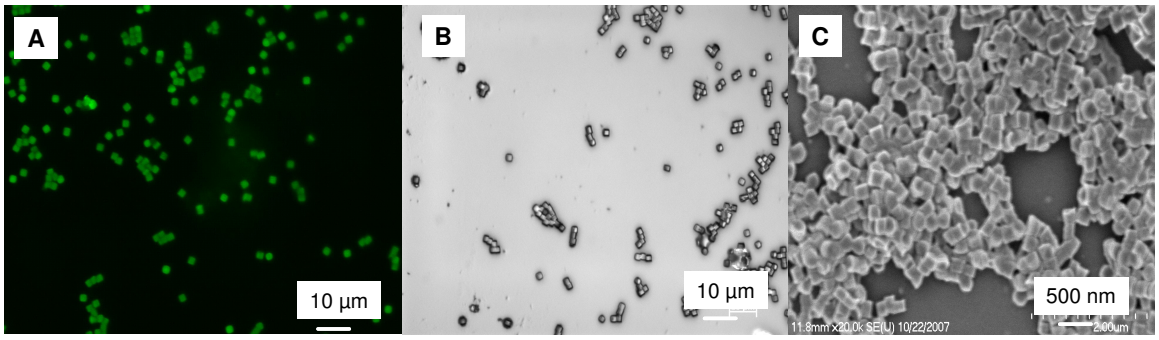

Figure 4-7. A) Fluorescent image of 2 µm particles. B) Optical image of 2 µm particles. C) SEM image of 200 nm particles

4.4.3.1 PRINT surface charge

Charged surfaces help to decrease the aggregation of particles and improve the interaction of particles with cells.[27,28] The surface charge of the elastomeric particles (2 micron) was studied by dispersing the particles in water at a concentration of 0.3 mg/mL and measuring the zeta potential. The zeta potential of the fabricated particles was -26 mV ± 0.54 mV, in the range for stable particles. Generally for amine containing particles, the surface charge is normally positive in distilled water and near + 15 ~ +20 mV depending on the polymer compositions.[35] The reason for the negatively charged particles can be traced back to the particle compositions. We incorporated 20 wt% of poly(ethylene glycol) (PEG) monomethyl ether monomethacrylate into the particle since PEG chains are well known for particle stabilization and extended circulation time.[9] Since the zeta potential for particles purely fabricated from PEG based polymers is around -35 ~ -40 mV in distilled water by our experiment, we believe that the PEG

composition formed a hydrophilic sheath around the particles and the surface charge is a result of the combined effects from the amine functional group and the poly(ethylene glycol) chains.

4.4.3.2 PRINT morphology in media

To study the influence of degradation on the particle size and shape, we further examined the particle morphology as immersed in pH 5 and pH 7.4 buffers over a period of 8 days. Particles (1 mg/mL) were suspended in the buffers, and each day, a drop of evenly dispersed solution was removed and sprayed on a glass slide. The size and shape of the particles were examined using an optical microscope (Figure 4-8). As can be seen by these images, the particles could maintain their original shape and size after 8 days of incubation in different buffers. This indicated that the degradation progressed via bulk erosion.[37]

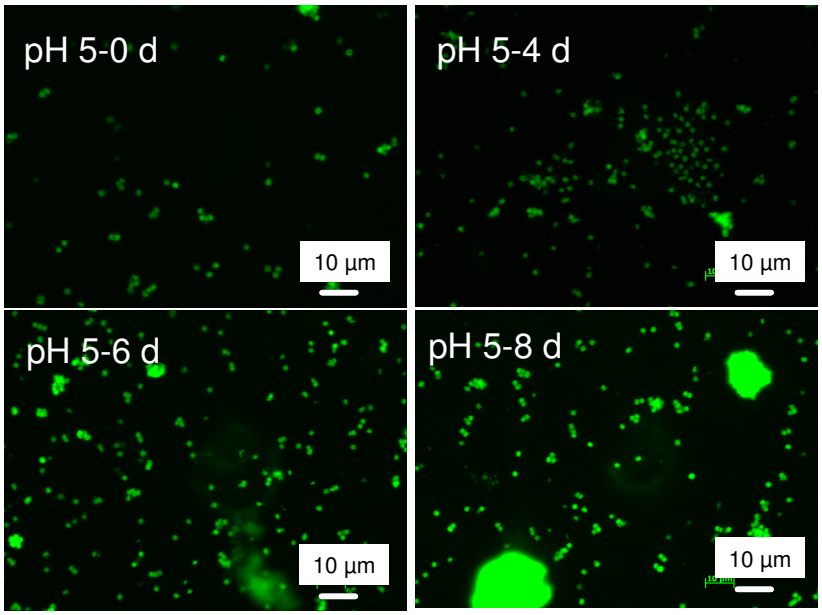

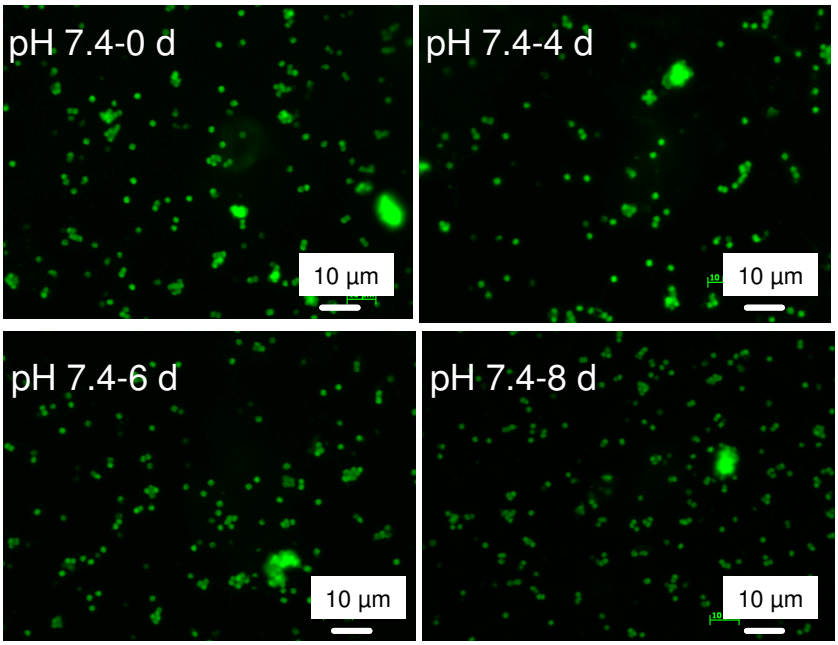

Figure 4-8. Microscopy images of particles in media for 8 days

4.4.3.3 Cytotoxicity of PRINT particles

We further studied the cytotoxicity of the fabricated particles using Hela cells. Particles (2 micron) in culture medium were incubated with HeLa cells (4.0×10^4) under different particle concentrations for 3 h, while the culture dish with only HeLa cells and medium was used as a control. At the end of the incubation, cell proliferation assay reagent was added to develop the colors. The viability was expressed as the ratio of the number of living cells to the original number of cells. Figure 4-9 shows high viability of the cells in the presence of high concentrations of microparticles, indicating the non toxic nature of the fabricated particles.

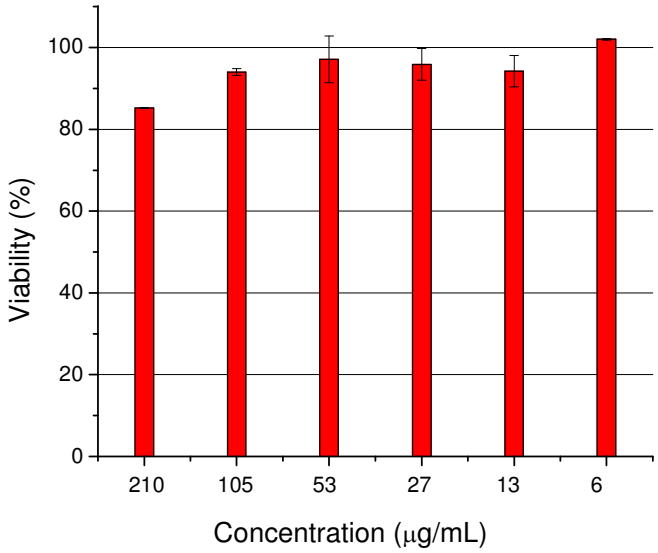

Figure 4-9. Cytotoxicity evaluation of the elastomeric particles. Percentage of Hela cell viability versus particle concentration

4.4.3.4 Cellular uptake of PRINT particles

When used drug release carriers, it is desired that particles can penetrate and release the drug inside cells, rather than only cell surface adhesion. We carried out the quantitative cellular uptake study by incubating a fixed population of the cells with graded concentration of particles. We wanted to explore the role of dose-dependency on the particle concentration. Hela cells were used for cellular uptake. Particles in different concentrations were added to Hela cell culture wells. The percentage of cellular uptake represents the fluorescein positive cells against all cells collected (Figure 4-10). For the 2 micron sized elastomeric particles, approximately 90% of the particles had been taken up by the cells at the concentration of 220 μg/mL, which was comparable to positively

charged particles of similar size[27] and indicated that the particles could be used as a potential drug release carrier.

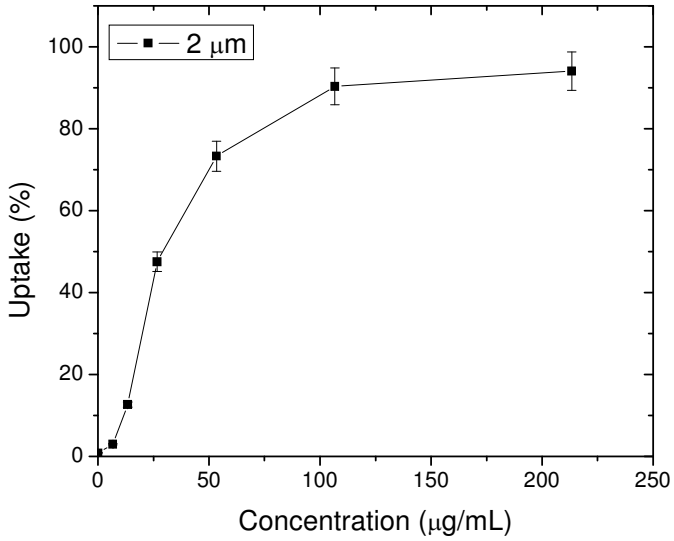

Figure 4-10. Cellular uptake of 2 micron sized particles by Hela cells in 3 h

4.4.4 Drug release study

In the following discussion, we studied first the applications of these elastomeric particles as drug release carriers for a hydrophobic drug model (Doxorubicin). Doxorubicin is a widely used hydrophobic anticancer agent, and numerous researchers are working in this field to develop its pH controlled release or protein sensitive release[13,18]. We are more interested in the pH adjusted drug release based on our elastomer structures. Furthermore, we incorporated a disulfide crosslinker to the drug release system and studied its adjustment to the Doxorubicin release. Lastly, we explored the amine-disulfide containing particles as a hydrophilic drug release carrier. Minocycline hydrochloride (MCH) was selected as a hydrophilic drug model. MCH, a member of the tetracycline antibiotic family, is useful in the treatment of a host of topical

bacterial infections. The tetracyclines are known to be moisture sensitive and unstable under conditions of low or high pH, heat and high humidity. Thus, a non-aqueous matrix was proposed to be a more appropriate vehicle for MCH because the absence of moisture in the matrix would prevent MCH degradation.[38] Our particles can be a good MCH release matrix given the nature of our fabrication method.

4.4.4.1 Doxorubicin release from the amine containing particles

First of all, Doxorubicin containing particles (2 micron) were fabricated using the following formulation: 77 wt% methacrylate endcapped prepolymers (Prepolymer 3), 20 wt% PEG monomethyl ether monomethacrylate, 1 wt% 2,2-diethoxyacetophenone, and 2 wt% Doxorubicin (DOX). Since we fabricated the particles with the drug homogeneously dispersed inside of the precursor, the loading efficiency is the same as the feed amount, which is an advantage over the current loading techniques in which the loading efficiency depends on the ratio of the DOX and the mixture.[18] After we fabricated the particles, we suspended them in pH 5 buffer and pH 7.4 buffer with the concentration of 2 mg/mL (particles/buffer) for 0.5 h. Then the suspensions were put into the dialysis tube and immersed in 20 mL buffer solutions. During each sampling point, 0.5 mL solution was taken out and UV-vis spectrometry was used to study the released DOX. Figure 4-11 shows the drug release profile of DOX in different buffer solutions, expressed as the percentage of accumulated amounts of DOX in the solution versus the study time. In the first 24 h, the drug released in both buffer solutions is similar, fast initial burst release followed by a slower release. After 24 h, the release differed for both solutions. For particles immersed in pH 5 buffer, the release amount was constant at 30% for the following 40 hours, and the release accelerated after 92 h to 45%. For particles immersed

in pH 7.4 buffer, the drug was almost linearly released after 24 h incubation in the medium to 76% after 92 h. The study of water uptake and degradation for the elastomers suggest that the DOX release is a degradation controlled process under these conditions. In pH 5 buffer, the polymer chains showed strong intramolecular interactions and the drug did not leach out very quickly. But for particles in pH 7.4 buffer, the particles began to degrade faster than in pH 5 buffer, and we can observe more DOX released in this system.

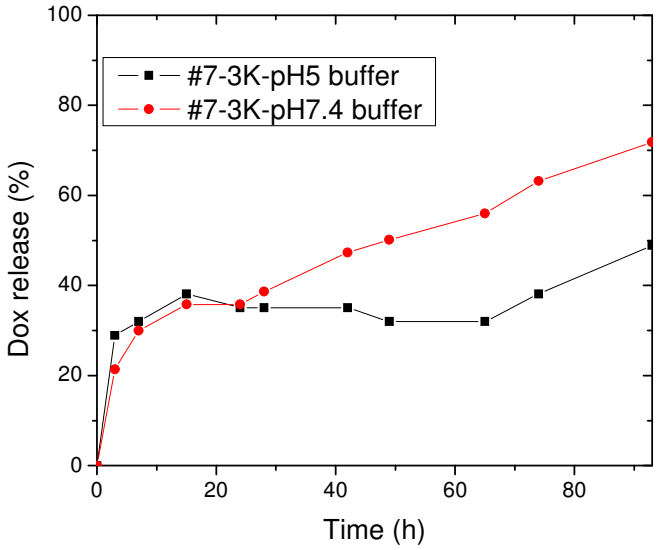

Figure 4-11. Percentage of Doxorubicin released in pH 5 and pH 7.4 buffers versus time

4.4.4.2 Doxorubicin release from amine-disulfide containing particles

One of the advantages of PRINT is that different raw materials can be easily incorporated into the particle matrix. We incorporated a disulfide crosslinker into our elastomeric particle matrix and the DOX release trend in pH 5 and pH 7.4 buffers switched. The synthesis of the disulfide crosslinker is shown in Figure 4-12. It is a yellow

liquid, and compatible with our photo fabrication process. ^{1}H NMR spectrum (in Appendix C) was consistent with the published results.[24]

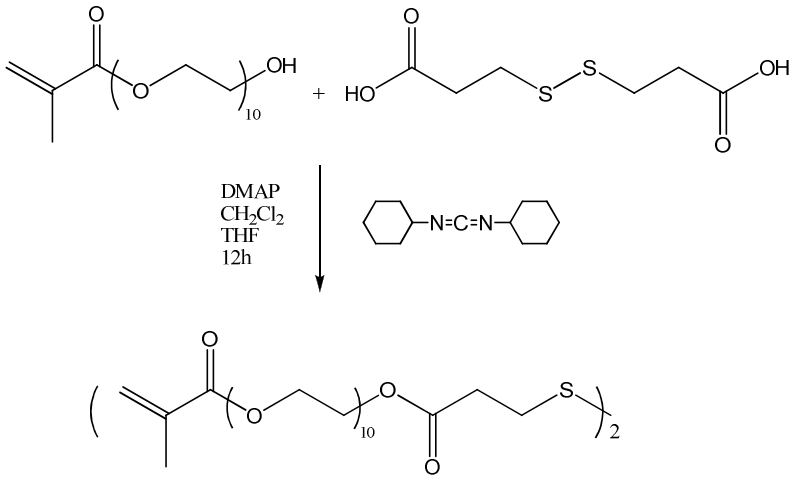

Figure 4-12. Synthesis of disulfide containing dimethacrylate

Doxorubincin loading particles were fabricated from the following formulation: 50 wt% methacrylate endcapped prepolymers (Prepolymer 3), 20 wt% PEG monomethyl ether monomethacrylate, 20 wt% PEG disulfide dimethacrylate, 9 wt% Doxorubicin and 1 wt% 2,2-diethoxyacetophenone. The drug release experiments were the same as above. As can be seen from the profiles (Figure 4-13), the incorporation of disulfide crosslinker changed the release trend of DOX in two buffers. Herein, DOX released faster in pH 5 buffer than in pH 7.4 buffer, which can be explained as the elastomers degraded faster in pH 5 than in pH 7.4 buffers (the data in Appendix C). The accumulative release for DOX in pH 5 buffer was 50% after 10 h release study, and 24% at pH 7.4 buffer after 6 h. It was surprising to notice that the absorbance of DOX decreased as the experiment progressed after 4 h in pH 7.4 buffer and 8 h in pH 5 buffer. We observed the decreasing amount of DOX in the release medium in the profiles. The reason for this phenomena is not sure, and it could result from the interaction of the disulfide groups with the released

drug since this phenomena did not show up in the previous experiments, where only the disulfide crosslinker was omitted.

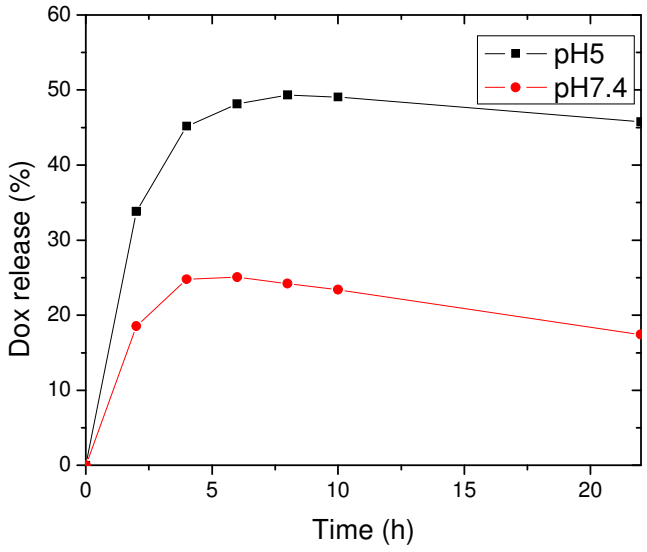

Figure 4-13. Percentage of Doxorubicin released in pH 5 and pH 7.4 buffers versus time

4.4.4.3 Minocycline hydrochloride release from amine-disulfide containing particles

Minocycline hydrochloride (MCH) was chosen as the hydrophilic drug model, and our particles showed promising result as this drug release vehicle. The formulation was as follows: 50 wt% methacrylate endcapped prepolymers (Prepolymer 3), 20 wt% PEG monomethyl ether monomethacrylate, 20 wt% PEG disulfide dimethacrylate, 9 wt% MCH and 1 wt% 2,2-diethoxyacetophenone. The fabrication method was the same and the procedures for the drug release study were the similar as above. The only difference is that 2.5 mg/mL Glutathione reduced ethyl ester was used along with the pH 5 and pH 7.4 buffer solutions. Glutathione is a tripeptide found within cells at millimolar concentrations. It is used as a reducing agent to degrade disulfide-containing polymers

and does not exhibit significant cytotoxicity at the concentration of 10 mM.[18] The *in vitro* release study was carried out at 37 °C with stirring. For each sampling point, we removed 250 μL release medium and measured the drug amounts by HPLC with acetonitrile/water as the eluents at 350 nm. The release profiles can be seen by Figure 4-14, where the percentage of MCH release was shown versus the release time for a total run of 45 h.

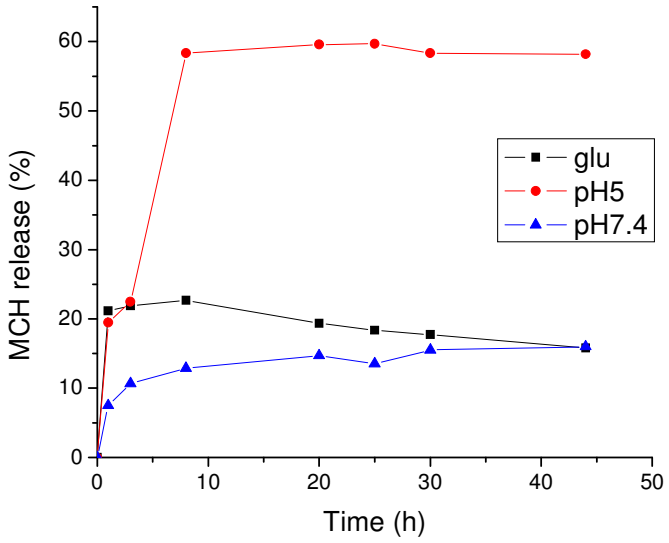

Figure 4-14. Minocycline hydrochloride (MCH) release study in different media at 37 °C

There were three trends indicated from the release profiles. First, the drug release in glutathione solution was not gradually increasing. After a burst release in the first hour, the release profile stabilized for around 10 h and then slightly decreased. By careful examination of HPLC profiles for the three systems, we observed the degradation components from the HPLC curves, which was not visible in the first several hours, and the amount was increasing as the study progressed. Moreover, we did not observe these peaks in the other two buffer systems. It is hypothesized that the reducing agent, glutathione, degraded the released minocycline hydrochloride. The total release after 45 h is around 16%. Second, the release in pH 7.4 buffer did not show burst release in the first

several hours, and the release was gradually increasing. After the 45 h study, the percentage of drug release is about 16%, which indicated that our disulfide-amine elastomeric particles could be a good system for controlled release of this type of drug. Third, the release of MCH in pH 5 buffer significantly differed from the others. During the first 3 h, the released amount of MCH was close to the MCH released amount in the glutathione solution. There was about 20% drug released in the medium. After that, the releases rate jumped up and then stabilized near 59%. The release trend of MCH in pH 5 and pH 7.4 buffers was slightly different from DOX release in these two buffers. The reason for the difference is still under study, and it is possibly from the nature of the two drugs (DOX is hydrophobic and MCH is more hydrophilic). It has been reported that the disulfide-based polyamide degraded faster in pH 5 buffer than it did in pH 7 and pH 9 buffers.[23]

4.5 Conclusions

In this chapter, we described the synthesis of novel amine containing photocurable polyesters. By controlling the feed ratio of the monomers, we can fabricate amorphous elastomers with variable molecular weight. By using the new developed PRINT technology, we fabricated monodispersed particles from this material. The cytotoxicity study indicated the fabricated particles are nontoxic to Hela cells and the cellular uptake study showed that a high percentage of particles can penetrate into Hela cells even at rather high concentration. Based on this information, we fabricated particles loaded with Doxorubicin (as a hydrophobic drug model) and Minocycline hydrochloride

(as a hydrophilic drug model) and studied the drug release in pH 5 and pH 7.4 buffers. The difference in the release behavior may come from the nature of the two drugs and/or from the composition of the particle formulation.

4.6 References

1. Lim, Y.; Choi, Y. H.; Park, J. *J. Am. Chem. Soc.* **1999***, 24,* 5633-5639.
2. Pillai, O.; Panchagnula, R. *Curr. Opin. Chem. Biol.* **2001***, 4,* 447-451.
3. Uhrich, K. E.; Cannizzaro, S. M.; Langer, R. S.; Shakesheff, K. M. *Chem. Rev.* **1999***, 11,* 3181-3198.
4. Gu, F.; Neufeld, R.; Amsden, B. *J. Control. Release* **2007***, 1,* 80-89.
5. Gu, F.; Younes, H. M.; El-Kadi, A. O. S.; Neufeld, R. J.; Amsden, B. G. *J. Control. Release* **2005***, 3,* 607-617.
6. Amsden, B. *Soft Matter* **2007**, 1335-1348.
7. Lynn, D. M.; Amiji, M. M.; Langer, R. *Angew. Chem. Int. Ed* **2001***, 40,* 1707-1710.
8. Lynn, D. M.; Langer, R. *J. Am. Chem. Soc.* **2000***, 44,* 10761-10768.
9. Shenoy, D.; Little, S.; Langer, R.; Amiji, M. *Mol. Pharmacol.* **2005***, 2,* 357-366.
10. Wu, C.; Hao, J.; Deng, X. *Polymer* **2007***, 21,* 6272-6285.
11. Anderson, D. G.; Akinc, A.; Hossain, N.; Langer, R. *Mol. Ther.* **2005***, 11,* 426-434.
12. Lim, Y. -.; Kim, C. -.; Kim, K.; Kim, S. W.; Park, J. -. *J. Am. Chem. Soc.* **2000***, 27,* 6524-6525.
13. Na, K.; Lee, E. S.; Bae, Y. H. *Bioconjugate Chem.* **2007***, 5,* 1568-1574.
14. Unger, F.; Wittmar, M.; Morell, F.; Kissel, T. *Biomaterials* **2008***, 13,* 2007-2014.
15. Zhong, Z.; Song, Y.; Engbersen, J. F. J.; Lok, M. C.; Hennink, W. E.; Feijen, J. *J. Control. Release* **2005***, 1-3,* 317-329.
16. Hermanson, G. T. Thiol-Reactive Chemical Reactions. In *Bioconjugates Techniques;* 1996; pp 146.

17. Ou, M.; Wang, X.; Xu, R.; Chang, C.; Bull, D. A.; Kim, S. W. *Bioconjugate Chem.* **2008***, 3,* 626-633.

18. Oh, J. K.; Siegwart, D. J.; Lee, H. -.; Sherwood, G.; Peteanu, L.; Hollinger, J. O.; Kataoka, K.; Matyjaszewski, K. *J. Am. Chem. Soc.* **2007***, 18,* 5939-5945.

19. Lin, C.; Lammens, T. M.; Zhong, Z. Y.; Gu, H.; Lok, M. C.; Jiang, X.; Hennink, W. E.; Feijen, J.; Engbersen, J. F. J. *J. Control. Release* **2006***, 2,* 79-81.

20. Lin, C.; Blaauboer, C.; Timoneda, M. M.; Lok, M. C.; van Steenbergen, M.; Hennink, W. E.; Zhong, Z.; Feijen, J.; Engbersen, J. F. J. *J. Control. Release,* **2008***, 2,* 166-174.

21. Lin, C.; Zhong, Z.; Lok, M. C.; Jiang, X.; Hennink, W. E.; Feijen, J.; Engbersen, J. F. J. *J. Control. Release,* **2006***, 2,* 130-137.

22. Emilitri, E.; Ranucci, E.; Ferruti, P. *J. Polym. Sci. Part A: Polym. Chem.* **2005***, 43,* 1404-1416.

23. Tsutsumi, H.; Okada, S.; Oishi, T. *Electrochimica Acta* **1998***, 43,* 427-429.

24. Oh, J. K.; Tang, C.; Gao, H.; Tsarevsky, N. V.; Matyjaszewski, K. *J. Am. Chem. Soc.* **2006***, 16,* 5578-5584.

25. Li, Y.; Armes, S. P. *Macromolecules* **2005***, 20,* 8155-8162.

26. Davis, K. A.; Matyjaszewski, K. *Adv. Polym. Sci* **2002***, 159,* 2-166.

27. Gratton, S. E. A.; Ropp, P. A.; Pohlhaus, P. D.; Luft, J. C.; Madden, V. J.; Napier, M. E.; Desimone, J. M. *PNAS* **2008**.

28. Gratton, S. E. A.; Pohlhaus, P. D.; Lee, J.; Guo, J.; Cho, M. J.; DeSimone, J. M. *J. Control. Release* **2007***, 121,* 10-18.

29. Ali, M. M.; Stover, H. D. H. *Macromolecules* **2004***, 14,* 5219-5227.

30. Lin, C.; Zhong, Z.; Lok, M. C.; Jiang, X.; Hennink, W. E.; Feijen, J.; Engbersen, J. F. J. *Control. Release* **2007***, 1,* 67-75.

31. You, Y.; Manickam, D. S.; Zhou, Q.; Oupický, D. *J. Control Release* **2007***, 3,* 217-225.

32. Zugates, G. T.; Peng, W.; Zumbuehl, A.; Jhunjhunwala, S.; Huang, Y.; Langer, R.; Sawicki, J.; Anderson, D. *Mol. Ther.* **2007***, 15,* 1306-1312.

33. Anderson, D. G.; Tweedie, C. A.; Hossain, N.; Navarro, S. M.; Brey, D. M.; Vliet, K. J.; Langer, R.; Burdick, J. A. *Adv. Mater.* **2006**, *18*, 2614-2618.

34. Pierce, B.; Ashby, V. *Unpublished results*.

35. Anderson, D. G.; Akinc, A.; Hossain, N.; Langer, R. *Mol. Ther.* **2005***, 11,* 426-434.

36. Olson, D. A.; Gratton, S. E. A.; DeSimone, J. M.; Sheares, V. V. *J. Am. Chem. Soc.* **2006***, 41,* 13625-13633.

37. Doi, Y.; Steinbuchel, A. In *Biopolymers: Polyester(3).* Wiley-Vch: Germany, Vol. 4, pp 398.

38. Chow, K. T.; Chan, L. W.; Heng, P. W. S. *Pharma. Res.* **2008***, 25,* 207-217.

CHAPTER 5

GENERAL CONCLUSIONS

This dissertation focused on the use of a photo curable method to prepare biodegradable soft materials which have improved properties over the current available biomaterials. Specifically, polycondensation polymerization techniques were utilized to prepare prepolymer liquids.

Chapter 2 served as the foundation for the rest of the work described in this dissertation. This chapter described the development of polymerization conditions and a full understanding of the properties of the resulting materials. By controlling the feed ratio of adipic acid and diethylene glycol or tetraethylene glycol, a series of hydroxyl endcapped polyester liquids with number average molecular weight ranging from $1x10^3$ g/mol to $7x10^3$ g/mol were prepared. With the help of triethylamine, the hydroxyl endcapped liquids reacted with methacrylol chloride to afford methacrylate group endcapped polyester liquids, which can be easily photocured in 2 min with only 0.1 wt% photoinitiator. At these conditions, we can fabricate completely colorless and amorphous elastomers with Young's modulus (G) ranged from 0.1-10 MPa and strain (ε) from 30-170%, which is in the mechanical range for some soft tissues inside of the body, such as knee articular cartilage (G = 2.1-11.8 MPa) and cerebral vein (G = 6.85 MPa and ε = 83 %). The degradation studies showed that these elastomers were rapidly degrading materials with weight loss up to 16% after 5 weeks of incubation in PBS at 37 ºC, which is one of the fastest degrading materials fabricated under similar conditions. The water-in-air contact angle results demonstrated that these elastomers were hydrophilic, and cytotoxicity studies indicated that these elastomers were nontoxic at the test conditions. All of these data implied that our elastomers could be good candidates as scaffolds for soft tissue replacement in tissue engineering.

Chapter 3 was the further study of the elastomers performance *in vivo.* We chose to subcutaneously implant these elastomers on the dorsal parts of rats. Similar approaches have been widely used in literature with the commercial biomaterial PLGA used as the control. Compared with the commercial biomaterial, which totally deformed after 3 weeks of the *in vivo* study, our materials could maintain their structural integrity throughout the experiment. This result meant that our materials were promising as the scaffolds in tissue engineering, since it is desired that the scaffolds be able to maintain their structure for a period of time until the newly formed tissue can function well. The weight loss results showed that the elastomers followed the same dependence on the prepolymer molecular weight as the *in vitro* degradation study, but with faster degradation rates, and the highest weight loss of 26% after 7 weeks of implantation. Although the mechanical properties decreased as the degradation progressed, our materials remained in the mechanical range of several soft tissues.

Since the photocurable method is easier to operate and faster than the thermal curing method, we fabricated bilayer scaffolds to mimic a small diameter blood vessel to take advantage of the mechanical properties, biocompatibility and fabrication method of our materials. The future direction for this project can be carried on to study the mechanical properties of this bilayer scaffold and tune the thickness of layers, pore size and distribution. As well, the nutrition flow, burst pressure and cell seeding on the scaffolds can be further explored.

Better than seeding cells on the scaffolds, there are numerous researches on growth factor eluting scaffolds. The photocurable method should be good at maintaining

the bioactivity of the growth factors. And also, porous and nonporous scaffolds in different shapes can be easily fabricated from the salt-leaching method.

Since the amine containing elastomers can be easily changed into cationic materials (in Chapter 4), it is possible to combine the neutral and cationic materials together to design some patterned surface to tune cell responsiveness and growth, which can be useful as micropatterned scaffolds.

Chapter 4 utilized the versatility of step growth polymerization to expand the functionality of the photocurable elastomers by incorporation of amine containing monomers into the polymer backbone. By controlling the amount of the two diols, we can prepare completely amorphous polyester liquids with $\langle M_n \rangle$ from $1x10^3$ g/mol to $6x10^3$ g/mol. As well, after endcapping with methacrylate groups, these liquids can be photocured at room conditions. We further studied the potential of these amine containing elastomers as drug release carriers. Instead of using the common drug loading particle methods, we fabricated monodispersed 2 micron sized particles from PRINT technology which have better control of shape, distribution and size of the fabricated particles, which proved to play important roles in the particle uptake by targeted cells and also the amount and speed of drug release. The cytotoxicity study indicated the non toxic nature of the particles and the cellular uptake study was similar to the reported literature. The 2 μm sized amine containing elastomeric particle showed pH sensitive drug release at pH 5 and pH 7.5 buffers for Doxorubicin (DOX), a widely used anticancer drug, where DOX released faster in pH 7.5 buffer than it did in pH 5 buffer with the cumulative release of 72% in pH 7.4 buffer after the 82 h study. The incorporation of disulfide crosslinker switched the drug release properties in the other direction, which released

more DOX in pH 5 than pH 7.4 buffers. At the same time, Minocycline hydrochloride (MCH), which is an antibiotic and useful in the treatment of a host of topical bacterial infections, was studied as the model of hydrophilic drugs. We fabricated the similar drug loaded particles and studied the release of MCH in different buffers. The release of MCH in pH 5 showed burst release and then stabilized around 59%. But for the release in pH 7.4 buffer, the MCH release showed a controlled and gradual release profile, which is promising for use as a drug release carrier. Moreover, our particle fabrication avoids using any aqueous medium, making it a more appropriate vehicle for MCH because the absence of moisture in the matrix would prevent MCH degradation. Still, the release of MCH in pH 7.4 can be further carried out to study the long term release, and the cumulative amount since our preliminary experiment was carried out in 2 days.

To further explore the application of these particles as drug release carriers, it is possible to tune the size and shape of these particles to study the dependence of drug release on the physical structure of the particles. Also, the formulation of the particles can be adjusted to meet different requirements and to further study the influence of the disulfide crosslinker incorporation on the reducing agent sensitive release.

APPENDIX A

SUPPLEMENTAL MATERIALS FOR CHAPTER 2

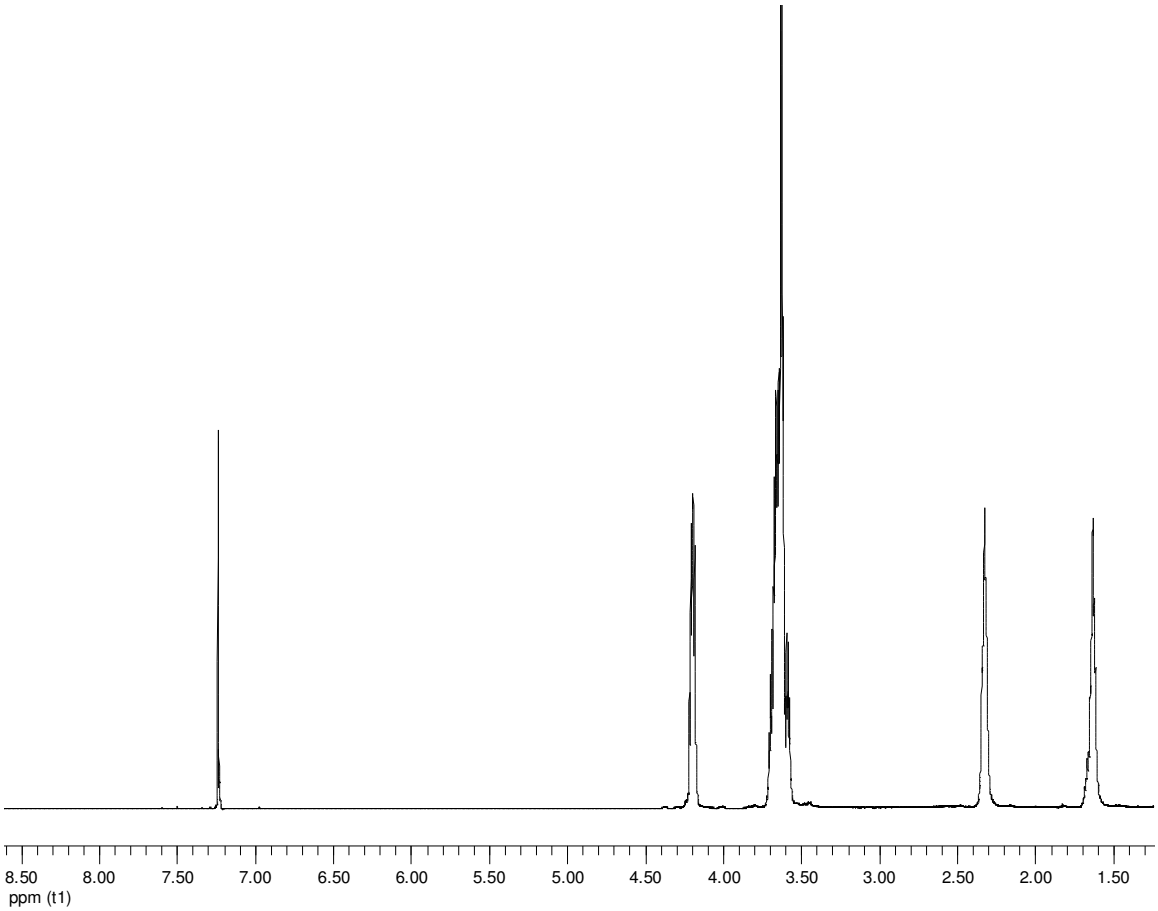

OH-AA-TEG-OH-2K

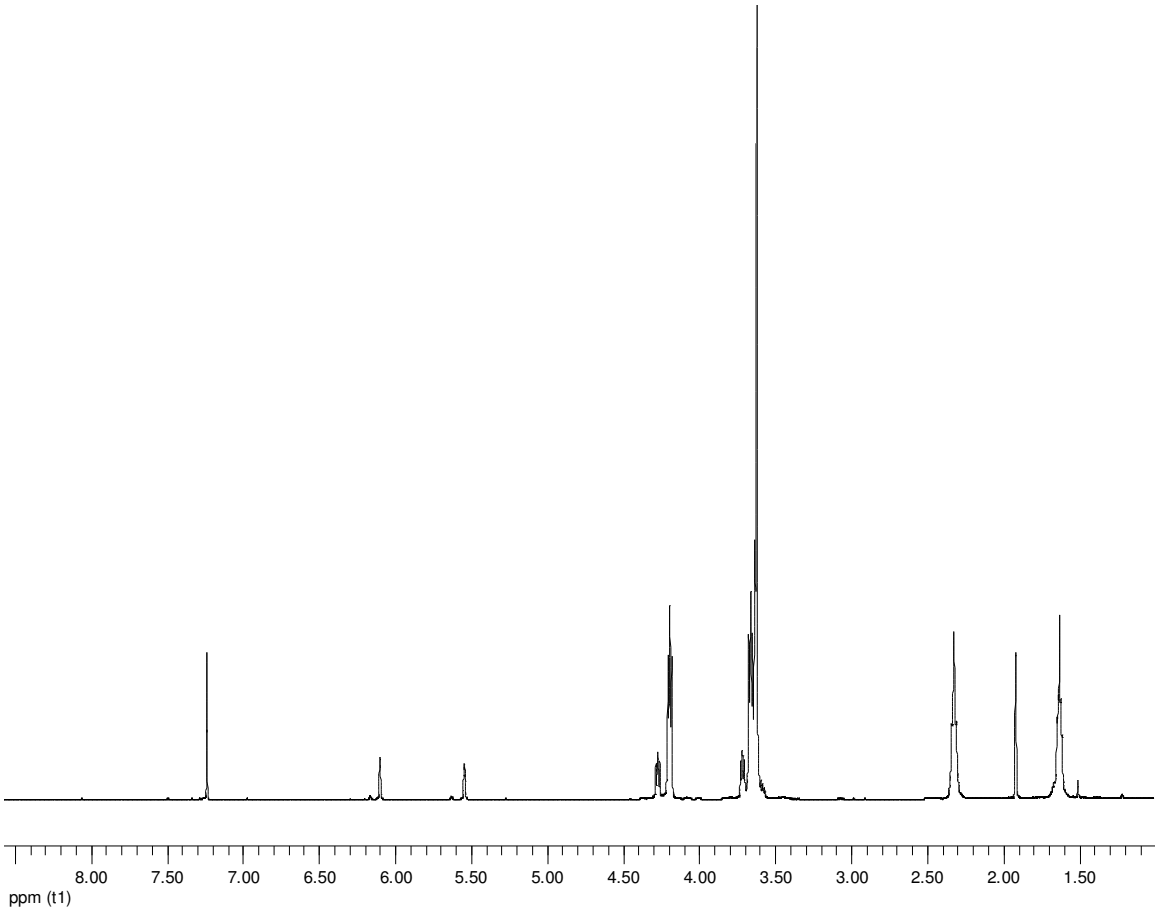

AA-TEG-2K

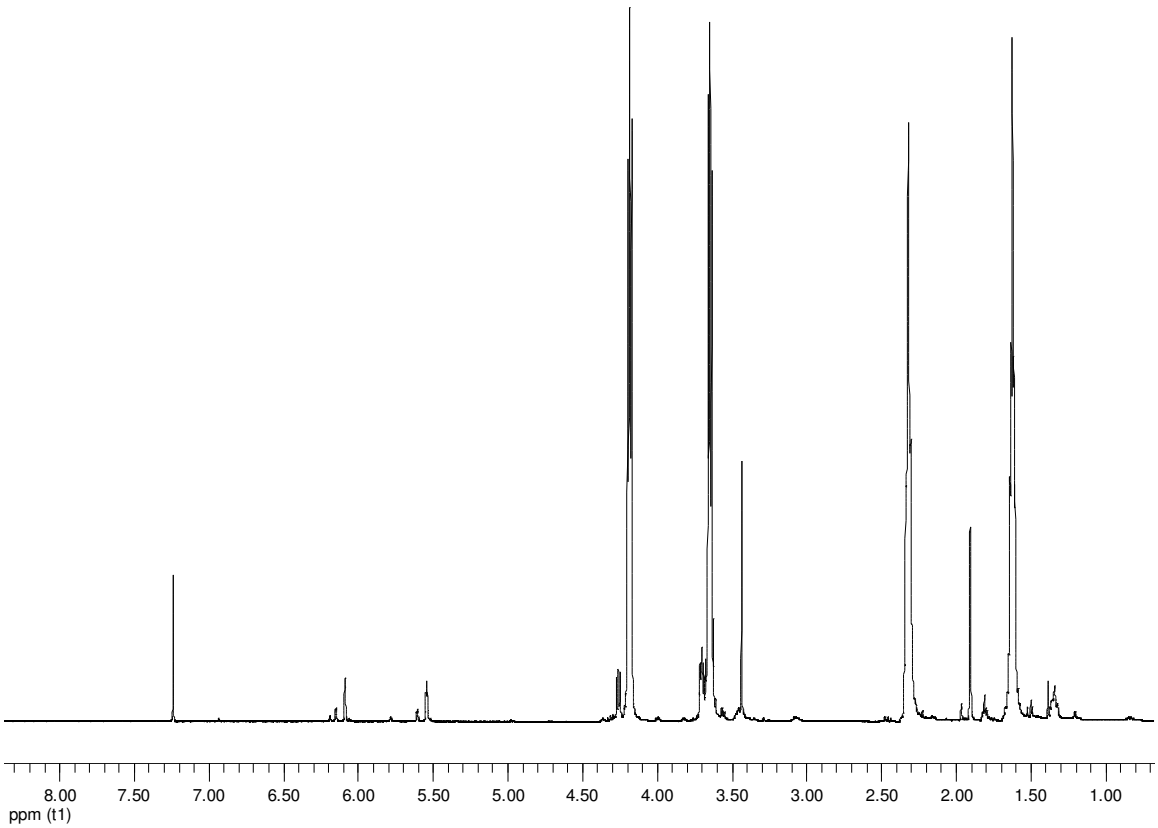
8.00
7.50
7.00
6.50
6.00
5.50
5.00
4.50
4.00
3.50
3.00
2.50
2.00
1.50
1.00
ppm (t1)

AA-DEG-4K-THF

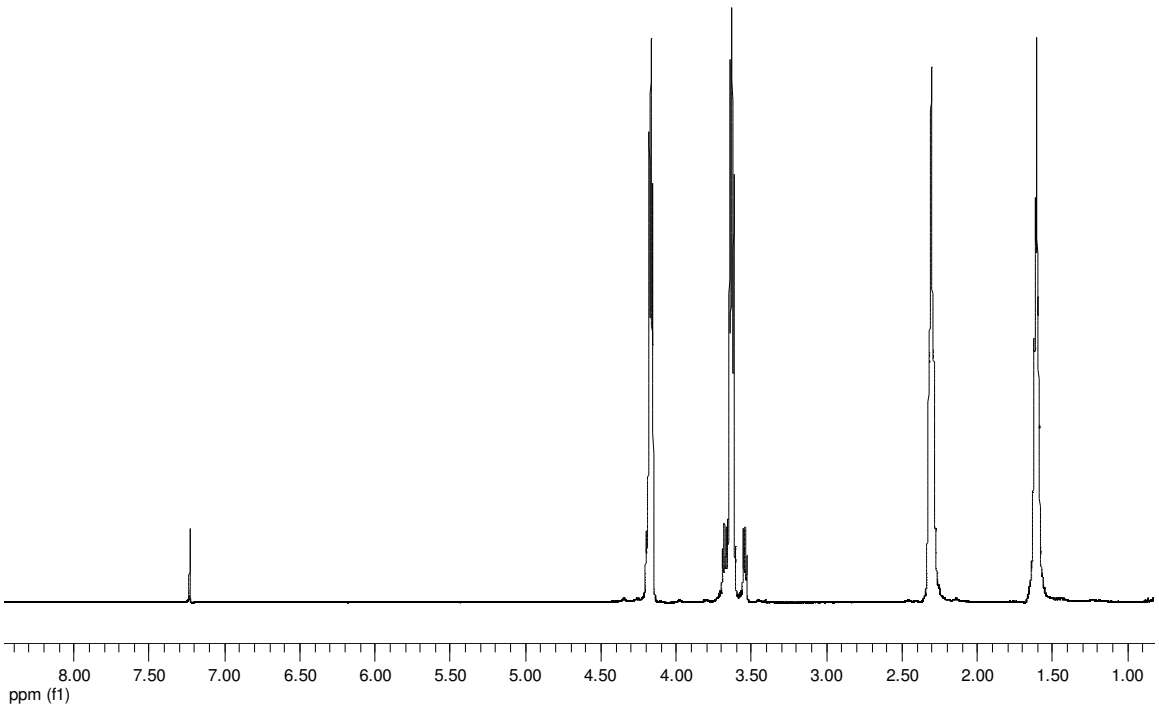

HO-DEG-AA-OH-4K

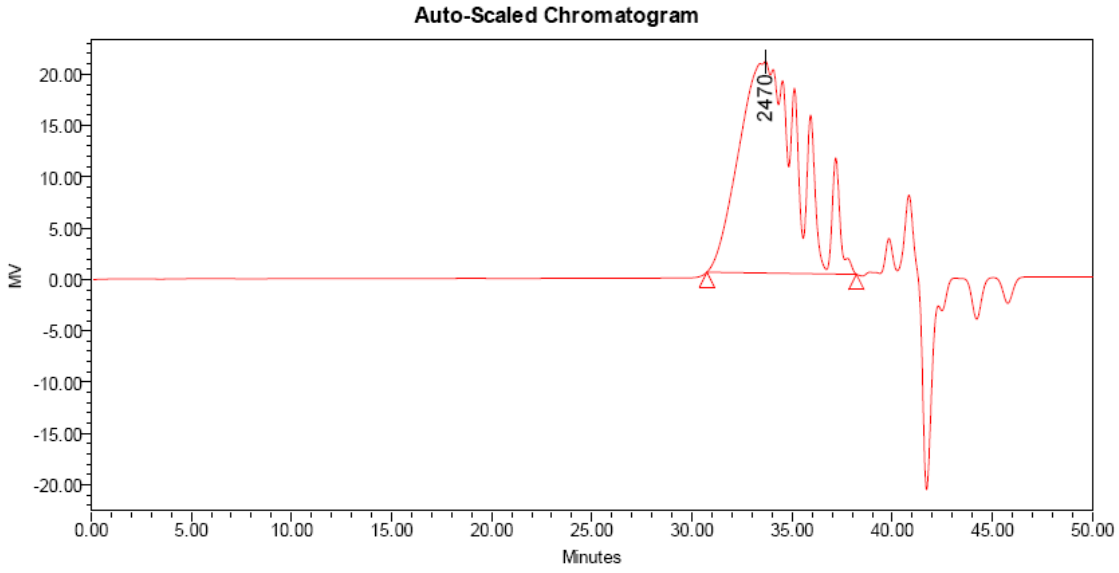

GPC Results

	Dist Name	Mn	Mw	Mv	MP	Mz	Mz+1	Poly dispersity	K	alpha
1		1368	2505		2470	3676	4695	1.831428		

DEG-1K

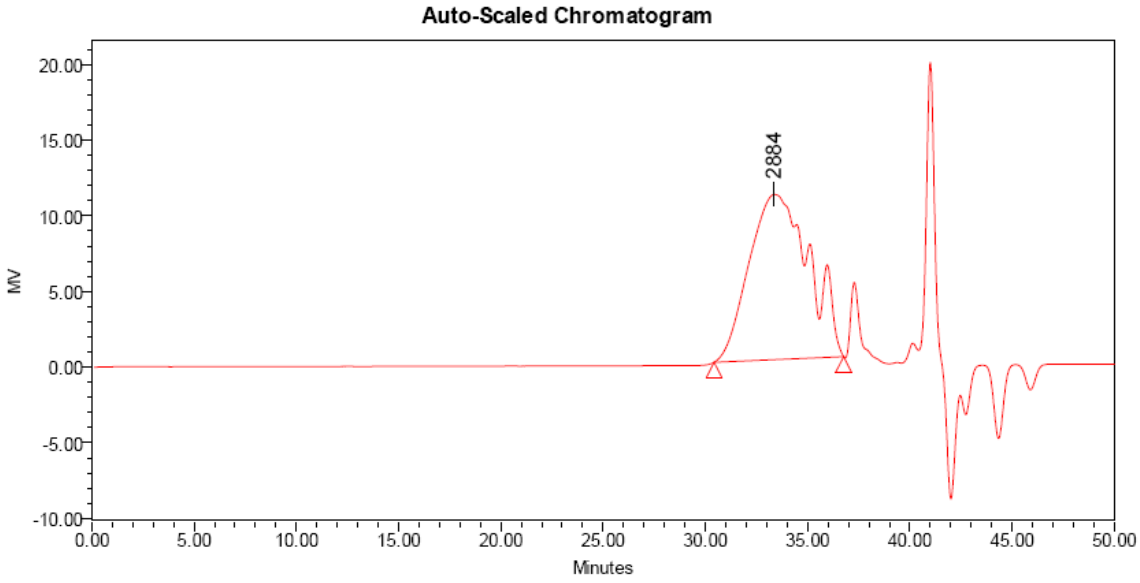

GPC Results

	Dist Name	Mn	Mw	Mv	MP	Mz	Mz+1	Poly dispersity	K	alpha
1		1904	2931		2884	4139	5289	1.539791		

DEG-2K

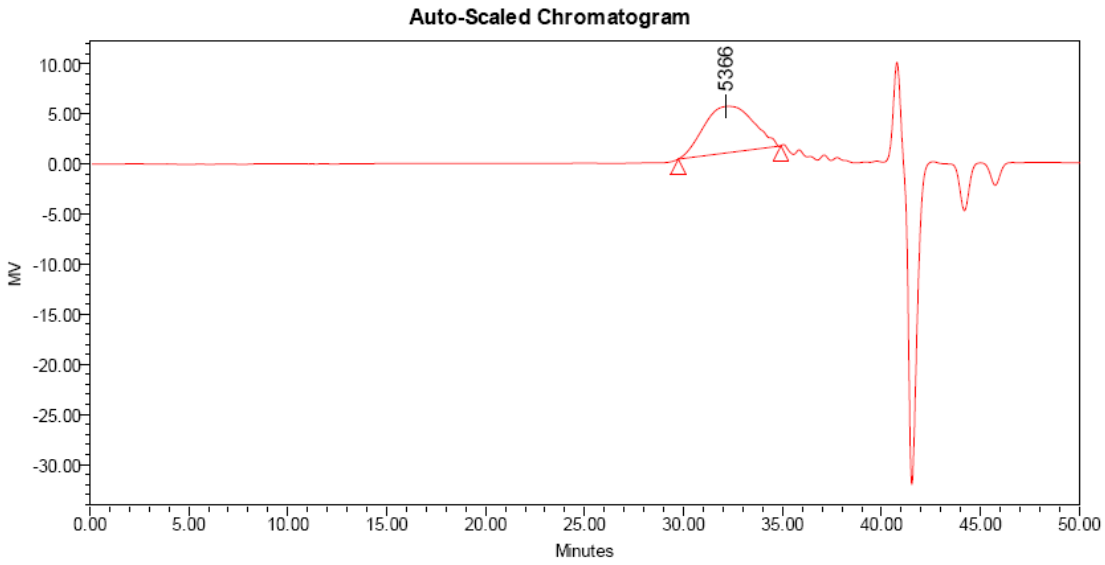

GPC Results

	Dist Name	Mn	Mw	Mv	MP	Mz	Mz+1	Poly dispersity	K	alpha
1		4341	5643		5366	7104	8516	1.299775		

DEG-4K

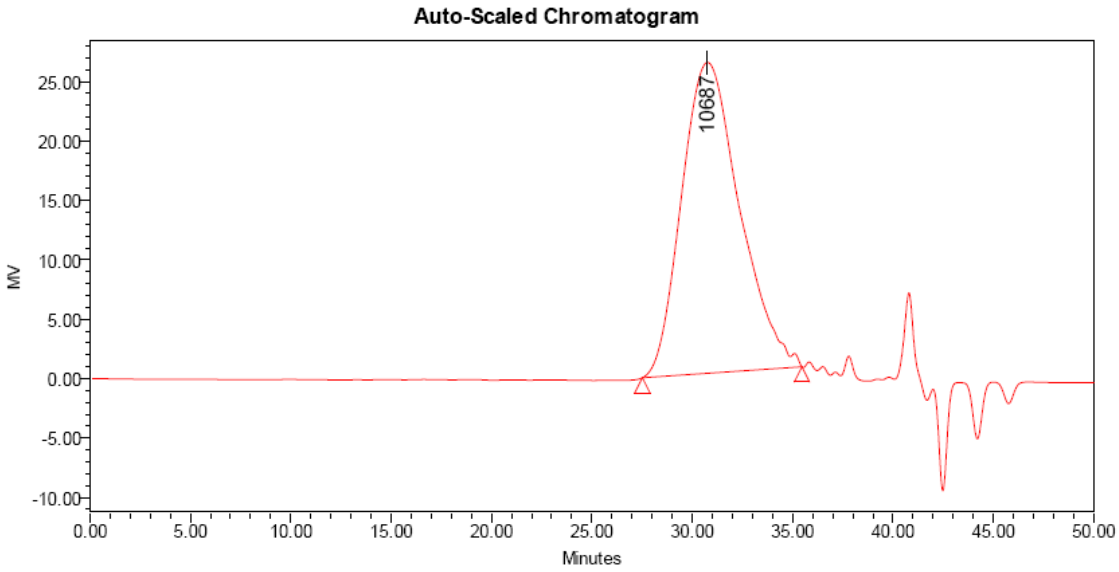

GPC Results

	Dist Name	Mn	Mw	Mv	MP	Mz	Mz+1	Poly dispersity	K	alpha
1		7069	11208		10687	15744	20215	1.585542		

DEG-7K

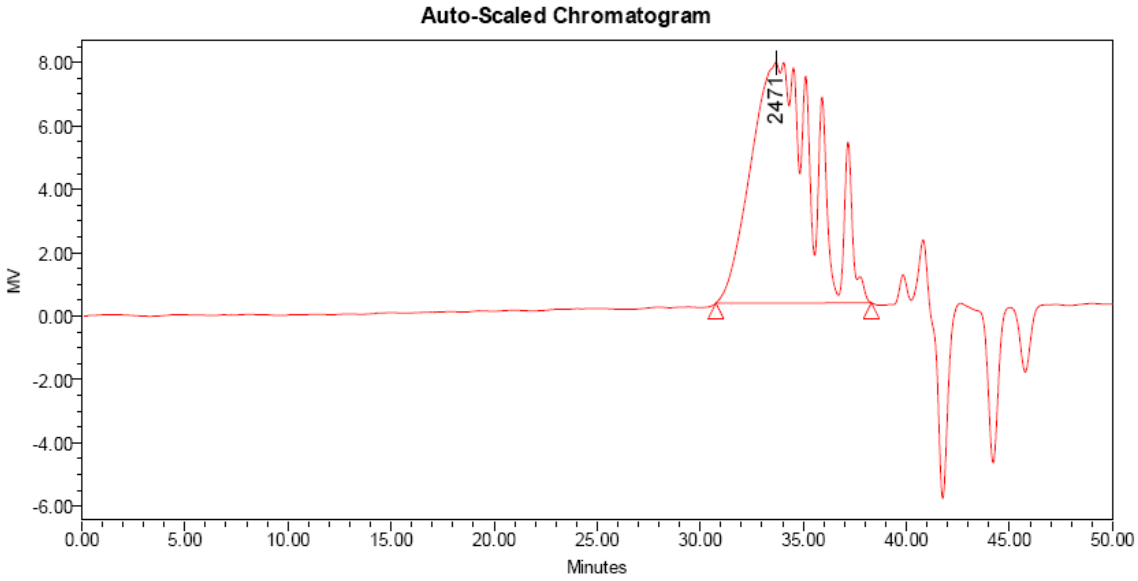

GPC Results

	Dist Name	Mn	Mw	Mv	MP	Mz	Mz+1	Poly dispersity	K	alpha
1		1252	2330		2471	3478	4491	1.861137		

TEG-1K

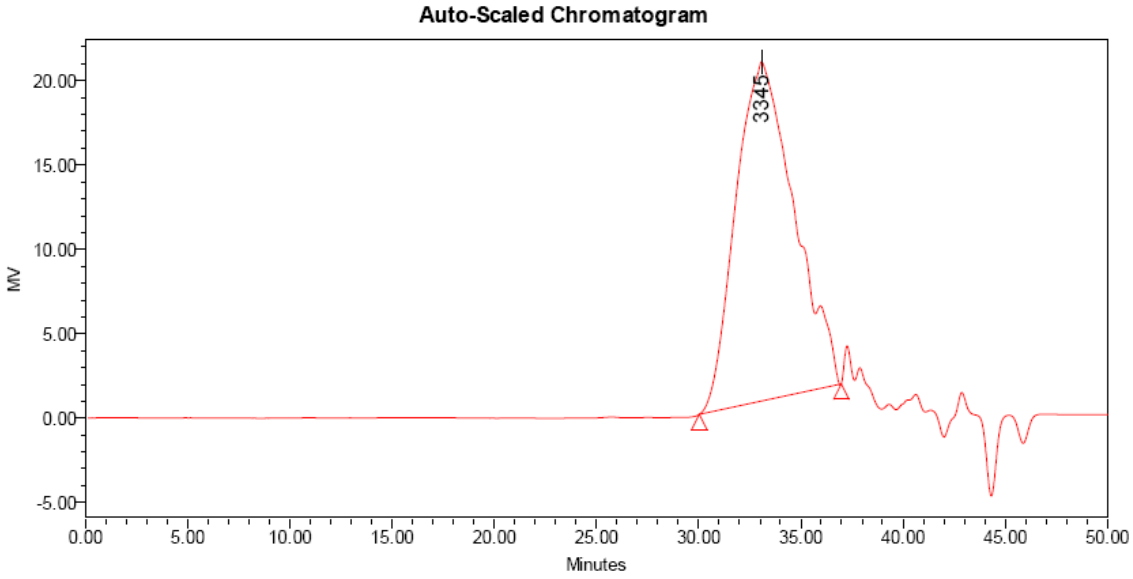

GPC Results

	Dist Name	Mn	Mw	Mv	MP	Mz	Mz+1	Poly dispersity	K	alpha
1		2205	3484		3345	4888	6187	1.580292		

TEG-2K

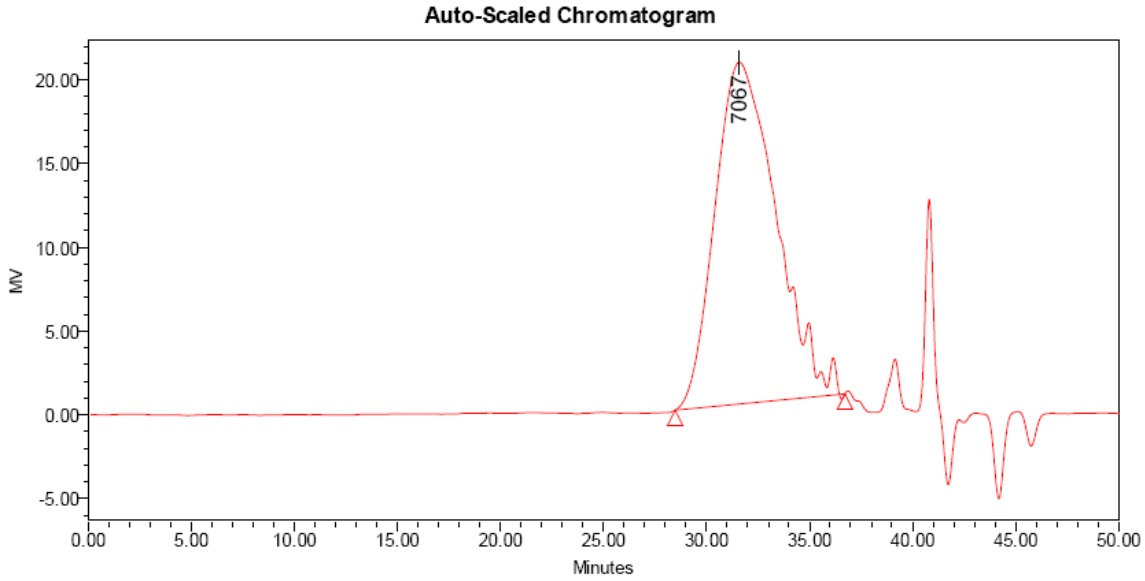

GPC Results

	Dist Name	Mn	Mw	Mv	MP	Mz	Mz+1	Poly dispersity	K	alpha
1		4134	6866		7067	9785	12591	1.661054		

TEG-4K

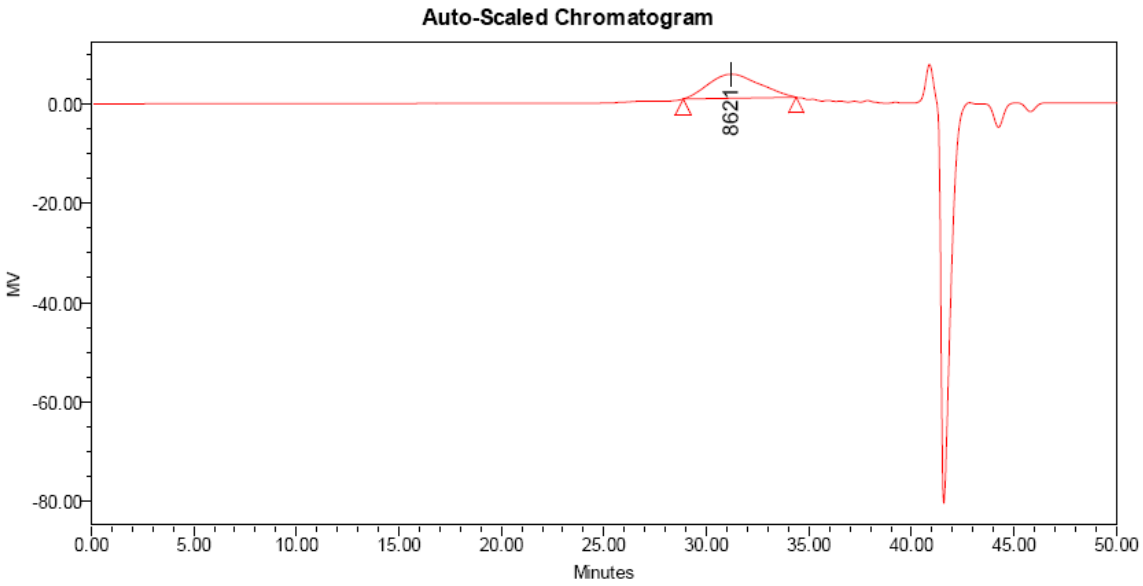

GPC Results

	Dist Name	Mn	Mw	Mv	MP	Mz	Mz+1	Polydispersity	K	alpha
1		6539	8755		8621	11156	13406	1.339009		

TEG-7K

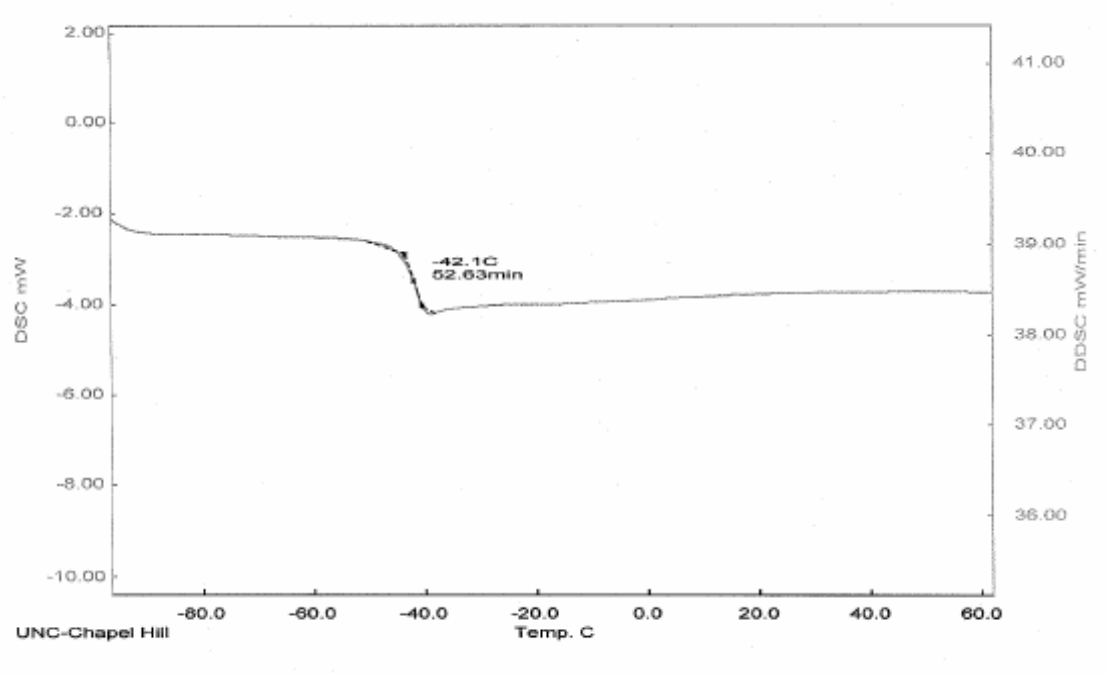

DEG-7K-Prepolymer

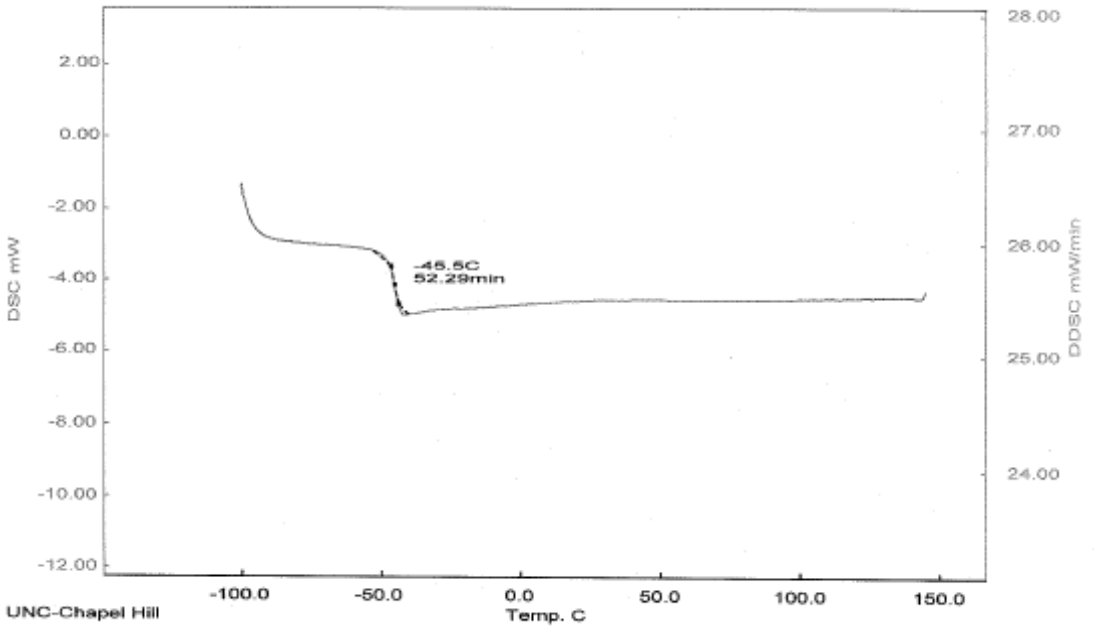

DEG-7K-elastomer

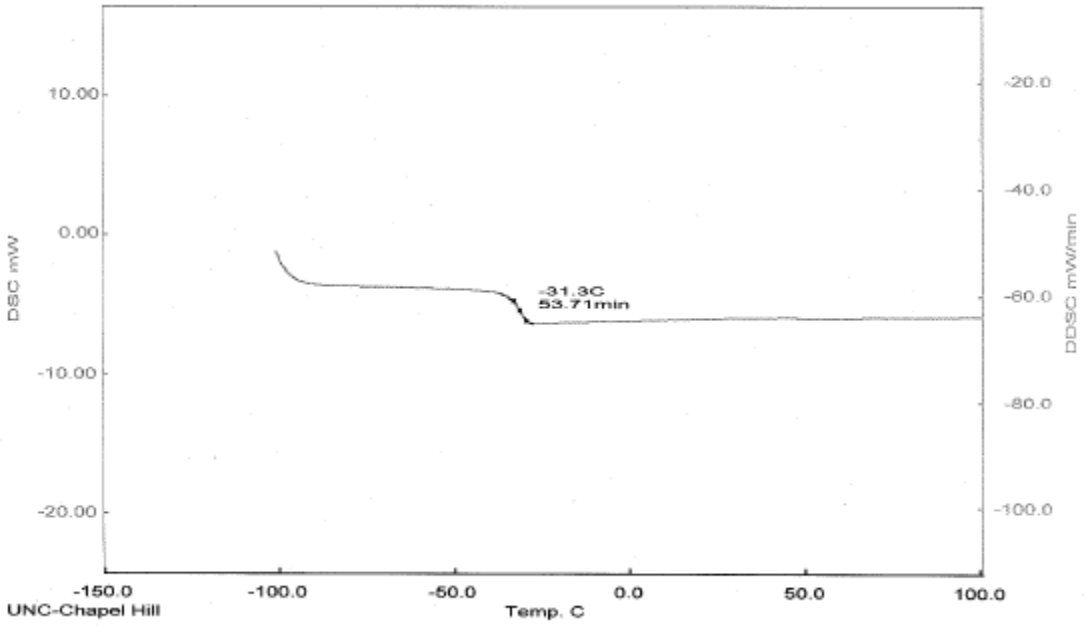

TEG-1K-Prepolymer

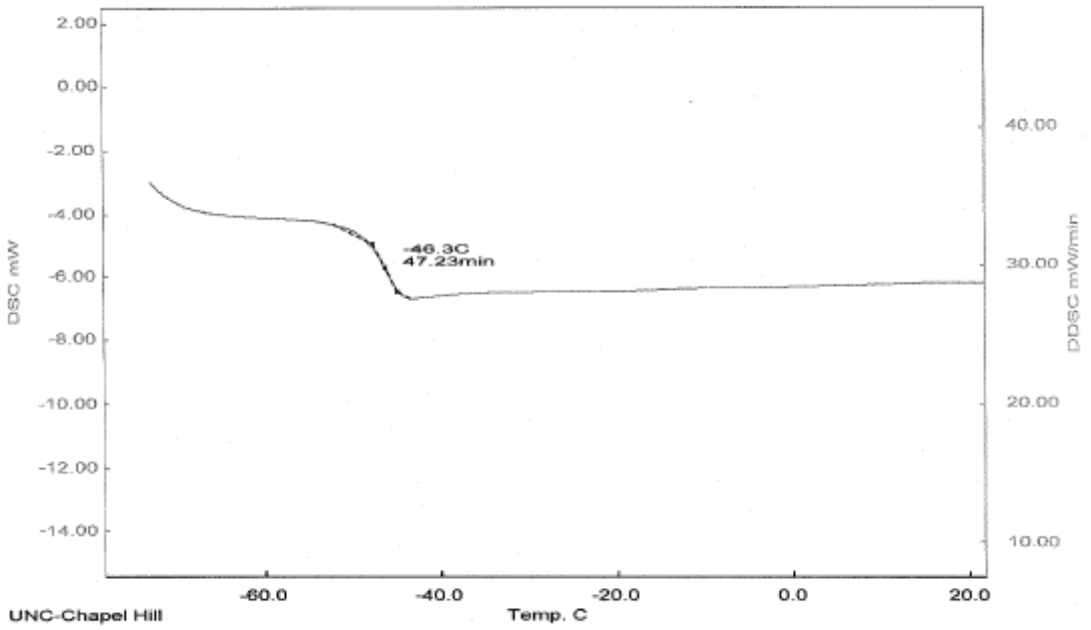

TEG-7K-Prepolymer

APPENDIX B

SUPPLEMENTAL MATERIALS FOR CHAPTER 3

Application to Use Live Vertebrate Animals

PI: Valerie S Ashby
Dept: Chemistry
IACUC ID: 07-217.0 Web ID: 9796

Title: in vivo biocompatibility study of a new biodegradable elastomer by subcutaneous implantation
Species: Rat (Sprague-Dawley female rats) ( )
Application Type: New Application
Multiple Species No
Total Animal Number: 15 (Dlam -)

IACUC Use Only

IACUC ID:	07-217.0-A
Renewal Date:	09/2008

No	1.1: Are there confidential or potentially patentable issues?
Yes	1.2: Will collaborator(s), other than the PI, Co-PI or approved personnel within the PI's laboratory, perform any procedures on animals in this animal use application?
Yes	3.1: Will animals be housed or used in any DLAM, investigator laboratory, or other space?
Yes	3.2: Are you requesting that DLAM conduct animal procedures?
No	3.3: Will animals be housed outside DLAM-managed area for >12 hours? (Satellite Facility Form)
No	3.4: Are study animals free-ranging wildlife?
Yes	4.1: Will animals experience potential pain and/or distress as a result of the study or phenotype?
No	5.1: Will animals be bred as part of this study?
No	5.2: Will animals be used in a terminal surgical procedure (non-survival surgery)?
Yes	5.3: Will animals undergo a surgical procedure from which they recover (survival surgery)?
No	5.4: Will tumors be induced in study animals or may they form spontaneously?
No	5.5: Will behavioral and/or conditioning experiments be conducted?
No	5.6: Will conscious animals be physically restrained?
No	5.7: Will animals experience weight loss as a result of this study?
Yes	5.8: Will tissues be collected from live or dead animals?
No	5.9: Will blood or body fluids be collected from live or dead animals?
No	6.1: Will animals be given food and/or fluids other than that provided by DLAM in regular husbandry? Will food and/or fluids be restricted?
No	8: Are you requesting an exception to established regulation or IACUC policy?
No	9: Will animal be used for monoclonal antibody production or mouse ascites production?
No	10: Will animals be immunized or used for polyclonal anitbody (non-ascites) production?
No	11: Will animals be treated with chemical, pharmacologic, toxicologic or radioactive agents (not anesthetics/analgesics)?
No	Schedule G: Are transgenic animals, recombinant DNA, viral vectors used or produced during this study? Requires Institutional Biosafety Committee approval.
No	Are Chemical Hazards used?
No	Are Radioactive Hazards used?
No	Are Biological Hazards used? (includes use of biological agents, human blood, tissue, body fluids, infectious agents etc.)
No	Will cell lines or other agents be passaged in animals? If yes, contact DLAM to have your cell lines tested.

Submission History:

10/08/2007 - Complete	09/28/2007 - In Process	09/26/2007 - Revised	09/17/2007 - Reopened
08/30/2007 - Under Review	08/29/2007 - Revised	08/24/2007 - Reopened	08/14/2007 - Submitted

Date Approved: 10/08/2007

1. Personnel Information:	Role(s):	
Charlene M Ross **PID:** 713635405 **Dept:** 4270 - Laboratory Animal Medicine **Campus Box:** CB: **Phone:** 843-7843 **Email:** cmross@email.unc.edu	Laboratory Coordinator Official Contact	
Ricardo Alberto Cortes **PID:** 710222099 **Dept:** 4270 - Laboratory Animal Medicine **Campus Box:** CB:7115 Thurston Bowles 1119A **Phone:** (919) 843-7843 **Email:** cortes@email.unc.edu	Animal Handler	**Technique(s)** / **Certified** Anesthesia - Monitoring: Yes CO2 Euthanasia: Yes Handling and Restraint: Yes Incision Site Prep: Yes Inhalational Anesthesia Vaporizer: Yes Inhalational Euthanasia: Yes Instrument Prep: Yes Scrubbing and Gloving: Yes Suture Placement: Yes Suture Removal: Yes Anesthesia - Administering: Yes Aseptic Technique: Yes Husbandry: N/A Tattoo: N/A
Charlene M Ross **PID:** 713635405 **Dept:** 4270 - Laboratory Animal Medicine **Campus Box:** CB: **Phone:** **Email:** cmross@email.unc.edu	Animal Handler	**Technique(s)** / **Certified** Anesthesia - Monitoring: No CO2 Euthanasia: No Handling and Restraint: No Incision Site Prep: Yes Inhalational Anesthesia Vaporizer: No Inhalational Euthanasia: No Instrument Prep: Yes Scrubbing and Gloving: Yes Suture Placement: Yes Suture Removal: Yes

Anesthesia - Administering	No
Aseptic Technique	Yes
Tattoo	N/A

Valerie S Ashby Principal Investigator
PID: 703283731
Dept: 3265 - Chemistry
Campus Box: CB:3290 15-26 Venable Hall
Phone: (919) 962-3663
Email: ashby@email.unc.edu

Jinrong Liu Email Contact
PID: 709983509
Dept: 3265 - Chemistry
Campus Box: CB:
Phone:
Email: ljramy@email.unc.edu

1.2 Collaborators and Core Facilities

2. Brief description of the procedure

We will use the core facility in Laboratory Animal Medicine. Charlene M Ross (Lab coordinator and animal handler) and her assistant will do the animal work. This core does not have its own animal use application, but instead works with investigator animals under the investigator's application.

Rats are anesthetized using Isoflurane and O2. While under a surgical plane of anesthesia (monitored for adequate anesthesia by monitoring wakefulness and response to handling and toe pinch) the rats are shaved of all hair on the dorsal portions of the right and left sides. The surgical areas are prepped with alternating applications of a 10 percent povidone-iodine solution and 70 percent ehanol. Four 1 cm longitudinal incison are made to allow the implantation of four 8mm*8mm*2mm pieces of polymeric materials. Three piece of each polymeric formulation and one piece of PLGA (Boehringer Ingelheim; as control) are implanted per rat. The incisions are closed using sterile 5-0 surgical suture and an injection of Bupreorphine of 0.05 mg/kg s.c. every 12 hours for 24 hours following the procedure.

3. Person(s) Performing Procedure	IACUC ID which person is approved
Charlene M. Ross	N/A
Ricardo Cortes	N/A

Funding Source :	Agency Deadline:	Funding Period:	Grant Number:
National Science Foundation - Research (NSF)		3 years	07-1605

3. Scientific Justification for Animal Species

Justify the species to be used by indicating

1. No This is a new model. (DLAM veterinarians available for consultation on new model development.)
No The results will be directly applicable to the health, care or welfare of this species

Yes Other -

The method we choose here is the regular experiment to check the in vivo biocompatibility for new materials application in tissue engieering field. we follow the experimental procedures from the following papers,

Yadong Wang, Robert Langer, ***Nature biotechnology***, 2002, 20, 602

Guillermo A. Ameer, ***Adv. Mater.*** 2004, 16, 511

Brian G. Amsden, ***Biomacromolecules***, 2006, 7, 365

2. No Will the PI conduct the same experiment in multiple species?

3. Features of the species (e.g. anatomic, physiologic, genetic, etc.) that make it desirable for this model.

the rats we used is Sprague-Dawley female rats from Charles River, 7-week-old, which is the normal species used for this kind of experiment.

3.1 Building - Room Number:	Housing Type :
Thurston Bowles -	DLAM

3.2 Procedures in Laboratory, DLAM/Satellite Housing & Confinement

1. No Will animals be removed from DLAM or approved satellite facility?

2. If animals will be removed from DLAM, approved Satellite Facility or taken to Investigator Laboratory, indicate the procedures to be performed, and the contact information:

» Procedure(s) to be performed:
» Contact Person:

4. Reduction, Refinement, Replacement, and Animal Numbers

1. Animal Number Reduction

a. Replacing vertebrate animals:
Are there computer simulation, non-living, or in vitro alternatives to the proposed use of animals described in your application? **No**

If yes, state why these alternatives are not appropriate:

b. Refining experimental procedures to minimize pain or distress:
Did you consider the use of pain-relieving drugs, or procedures that avoid or minimize discomfort, distress and pain, and humane endpoints in the design of the experiment? **Yes**

If not considered, state why the alternative was not applicable:

c. Reduction in the number of animals:

Yes Rational selection of group size (e.g., pilot studies to estimate variability, power analysis)

Yes Careful experimental design (e.g., appropriate choice of control groups)

Yes Maximizing use of animals (e.g., selecting the minimal number of animals per group required for statistical verification, sharing tissues with other investigators)

Yes Minimizing loss of animals (e.g., good post-operative care, avoidance of unintended breeding)

If you selected none of the above choices, state why they are not appropriate:

2. Using the specifics of your experimental plan, justify the number of animals requested and list the number of animals used for each pain category (B, C, D, E):

There are 3 types of test samples and 1 control sample from a commercial FDA approved product.

there will be 15 rats used in the experiment. They are divided into 5 groups. each group have 3 rats and each rats will be implanted 3 samples and 1 control. Each implantation size is around 1 cm in longitude. the samples are different in each group are different. Every week one group of rats will be euthanized with CO_2 and then 12 tissues will be harvested.

the rats are anesthetized using Isoflurane and O_2 before the implantation. And after implantation, The incisions are closed using sterile 5-0 surgical suture and an injection of Bupreorphine of 0.05 mg/kg s.c. every 12 hours for 24 hours following the procedure. There may be slight inflammation over the implantation site but it is not expected to have any adverse affect on the animal

3. Estimate the following animal number totals required for this study during the three-year approval period>

Pain Category	Unweaned	Breeders	Adults
B	0	0	0
C	0	0	0
D	0	0	15
E	0	0	0

Total Animal Number = **15**

4. Category E Justification:

5. Transfer of Existing Animals: No

4.1 Alternatives to Animals Classified in USDA Pain Categories D or E

1. Details About Alternatives Search

a. Literature search conducted:

Other: 8/24/2007 -
scifinder,

sciencedirect

pubs.acs.org

b. Keywords used in database searches

in vivo study of biodegradable scaffold

c. Years Search: 1999-2007

d. » Information Services and other Literature Sources:

No Animal Welfare Information Center
No Lab Animal Welfare Bibliography (NLM)
No Laboratory Animal Science Journal
No Alternatives to Laboratory Animals Journal (FRAME, U.K.)
No Quick Bibliography Series (AGRICOLA)
No Peer Review -

No Other -

» **Knowledge of Field/Consultants:**

» **Other Methods or Sources Used:**

e. **Other Search Sources:**

by published methods from the following papers. they all used the similar methods to do the in vivo study for the biodegradable scaffold in tissue engineering field.

Brain G. Amsden etc., *Biomacromolecules* 2006, 7, 365-372

Robert Langer, *Nature technology*, 2002, 602-606

Guillermo A. Ameer, *Advanced Materials*, 2004, 16, 511-516

5. Details of Animal Use:

1. Goals and objective(s) of your research.

biodegradable polymers have significant potential in various fields of bioengineering, such as tissue engineering, drug delivery and in vivo sensing. Because many biomedical devices are implanted in a mechanically dynamic environment in the body, the implants must sustain the mechanical strength and no irritation to the surrounding tissues. Our lab synthesized a new biodegradable material, which is soft, tough with properties resemble thos of extracellular matrix, which provide mechanical stabilityand structural integrity to tissues and organs. we want to explore its appliation in tissue engineering field as a biodegradable scaffold. the in vitro biocompatibility and in vitro degradation studies have been done, so the in vivo biocompatiblity study is vital to evaluate the material application as a scaffold.

2. If this application is a continuation of an ongoing project, state concisely how these goals differ from those in the original application and what was accomplished during the prior approval period. If this is a new project, please indicate so.

it is not a continuation of an ongoing project.

3. Describe the specific experimental manipulations and treatments of the animals in terms that are intelligible to a non-scientist.

The main purpose for this experiment is to study the new polymeric material performance after implanted in the rat. The rats will be subcutaneous implanted with some samples. the experiment will go 5 weeks. each week, 3 rats will be euthanized with carbon dioxide and some samples will be explanted for mechanical study and some sample will be harvested with the tissues for histologic examination.

5.3 Survival Surgery

1. **Will this surgery or surgeries be performed in the Berryhill Hall DLAM veterinary surgical suite under DLAM veterinary services supervision? No**
Location(s) for surgical procedure: Thurston Bowles -

2. **Will any animal undergo more than one major survival surgical procedure? No**
» **Number of Surgeries on each animal:**
» **Scientific Justification:**

3. Approximate time length of anesthesia for each procedure:
the rats will only be anesthetized in the beginning of the implantation. it is around half an hour.

4. Neuromuscular paralytics used?: No

5. Monitoring of distress, discomfort, or depth of anesthesia during surgery

No Heart Rate
No Blood Pressure
No EKG
No Body Temperature
No Fluid Balance
No Respiratory Rate
Yes Other
Other Description -

Monitored for adequate anesthesia by monitoring wakefulness and response to handling and toe pinch.

6. Assesing Depth of Anesthesia:
Means by which a surgical plane of anesthesia is established, maintained, and monitored: Toe pinch reflex

7. Anesthetic agents and other information:

Anesthetic Agent:	Isoflurane
Dosage:	2%
Route:	
Schedule:	
Procedure:	
Volume:	

Anesthetic Agent:	oxygene
Dosage:	200 mL/min
Route:	
Schedule:	
Procedure:	
Volume:	

8. Detailed description of each surgical procedure. Include the surgical anatomy and organs involved; location and size of incisions; method and materials of wound closure; and description and size of implanted materials/devices:

Before the experiment, all the samples will be strelized with UV radiation for 15 min.

Rats are anesthetized using Isoflurane and O2. Sterile ocular ointment is applied to the eyes to prevent desiccation. Throughout the procedure the animal is maintained on a Deltaphase Isothermal heating pad. While under a surgical plane of anesthesia (monitored for adequate anesthesia by monitoring wakefulness and response to handling and toe pinch) the rats are shaved of all hair on the dorsal portions of the right and left sides. The surgical areas are prepped with alternating applications of a 10 percent povidone-iodine solution and 70 percent ehanol. four 1 cm longitudinal incison are made to allow the implantation of four 8mm*8mm*2mm pieces of polymeric materials. Three piece of each polymeric formulation and one piece of PLGA (Boehringer Ingelheim; as control) are implanted per rat. The incisions are closed using sterile 5-0 surgical suture and an injection of Bupreorphine of 0.05 mg/kg s.c. every 12 hours for 24 hours following the procedure.
At each week sampling point, 3 rats will be euthanized with CO2 and tissue around the implanted materials will be harvested with the materials.

9. Period of time animals will survive after surgery:

after surgery, the longest survival time is 5 weeks. For each week, 3 rats will be euthanized with CO_2 .

10. Postoperative monitoring and care to be given:

Rats will be monitored daily by the Animal Studies Core. This monitoring will include weekends and holidays. Charlene Ross will be contacted for after hours or emergency issues.

11. Are post-operative analgesics provided? Yes

» **Administered by:** DLAM

Analgesic Agent:	Buprenorphine
Dosage:	0.05 mg/kg
Route:	
Schedule:	every 12 hours
Procedure:	
Volume:	

12. Complications that may occur and how they will be handled:

there may be slight inflammation over the implantation site but I don't expect it to have any adverse affect on the animal.

If the animals reject the material or a site becomes infected, the animals will be sacrificed. But I don't expect it to happen since we did the outside of body cytotoxicity test for 8 days and the results showed that the materials are biocompatible.

13. Surgeon(s):

Surgeon(s):

Surgeon:	Experience of surgeon with animal model:
Ricardo Cortes	Ricardo Cortes is a member of the Animal Studies Core. He has been trained by Charlene Ross and performs rodent aseptic survival surgeries on a daily basis. He successfully completed the IACUC's aseptic techniques class.
Charlene Ross	Charlene Ross is the manager of the Animal Studies Core and has over 7 years experience with rodent surgical models. She performs aseptic surgical procedures for the Core on a daily basis. She has successfully completed the IACUC's aseptic techniques class here at UNC-CH.
NULL	

5.8 Collection of tissue from live or dead vertebrate animals

1. Will tissue be collected from dead animals? Yes

Collected Tissue: the implant and surrounding tissue of the dorsal portion of the rats.

2. Will tissue other than rodent tail and toe be collected from live animals? No

3. Will anesthesia be used? No

4. a. Is tail tissue harvested for genotyping or other purposes? No

b. Will vertebra(e) be cut? No

5. **a. Is toe tissue harvested for genotyping or other purposes?** No

b. Will rodents be greater than 10 days of age when toes are clipped? No

6. Animal Care

1. Animal ID Method:

No Ear Tag
No Ear Punch
No Microchip
Yes Tattoo
No Toe Clip
No Not Applicable
No Other
Other Explanation -

2. How will animals be monitored?

Rats will be monitored daily by the Animal Studies Core. This monitoring will include weekends and holidays. Charlene Ross will be contacted for after hours or emergency issues.

If special monitoring has been arranged with DLAM facility supervisor, provide DLAM contact name:

3. Should DLAM contact PI/emergency contact if animal(s) found dead? Yes

4. Indicate requests for special handling of sick and dead animals:

Charlene Ross should be contacted in the event of an emergency, this includes sickness and death of the animals.

5. Special Housing (DLAM):

Will any special housing or care be necessary? No

Deviations from standard DLAM husbandry procedures, Guide recommendations or special animal care needs:

6. Special Diets (DLAM)

Are special diets, additives to food and/or water (e.g. colyte) and/or antibiotics administered? No

7. Endpoints (time points, tumor sizes etc.) and/or the maximum time length of study:

the study will take 5 weeks. each week there will be a tissue harvest time.

8. Will animals be euthanized as part of the study? Yes

the rats will be euthanized with CO_2

» Euthanasia Methods

Yes CO2-compressed carbon dioxide gas in cylinders followed by a physical method to ensure death
No Barbituate overdose
Dosage and route:

No Cervical Dislocation
If no anesthesia, scientific justification:

No Decapitation
If no anesthesia, scientific justification:

No Overdose of gas anesthetic
Specify Agent:

No Anesthesia - followed by physical euthanasia
Agent, Dose and Route:

Yes Other Method of Euthanasia
CO2 euthanasia followed by a thoracotomy.

9. Would the PI be willing to share, donate or make available extra animal tissues or organs to other PI's? Yes

7. Anticipated Animal Pain & Distress

1. Are there any clinical, behavioral, or physiological manifestations expected to result from experimental manipulation such as surgery, diet, tumor, chronic disease, radiation sickness or toxicity, or potential health problems due to animal phenotype?Yes

a. Expected clinical and/or behavioral signs of pain and distress in animals

No Decreased weight
No Changes in food/water consumption
No Decreased ambulation
No Ruffled fur
No Skin abnormality
No Urinary problems
No Hunched posture
No Paw guarding
No Porphyrin Staining
No Lethargy
No Diarrhea
No Other
Other Explanation -

there may be slight inflammation over the implantation site but that I don't expect it to have any adverse affect on the animal.

b. Methods of dealing with the above complications:

No Analgesics
No Anesthetics
No Sedation or tranquilization
No Increased bedding
No Other
Other Explanation -

1b. continued...

b. Agents used in dealing with complications

2. Animals experiencing unrelieved pain or distress prior to the endpoint, as defined by institutional policy, must be humanely euthanized, unless an exception to policy is requested and approved. Is exception required? No

a. Criteria for euthanasia that will used for this exception:

b. Scientific justification for not using an earlier endpoint:

Application to Use Live Vertebrate Animals

PI: Valerie S Ashby
Dept: Chemistry
IACUC ID: 07-217.0 Web ID: 9796

Application Certification

I agree to the following statements. Signify your agreement by signing at the bottom

- I certify that I am familiar with and assure compliance in this Project with the legal standards of animal care and use established under the Federal and State laws and the policies on animal welfare of the National Institutes of Health and the University of North Carolina.
- I assume responsibility for ensuring that all persons working with animals on this project are familiar with and are trained in relevant animal procedures and that they will comply with established laws and policies regarding animal care and use. Applications will not be approved for investigators that have taken the IACUC orientation but have not completed required Laboratory Animal Coordinator certification. Contact the IACUC office to arrange training.
- I will appoint a Laboratory Coordinator to manage all animal use in the lab. I will ensure that the Coordinator receives required training and certification. I will ensure that after being certified, the Coordinator or IACUC representative will train and certify all individuals working with animals in the lab.
- I certify that all individuals working with animals on this project will register with the University Employee Occupational Health Clinic (UEOHC) by completing and submitting the "Research Animal Handlers & Animal Caretakers" medical history questionnaire (each individual who works with animals must complete the questionnaire during online orientation - UEOHC will assess the PI a processing fee).
- I certify the following: the research proposed herein is not unnecessarily duplicative of previously reported research; appropriate non-animal alternatives for this research do not exist; no alternatives to the potentially painful and/or distressful procedures conducted in this project exist. I have indicated methods used to make these determinations in the appropriate section of this animal use application.
- I will secure IACUC approval before changing procedures or personnel associated with this study (including adding personnel)
- I assure that I and personnel under by direct supervision will use the animals acquired for the activity described herein solely for said purpose. I also certify that if live animals are shared with other PIs or are used in any procedure other than those described in this application, I will provide the details in the form of a written amendment to the original application prior to their use.
- I acknowledge that veterinary care will be administered to moribund animals or animals experiencing more than momentary or slight pain or distress. Division of Laboratory Animal Medicine (DLAM) veterinary staff will attempt to contact me regarding the care of treatment of a moribund animal, but will institute treatment or euthanasia, as needed, if PI cannot be reached.
- I assure the IACUC and the University of North Carolina at Chapel Hill that the general procedures involving animals described in my grant application have been described in the animal use application and submitted to the IACUC for review.
- I assure that I have read "Notes on Euthanasia" of animals used in research and understand how it applies to animals in this animal use application.

NOTE: Consultation of a DLAM veterinarian regarding space allocation is recommended prior to submission of application. IACUC approval of application does not assure DLAM space availability. Please contact DLAM for pre-study strategy meeting prior to ordering animals to dicuss availability of housing.

NOTE: Cell lines that have been passaged in animals or maintained using animal serum may contain murine viruses that can alter the outcome of the study and may cause an outbreak of disease among other mice. ATTCC does not screen cell lines for murine pathogens. Cell lines that have been passaged in animals or grown in media containing rodent serum should be tested for murine pathogens prior to use in animals. Please contact DLAM for more information on testing of your cell lines.

PI Signature Date

Co-PI Signature Date

Date Approved: 10/08/2007

APPENDIX C

SUPPLEMENTAL MATERIALS FOR CHAPTER 4

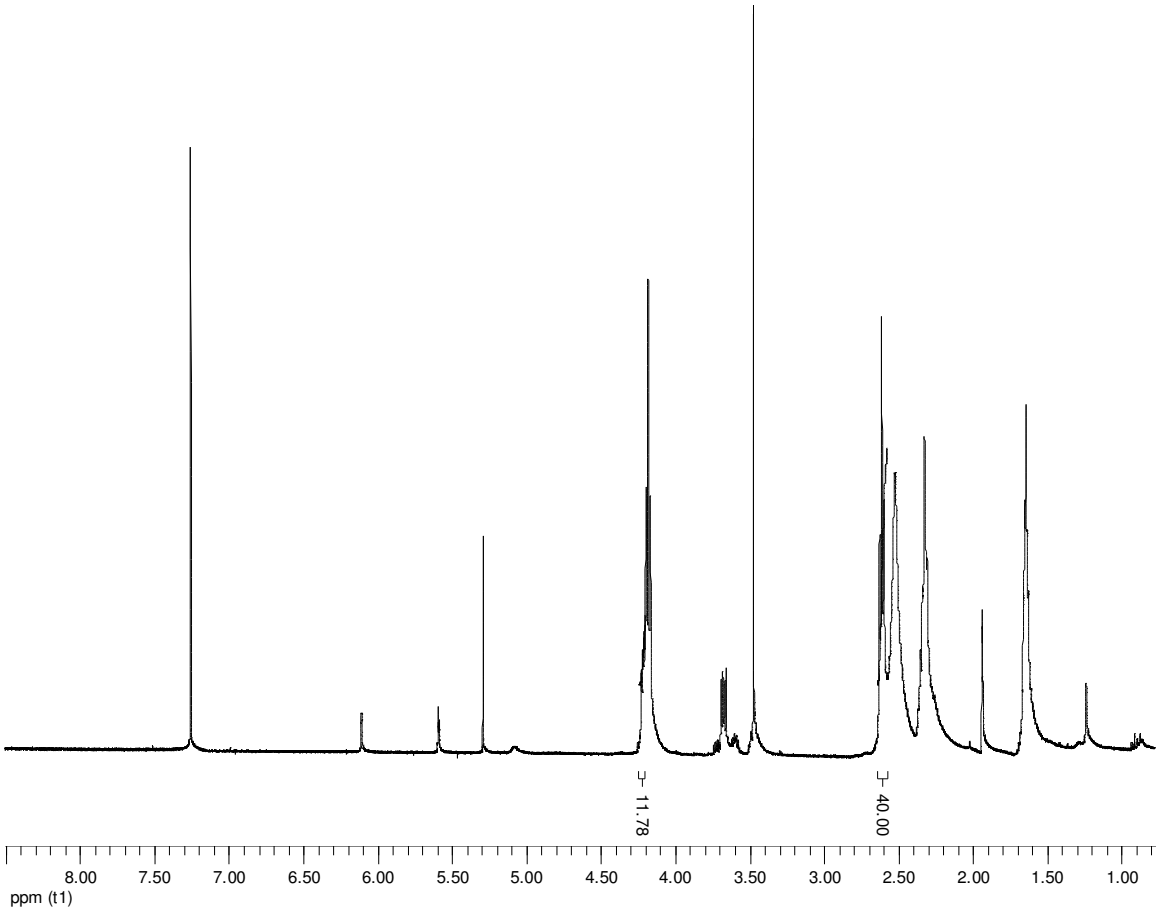

Elastomer, PIP:DEG=40:10

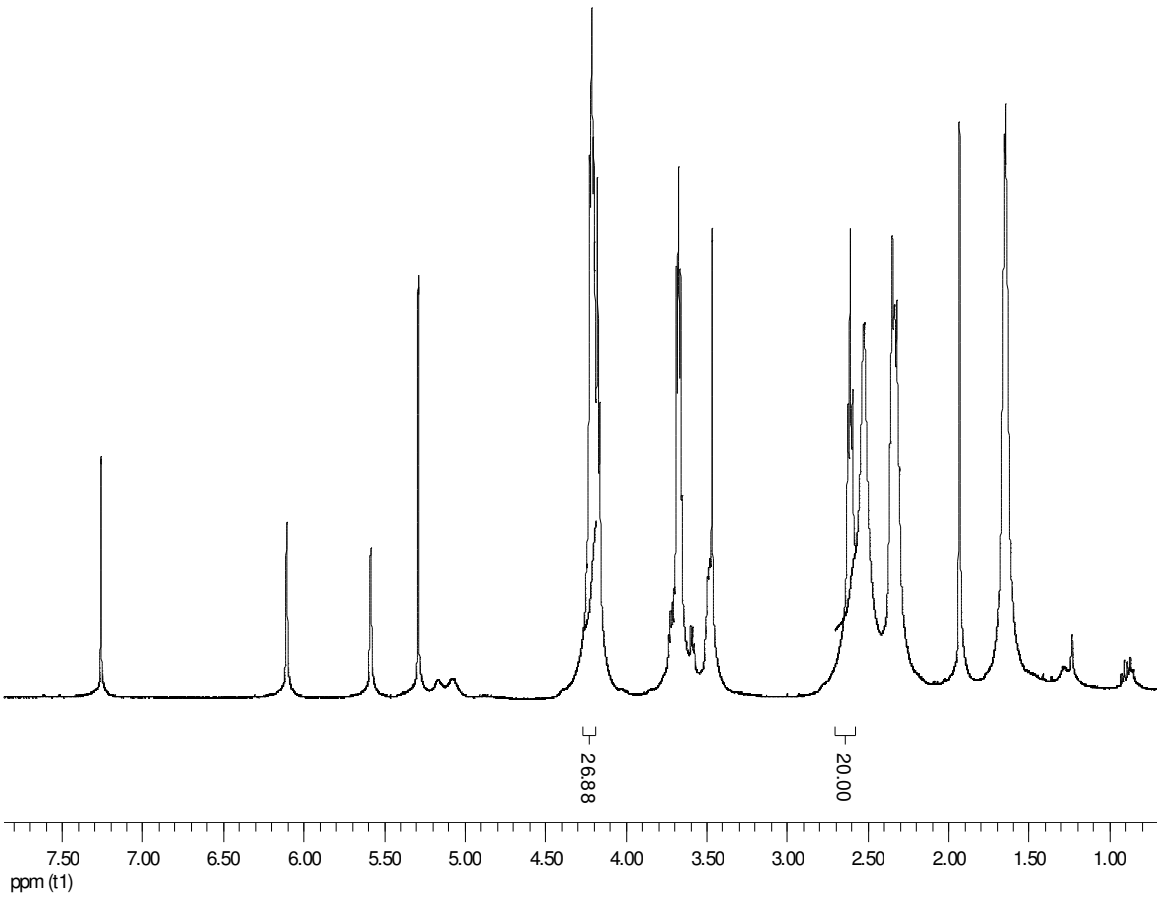

Elastomer, PIP:DEG=20:30, 2K

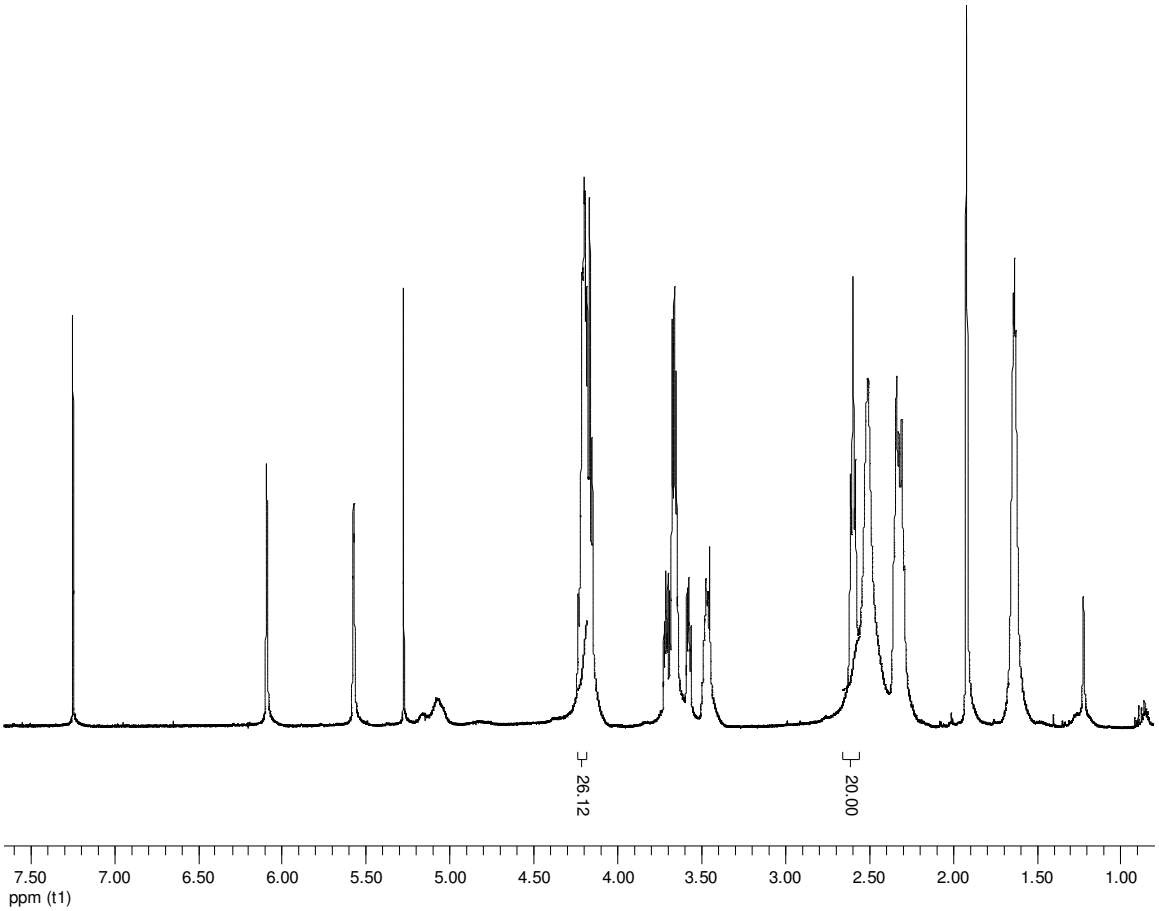

Elastomer, PIP:DEG=20:30, 1K

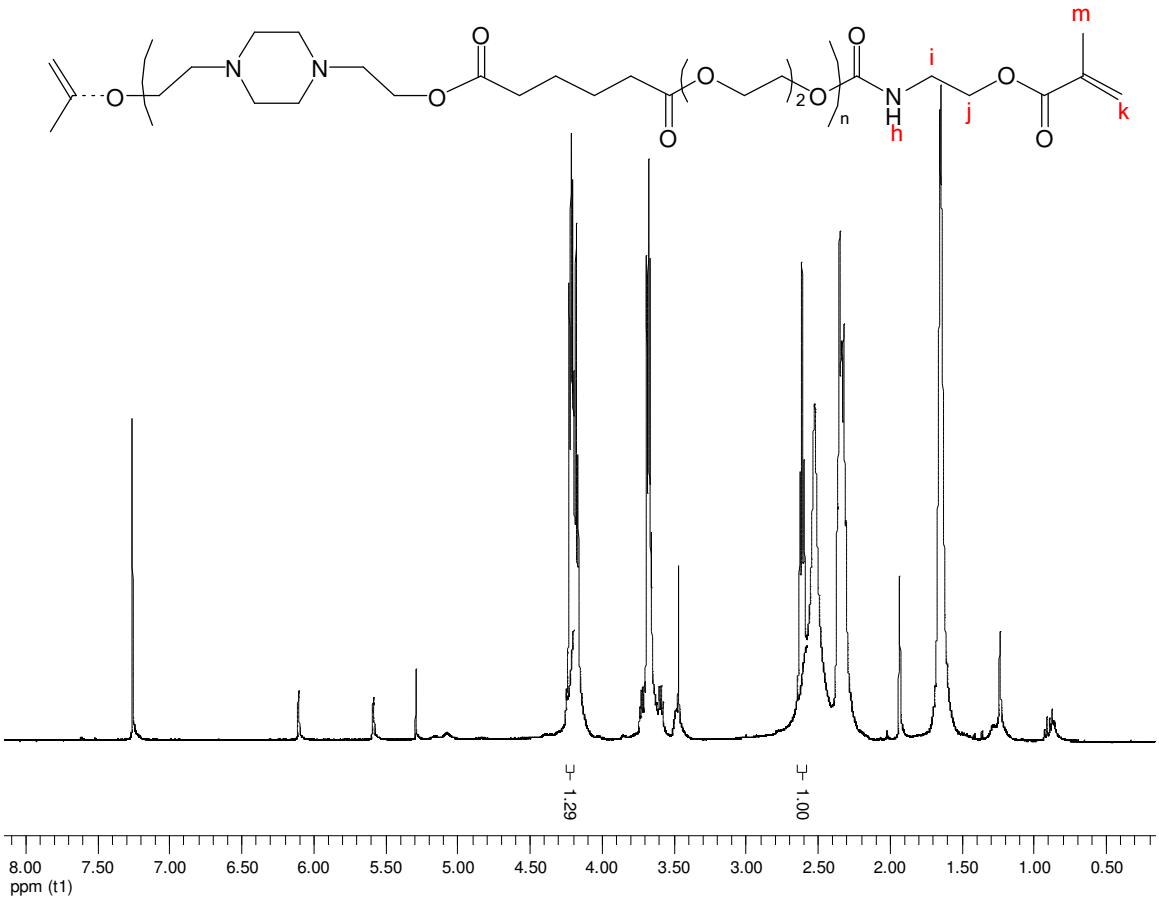

Elastomer, PIP:DEG=20:30, 6K

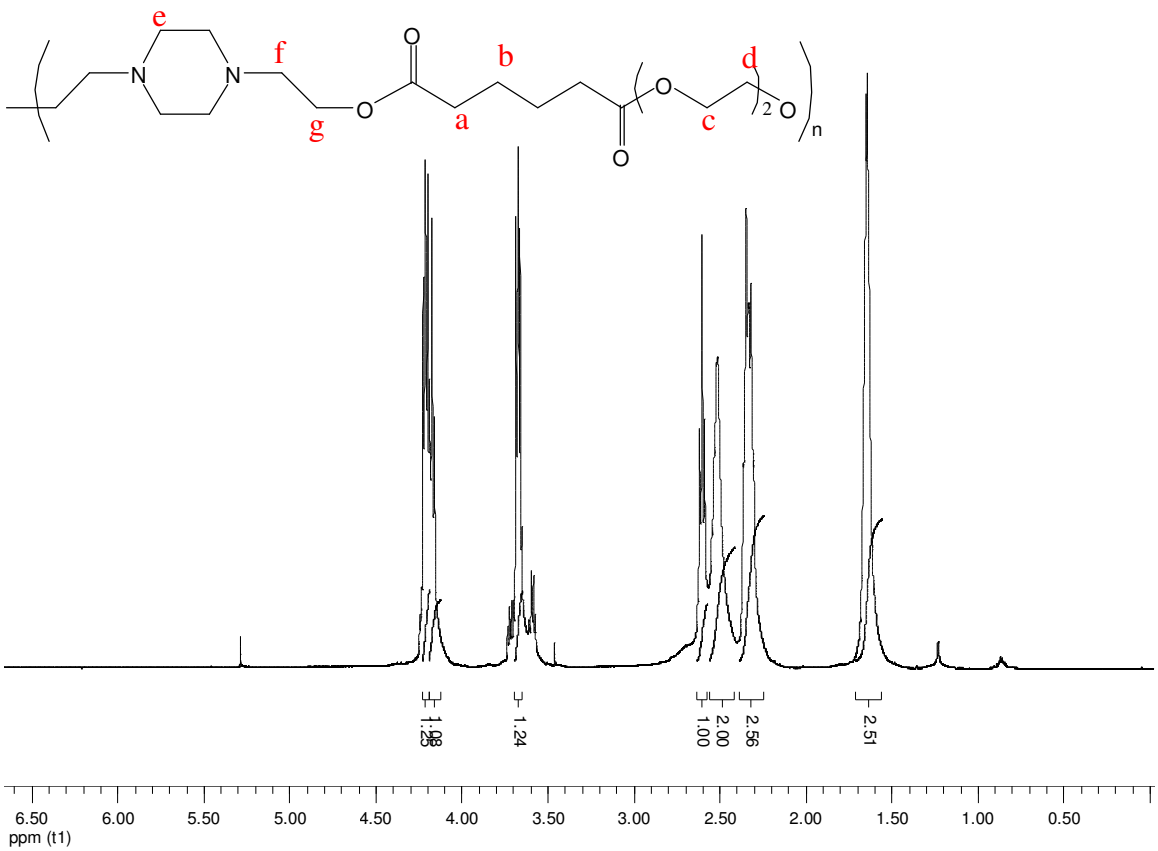

HO-PIP-AA-DEG-OH, PIP:DEG=20:30, 6K

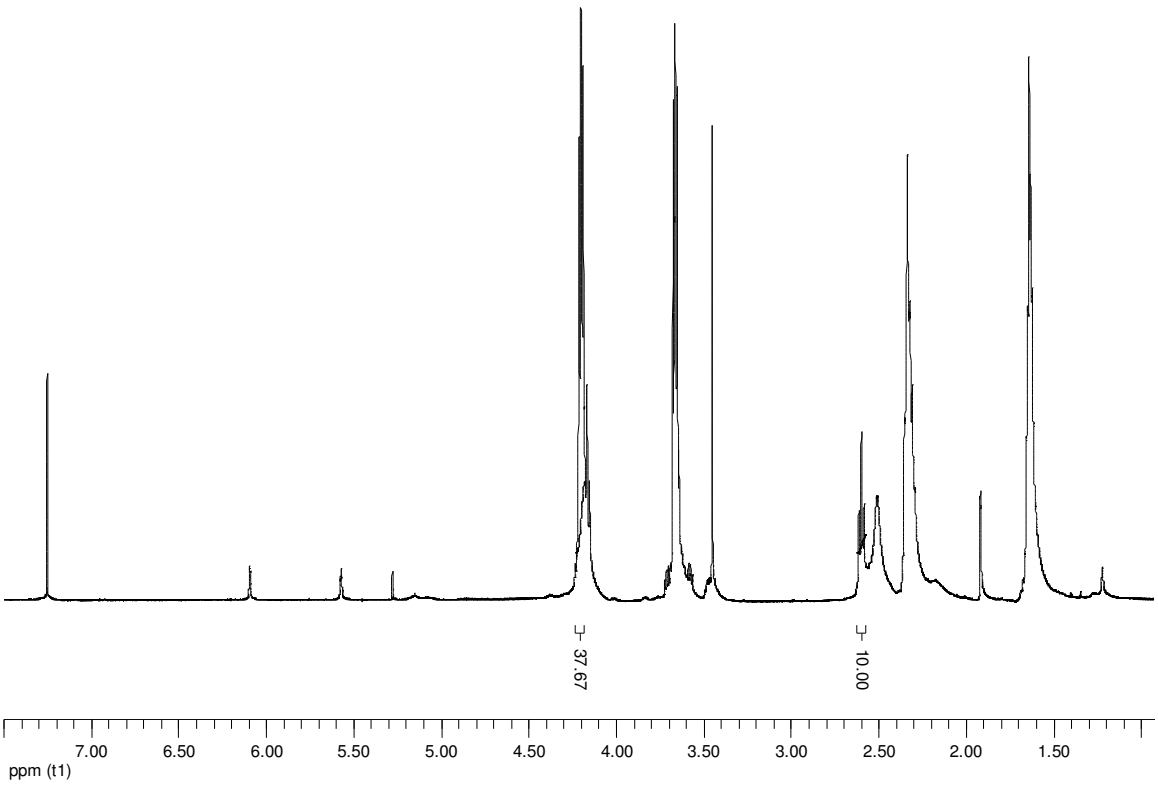

Elastomer, PIP:DEG=10:40

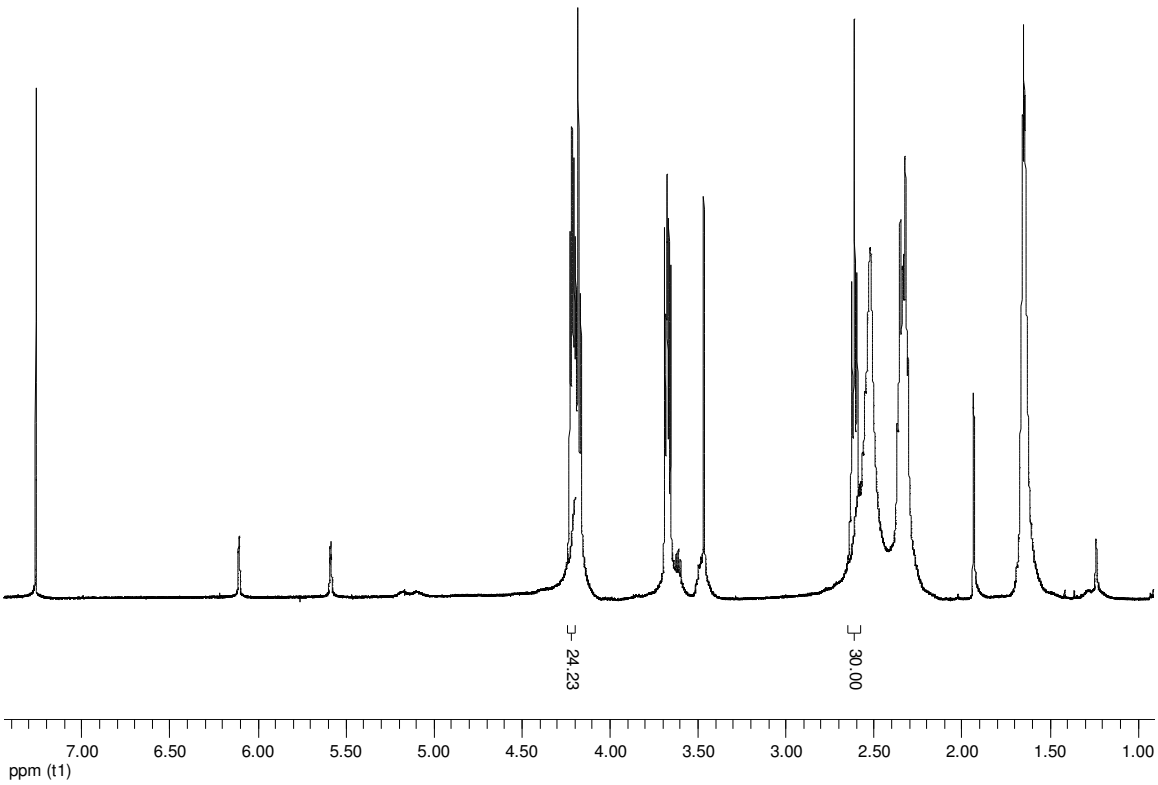

Elastomer, PIP:DEG=30:20

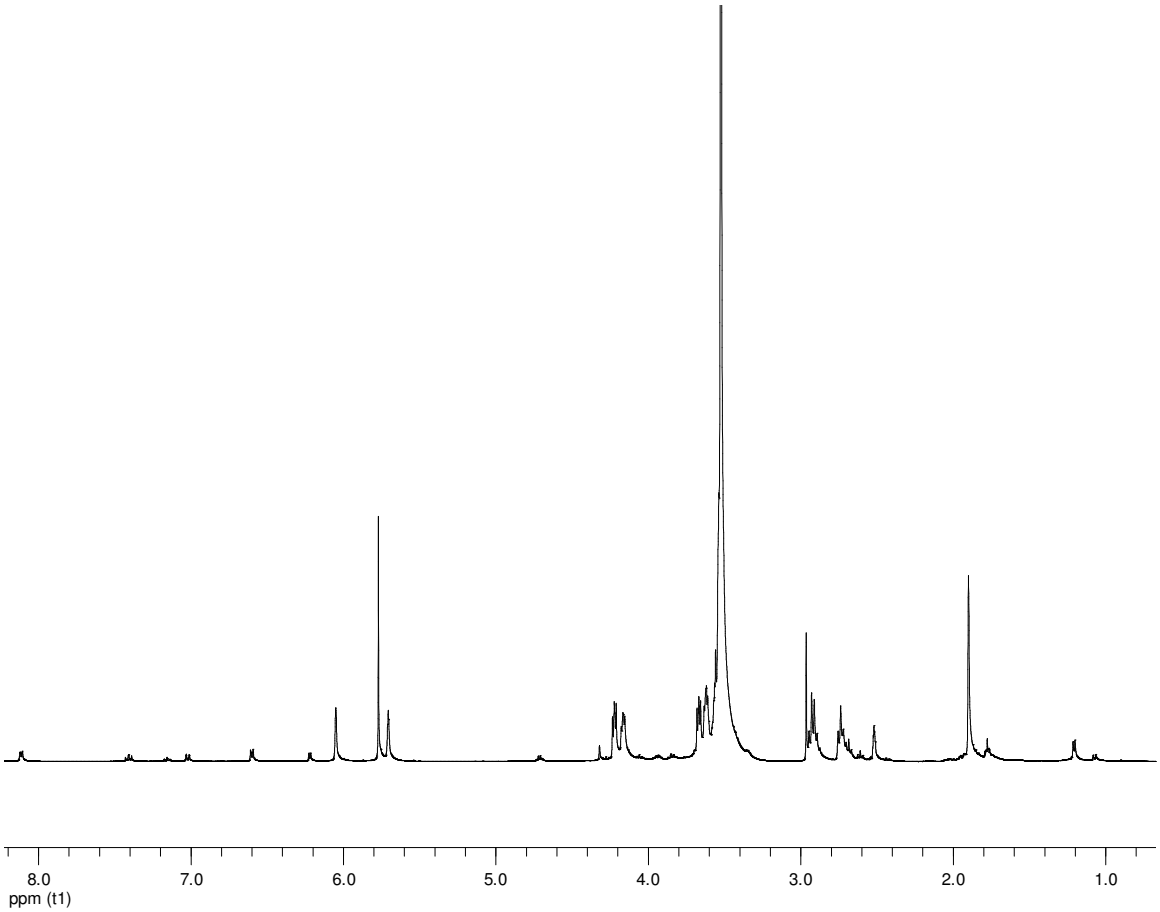

Disulfide crosslinker

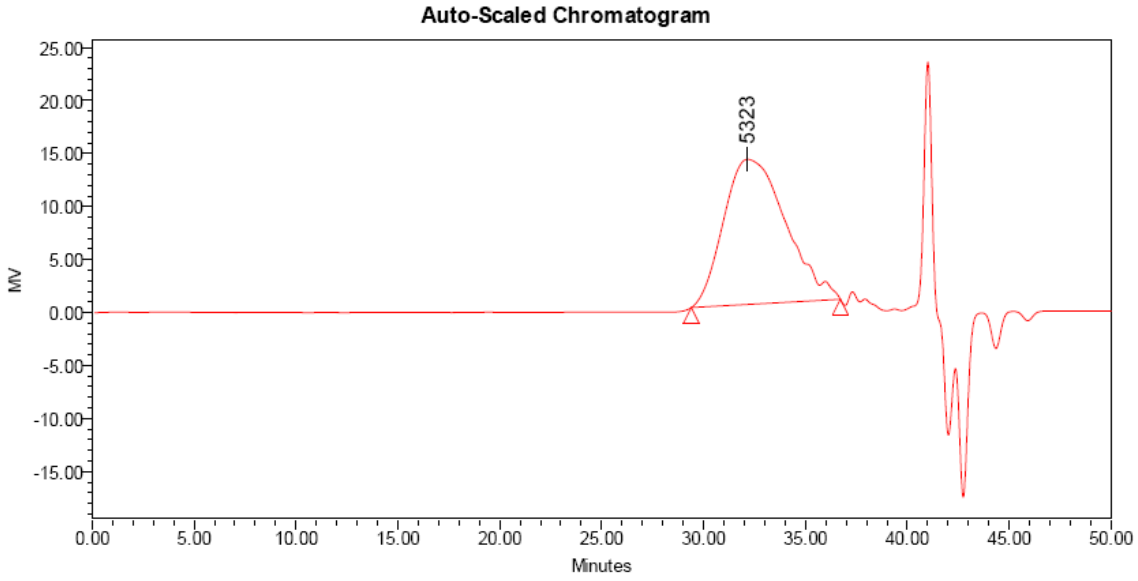

GPC Results

	Dist Name	Mn	Mw	Mv	MP	Mz	Mz+1	Poly dispersity	K	alpha
1		3105	5042		5323	7115	9018	1.623677		

HO-PIP-AA-DEG-OH, PIP:DEG=20:30, 3K

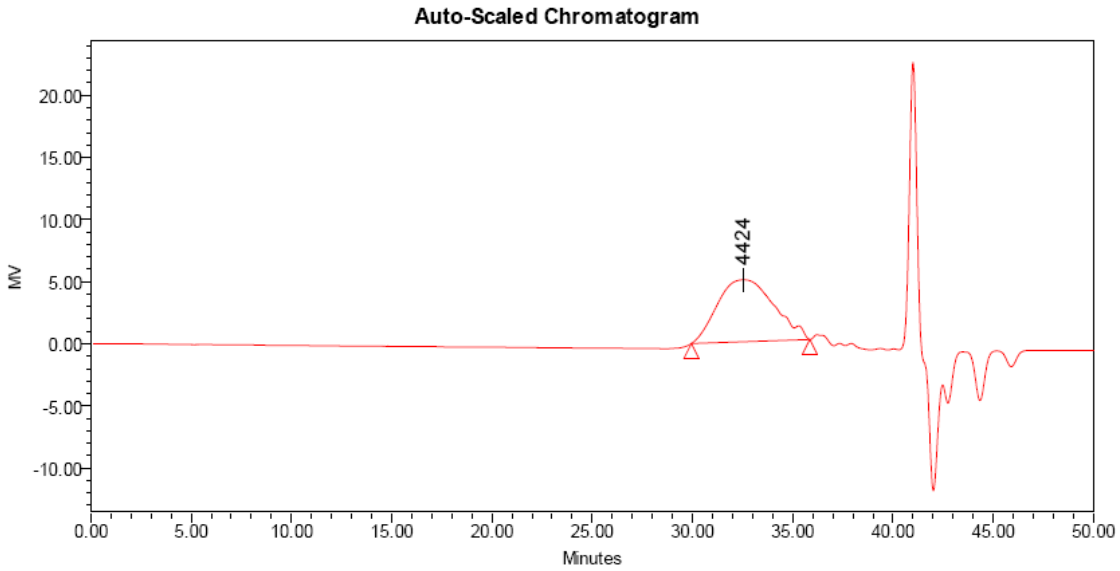

GPC Results

	Dist Name	Mn	Mw	Mv	MP	Mz	Mz+1	Poly dispersity	K	alpha
1		3246	4661		4424	6210	7630	1.435982		

PIP:DEG=20:30, 3K

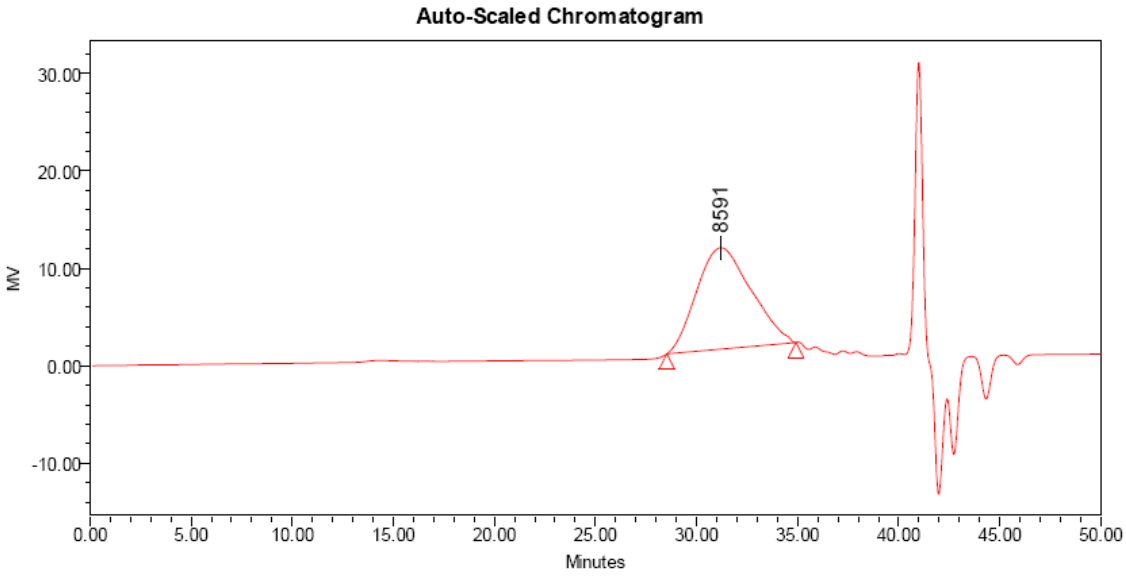

GPC Results

	Dist Name	Mn	Mw	Mv	MP	Mz	Mz+1	Polydispersity	K	alpha
1		6241	8903		8591	11831	14606	1.426494		

PIP:DEG=20:30, 6K

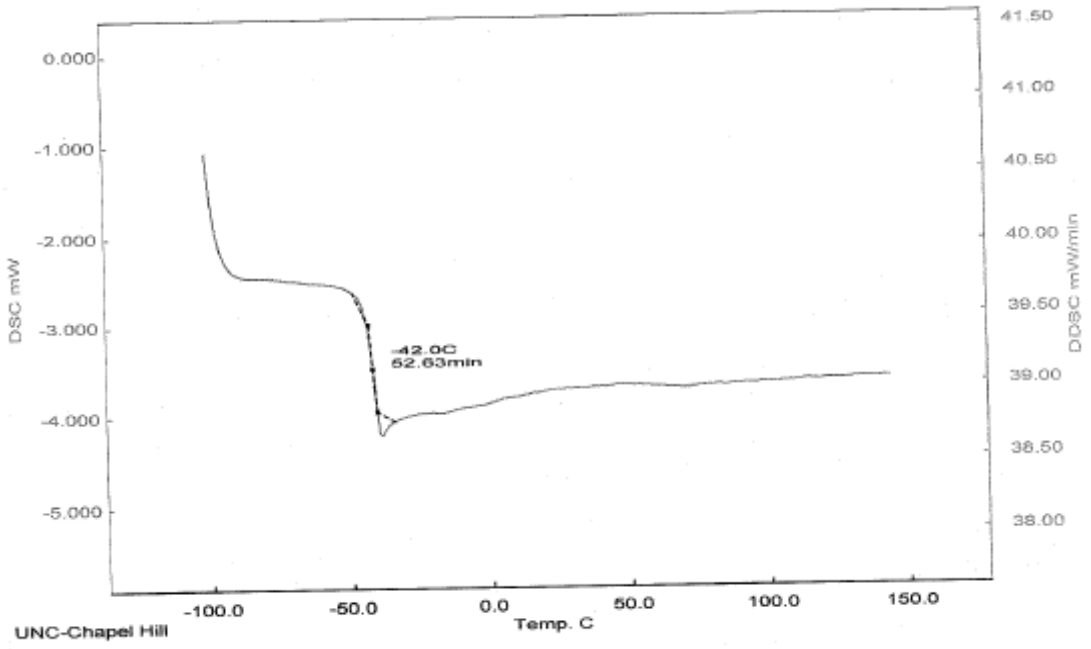

PIP:DEG=20:30, 3K

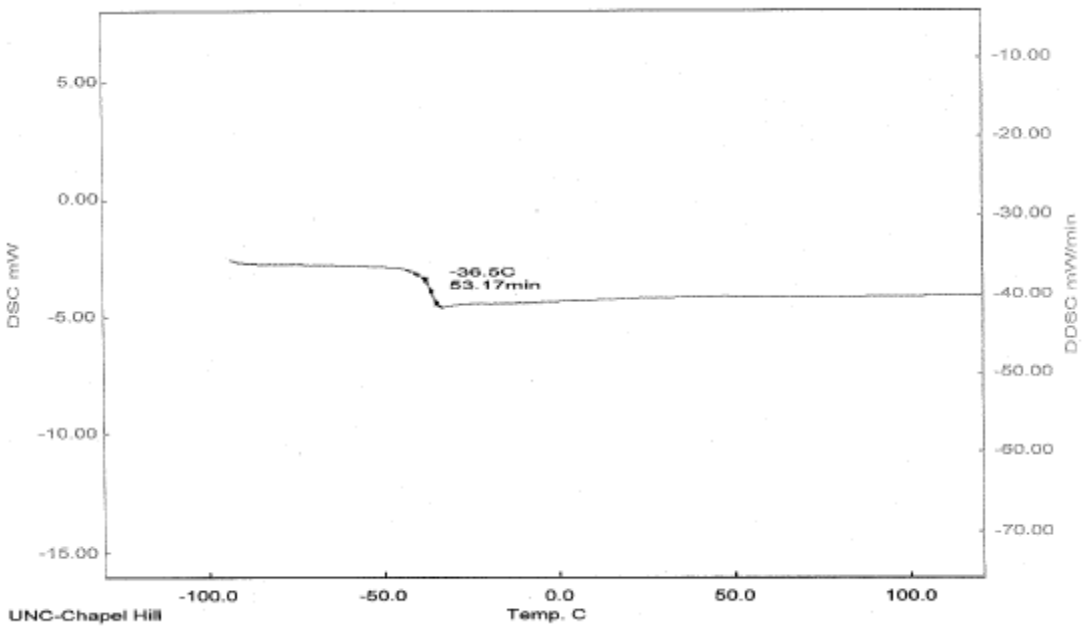

PIP:DEG=20:30, 6K

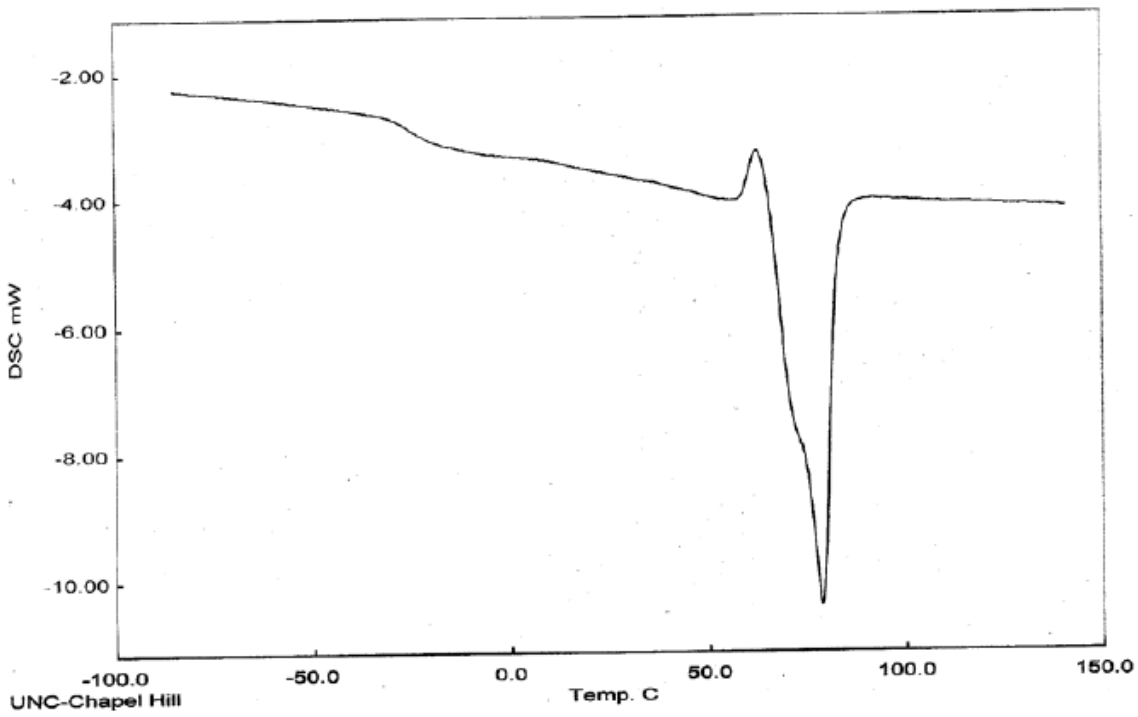
-2.00
-4.00
-6.00
-8.00
-10.00
DSC mW
-100.0
-50.0
0.0
50.0
100.0
150.0
Temp. C
UNC-Chapel Hill

PIP:DEG=40:10

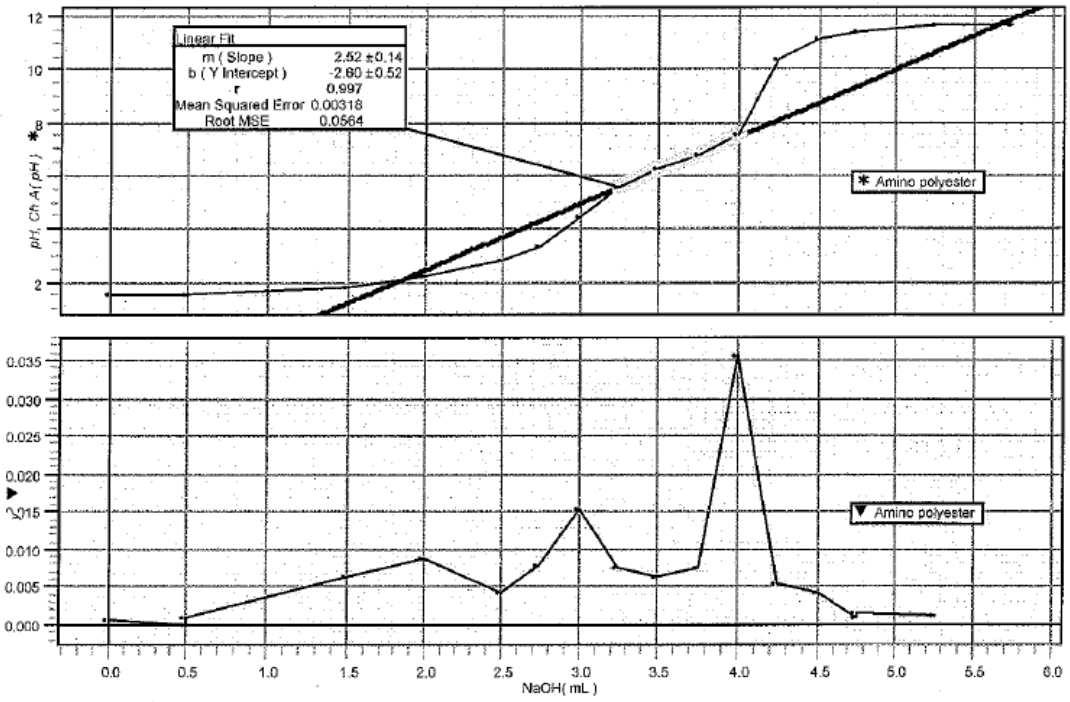

pKa of amino polyester

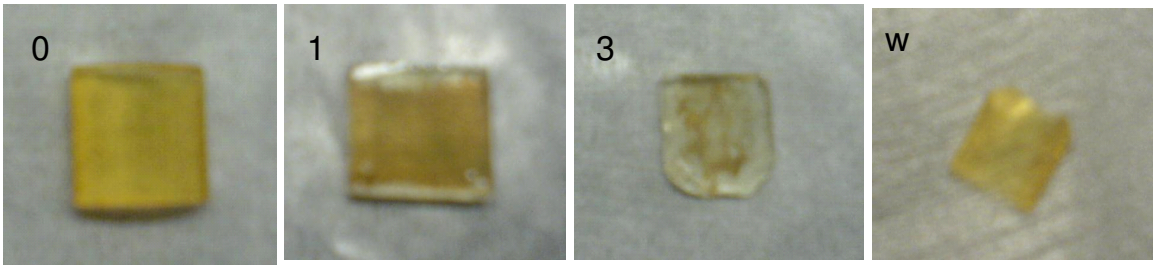

Disulfide containing elastomers degradation in 1 wt % $NaBH_4$ for 0 day, 1 day, 3 day and in water.

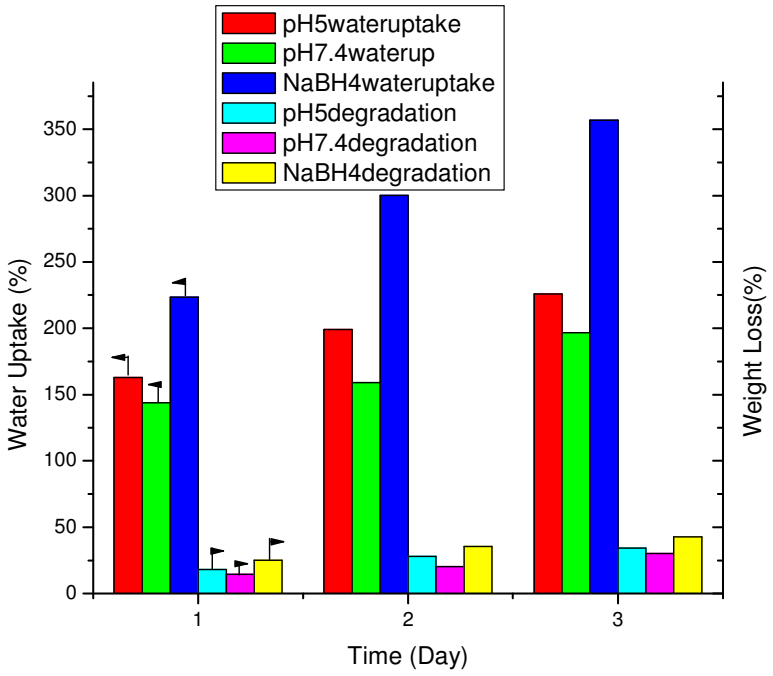

Percentage of water uptake and weight loss against the experiment time in different media. (disulfide-amine containing elastomers)

Standard curve of Dox (500nm) in pH 5 buffer, UV-vis

Concentration mg/mL	Absorbance (OD)
0.00344	0.0368
0.006875	0.081
0.01375	0.1698
0.0275	0.339
0.055	0.6891
0.11	1.3598

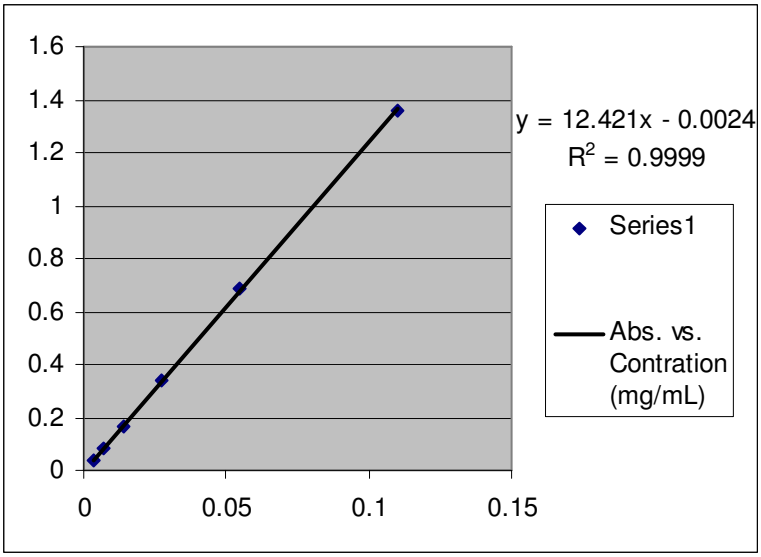

Standard curve of Minocycline hydrochloride (350nm), HPLC

Concentrations (µmol/L)	Area (a.u.)
0.1	
1	
5	
10	279743
25	
50	
100	2498860
200	4879613
250	
400	9644892
500	11438938
600	13535596
800	17988068
1000	24566791

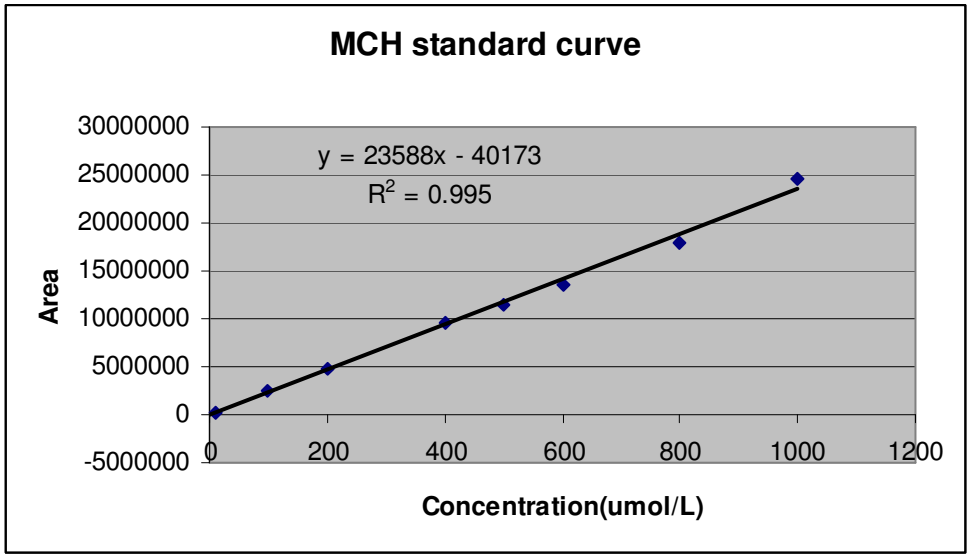

MCH release

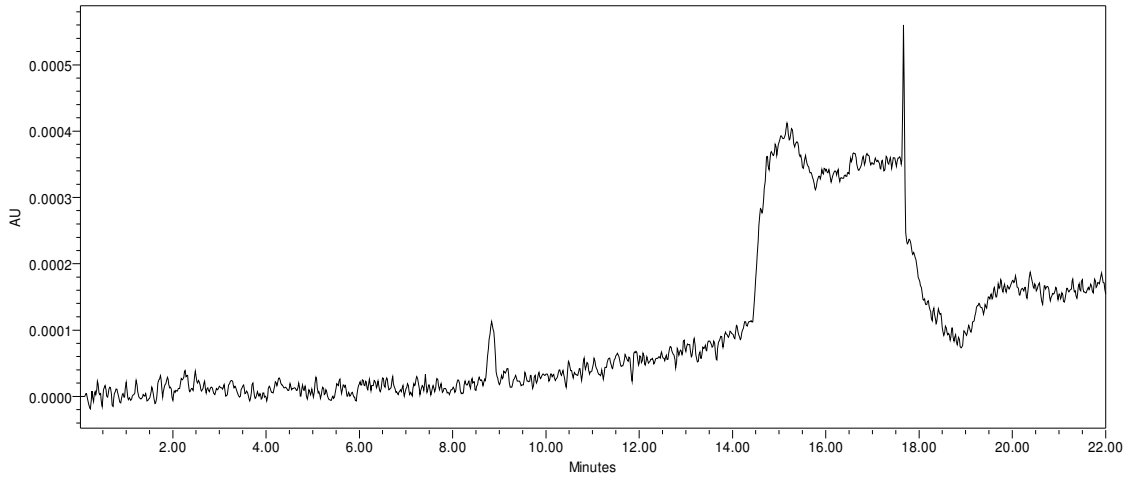

PBS-1h

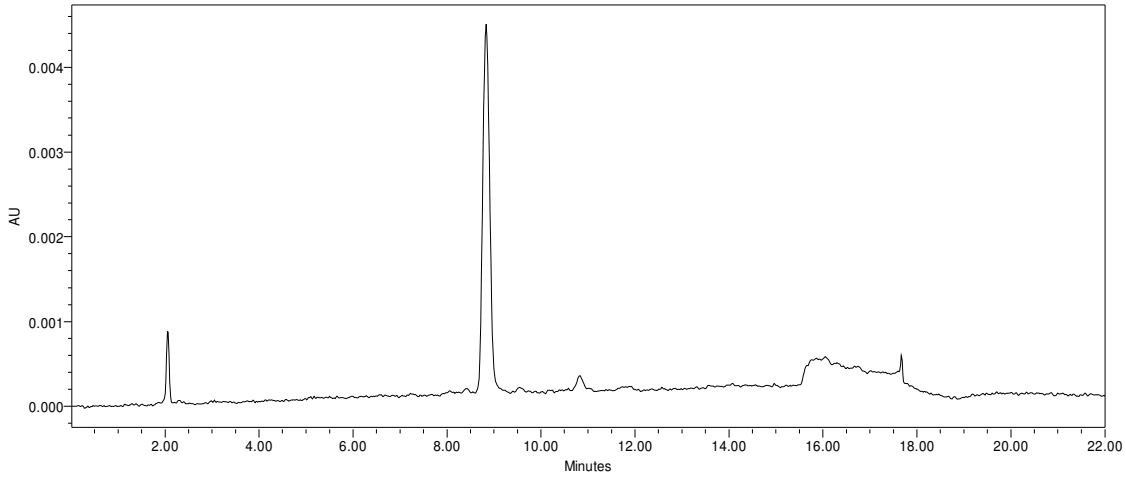

PBS-20h, MCH release

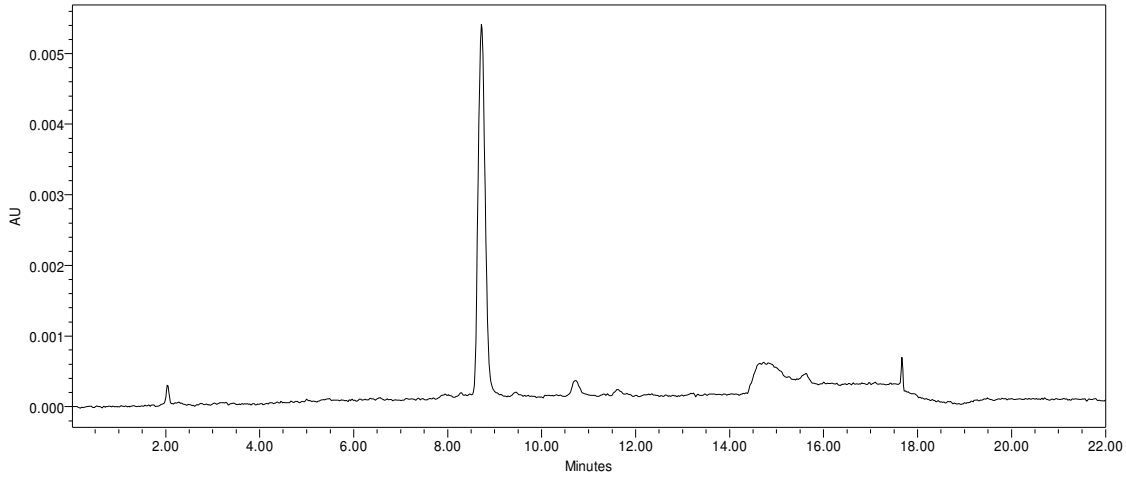

PBS-44h ,MCH release

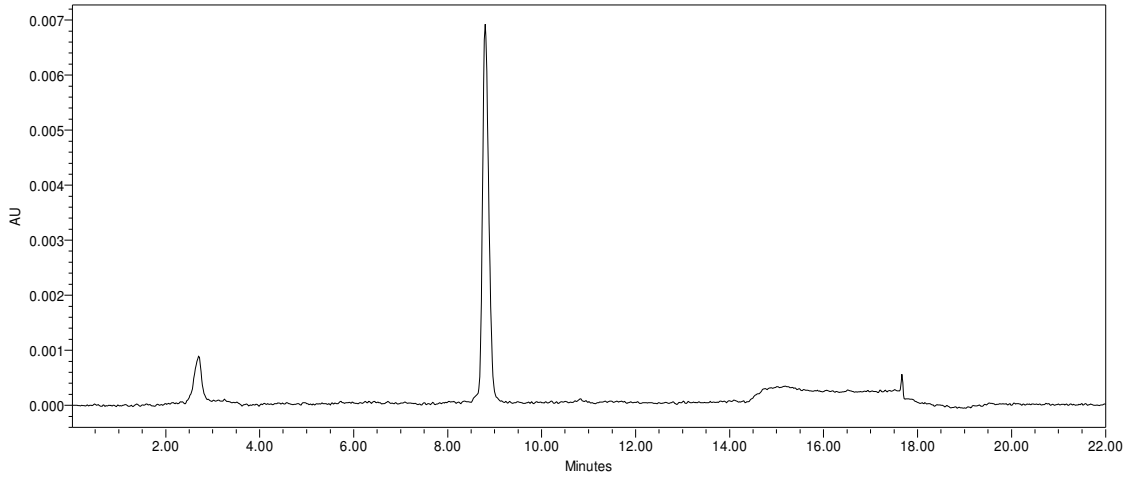

pH 5 - 1h, MCH release

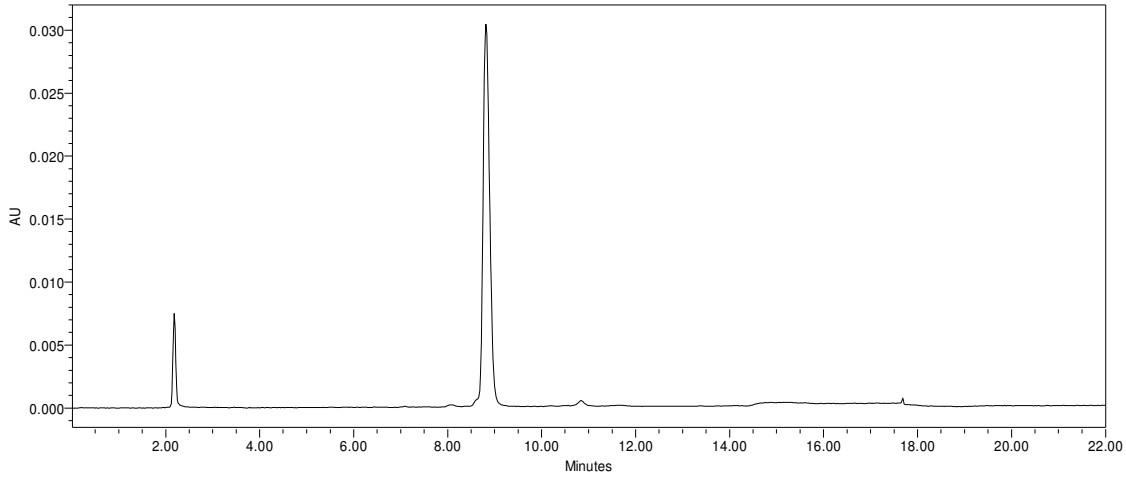

pH5-20h, MCH release

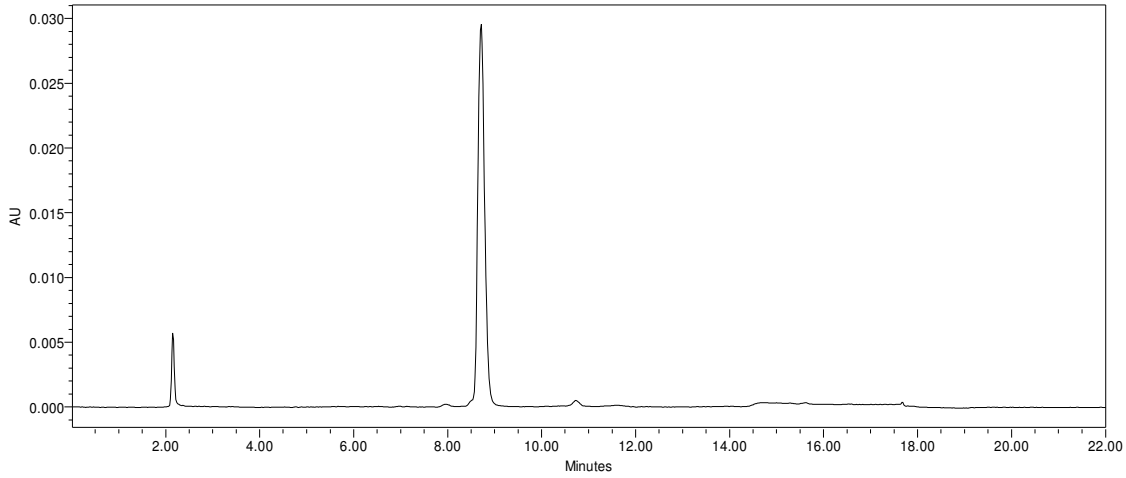

pH5-44h, MCH release

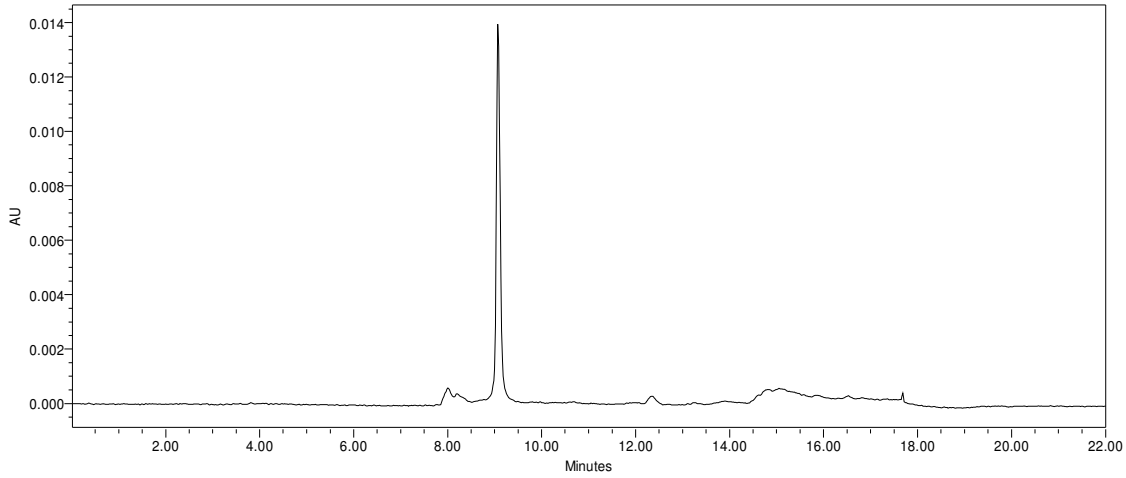

gluto- 1h ,MCH release

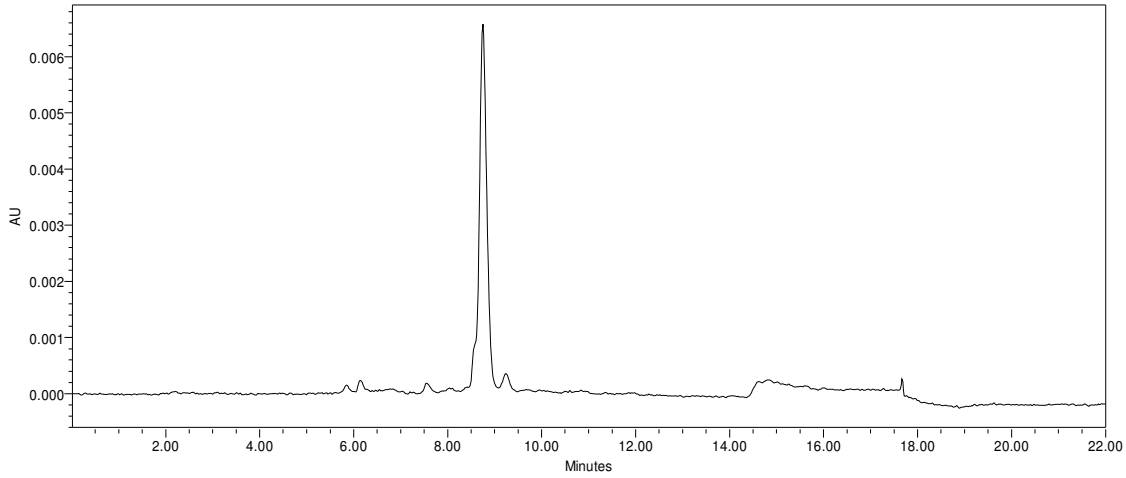

gluto-20h, MCH release

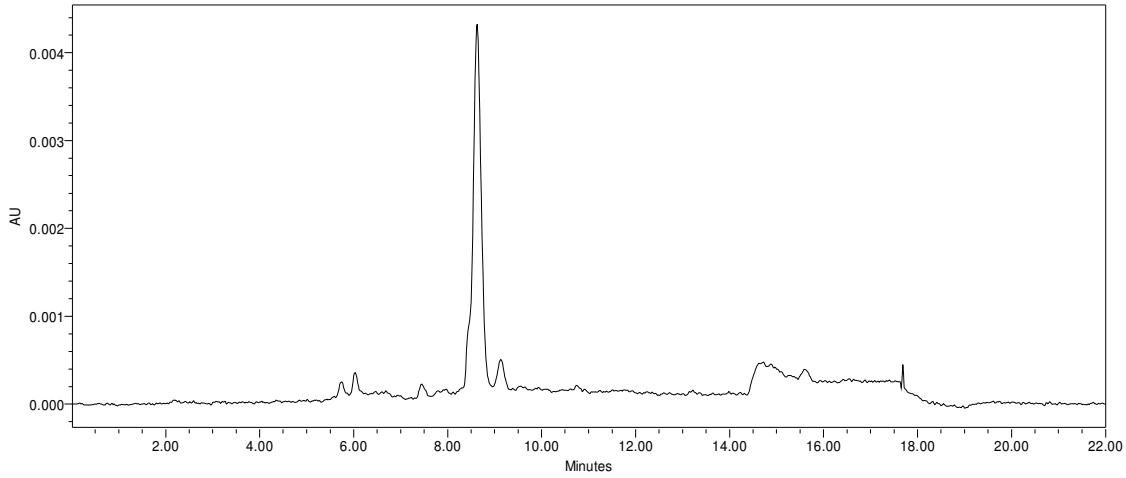

gluto-44h ,MCH release

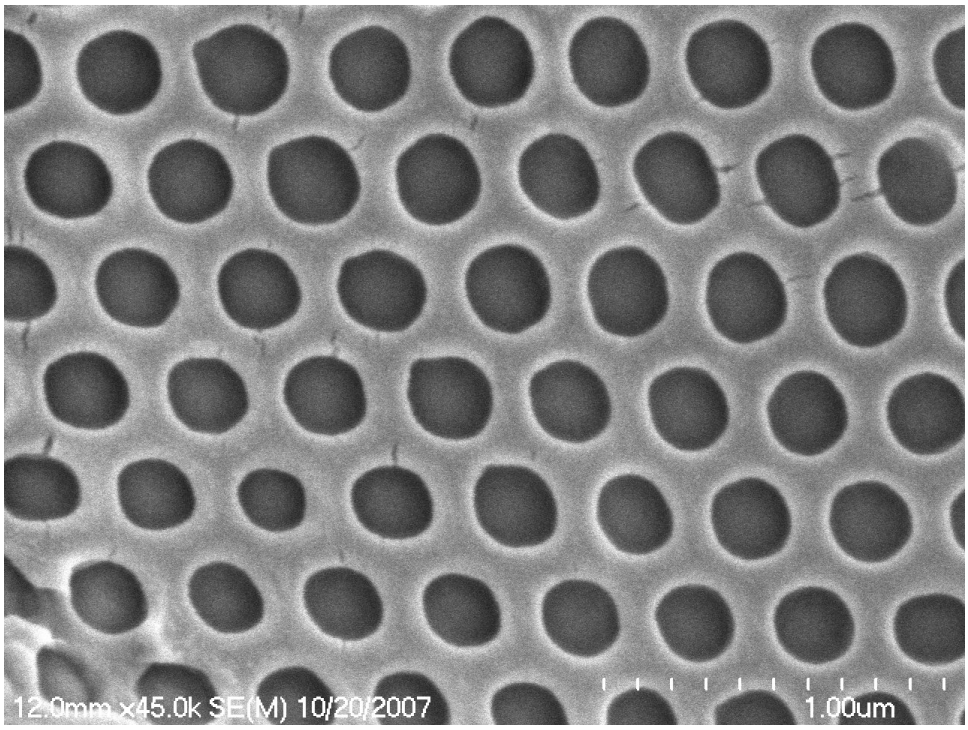

2 micron Mold

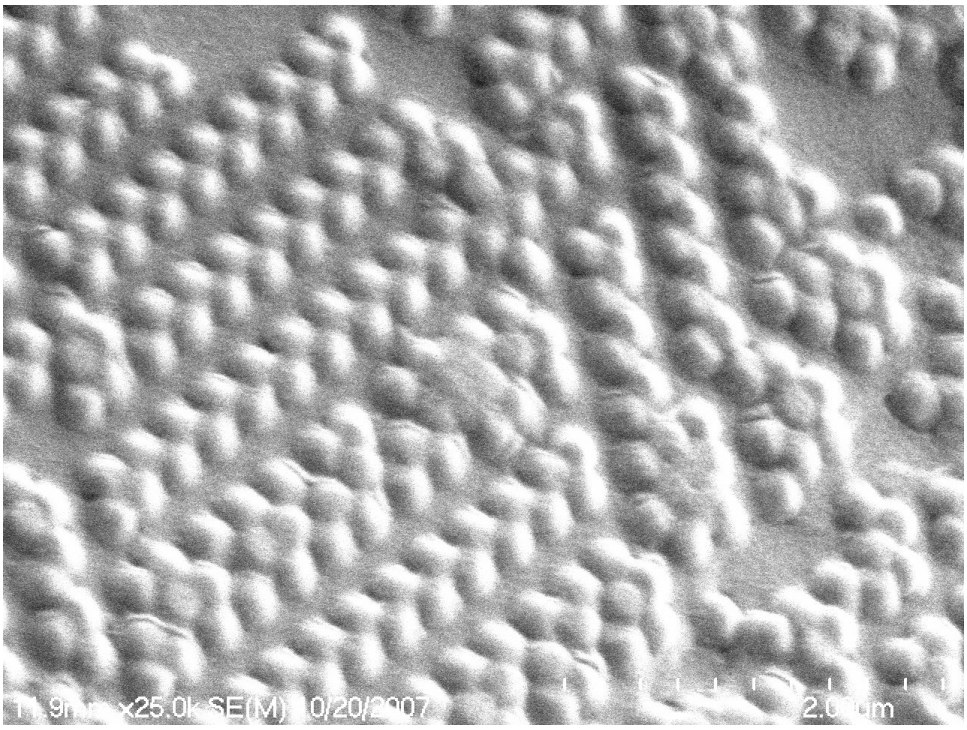

Scum layer

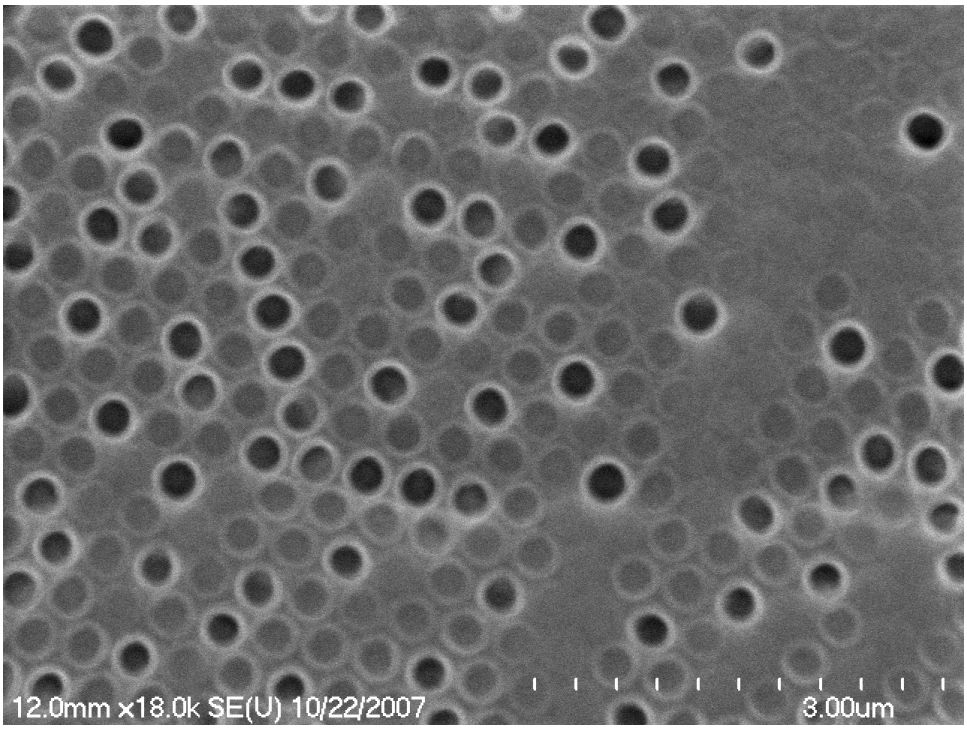

Mold filled with elastomers

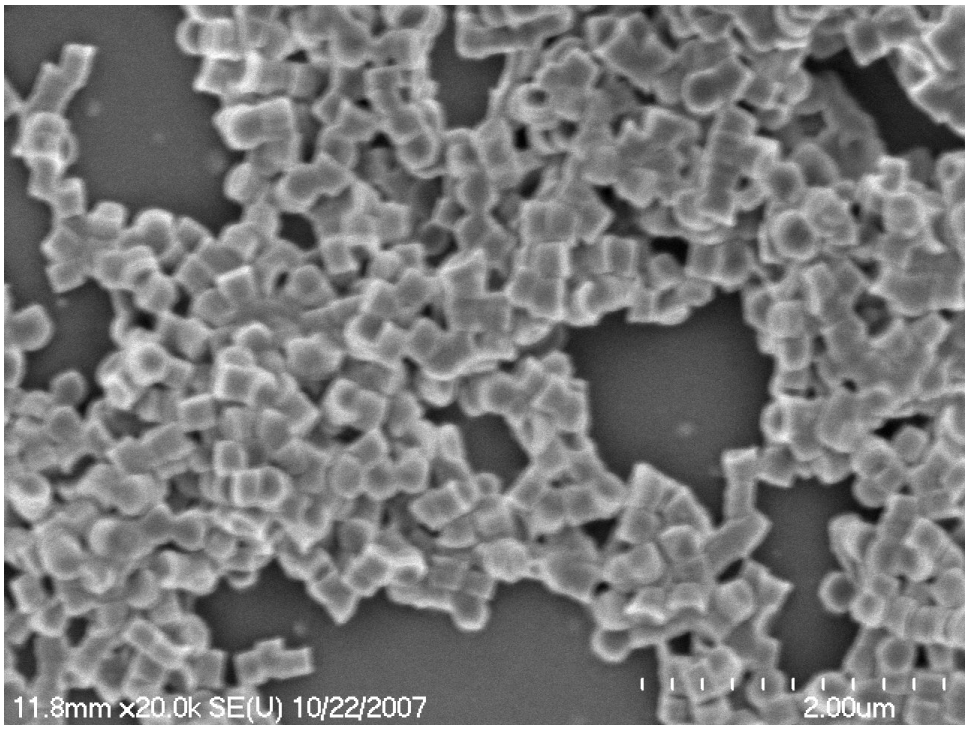

Particles

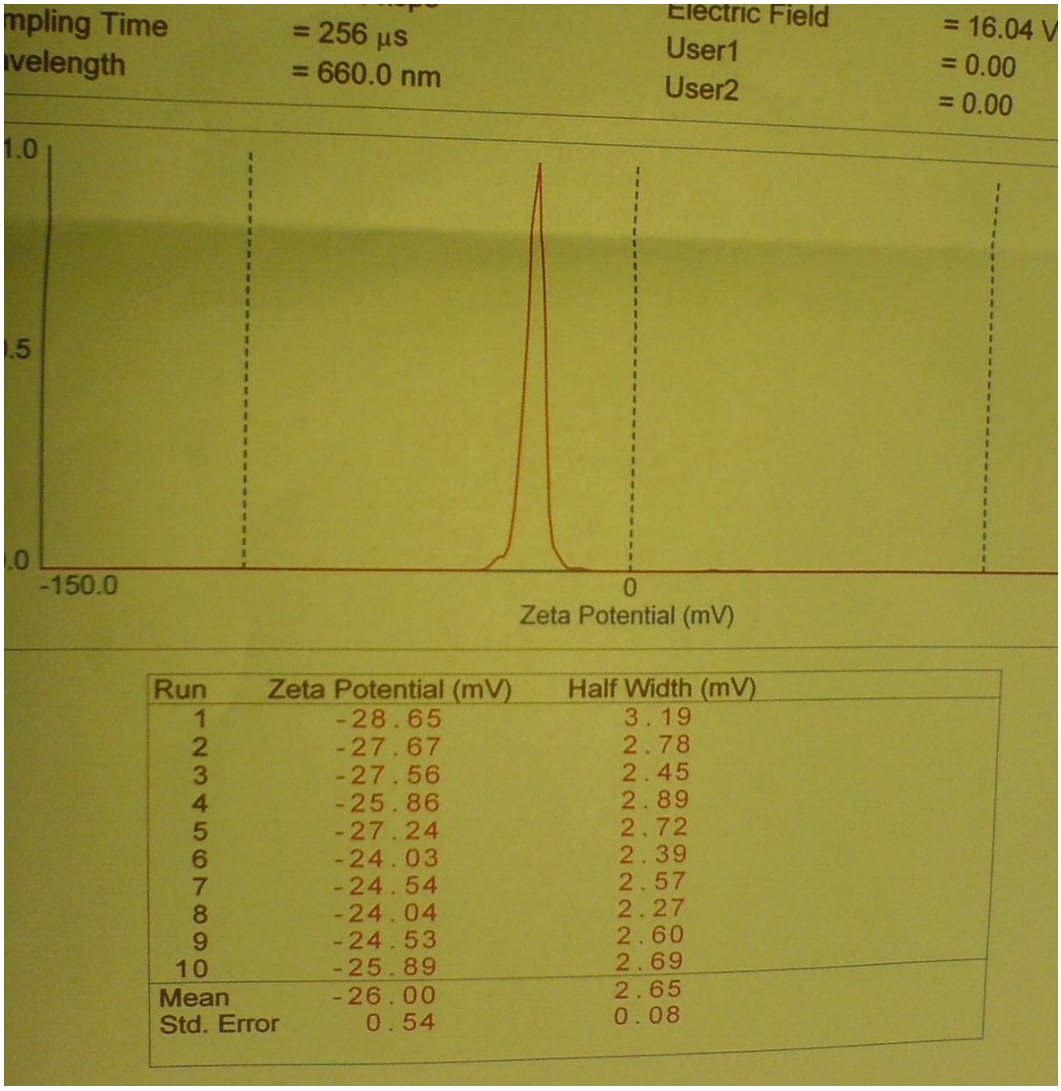

Run	Zeta Potential (mV)	Half Width (mV)
1	-28.65	3.19
2	-27.67	2.78
3	-27.56	2.45
4	-25.86	2.89
5	-27.24	2.72
6	-24.03	2.39
7	-24.54	2.57
8	-24.04	2.27
9	-24.53	2.60
10	-25.89	2.69
Mean	-26.00	2.65
Std. Error	0.54	0.08

Zeta potential of particles

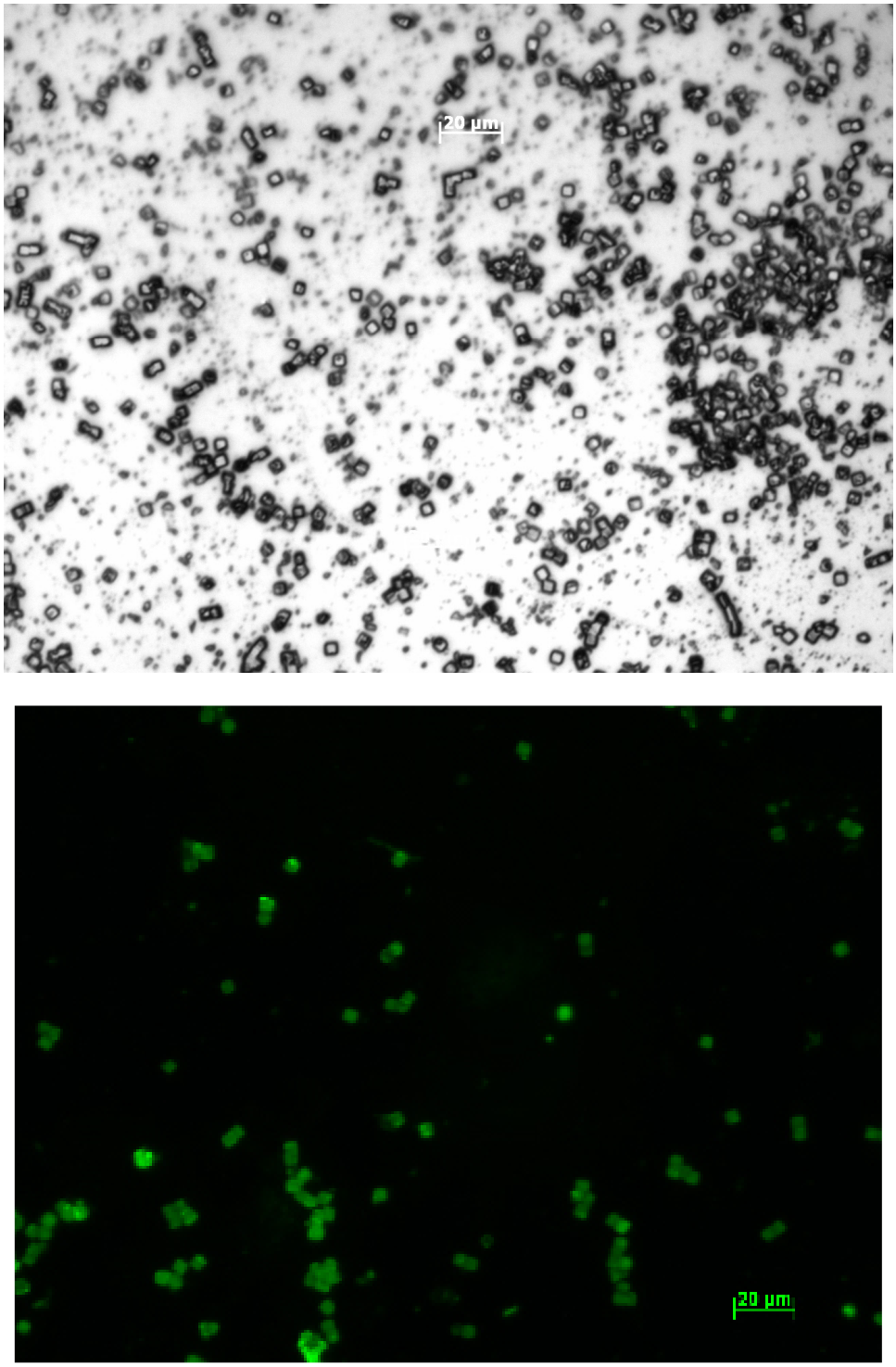

DOX loaded particles (2 micron)

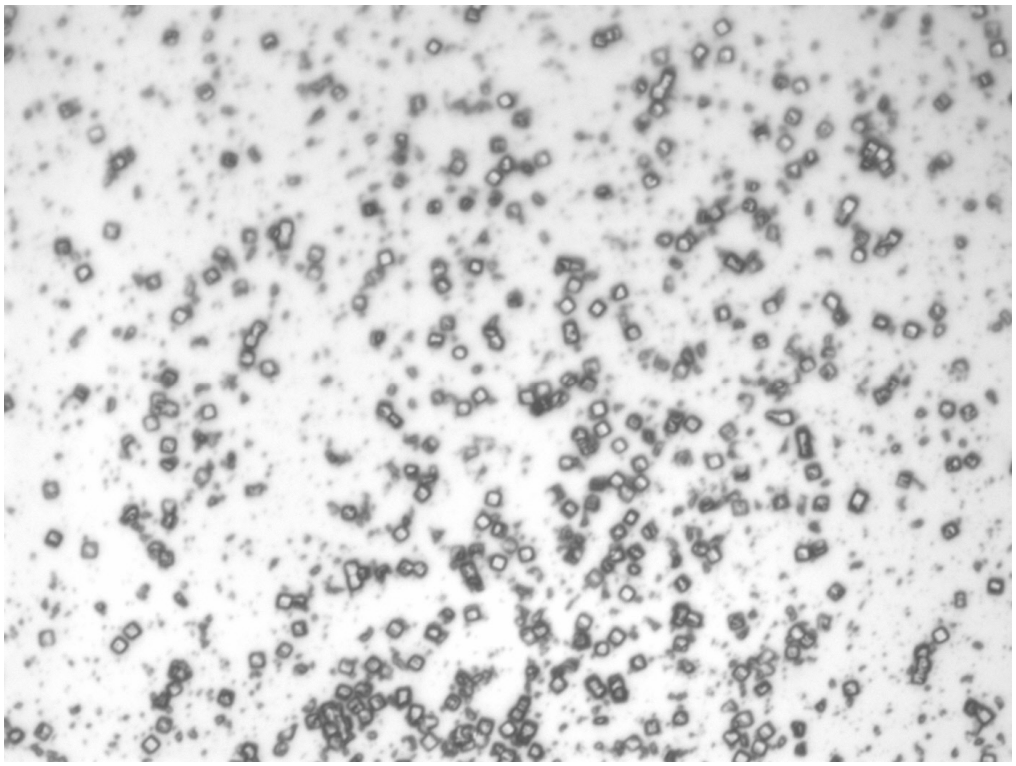

MCH loaded particles- 2 micron